Dissertation
submitted to the
Combined Faculties for the Natural Sciences and for Mathematics
of the Ruperto-Carola University of Heidelberg, Germany
for the degree of

Doctor of Natural Sciences

presented by
Sushma Nayak
Born in: Bilaspur, India

Oral-examination: 3rd March 2015

Mechanisms of Chromosomal Instability in Glioblastoma

Supervisors:

Dr. Anne Régnier-Vigouroux

Prof. Dr. Alwin Krämer

To

My Parents

Acknowledgements

I would like to thank Alwin for taking me into his lab when I was in need. I am grateful to you for giving me this interesting topic and for your enthusiasm and support. Thank you for providing me with a wonderful research environment and for making these last three years a great learning experience.

I would like to thank the members of my thesis advisory committee, Anne and Anna, for their expertise and invaluable advice over the years. I would like to thank Dr. Renata Voit and Dr. Karsten Rippe for joining my defense committee.

I would like to thank all the members of the Kramer lab, past and present. Most importantly I would like to express my heartfelt gratitude to Bettina Maier for her selfless help, encouragement, support and intellectual advice and thanks for being kind enough to read the rough drafts of this thesis during your holidays. Sigi and Michael for being the backbone of the lab, Thank you. Bianca thank you for your advice and help during trying times. I would like to extend a special thanks to the girl's Fengying, Lena, Julia, Nur, Elena, Viani, Jing, Anna, Anik, Anne-Mari, Corrina and Alex for being cheerful and supportive. Marco thank your for introducing cytogenetics to a complete novice like me. Tillman, thank you for spending endless hours scoring FISH slides and Gleb for driving me to work on those cold winter mornings. You all made going to lab so much fun!

A big thank you to the people in Korbel group and Jauch group for their contribution to this project that helped steer it into the right path. In particular Balca and Brigitte, I am grateful for all your technical help. To the many friends from other labs who took time out of their busy lives and provide me with expertise, probes, advice, or just to listen to my questions, specially Ivana thank you. I would not have been able to complete much of my research without invaluable advice from you.

I would like to give my special thanks to my friends and family in Germany who made this place feel home Laureen, Alex, Anastasia, Kathrin, Tim, Daniel, Jessi, Niko, Julia, Arne, Roswitha and Schuffi. My little India here, I could never thank you enough for being there Shariq, Ashwin, Soniya, Taro, Devanjali, Asrar, Aishwarya, Bharat and the Manvi's. A big thank you to the graduate school for the stipend that provided me with this opportunity of a lifetime and team Lindsay for making DKFZ a great place for PhD students.

To Martin, thank you for all the love and encouragement, for sharing all the good and not so good times, and reminding me to "stay strong". I love you.

Most of all, my family, Baba, Bai, Mama, Mami, Sahana and Saahil, I am so grateful for your love and support. Thank you Mom and Dad for letting me dream and for leaving no stone unturned to make my dreams come true and Sameer for all you support through thick and thin. Thank you for reminding me what is most important, I am what I am because of you and hope I have made you proud.

Index

1 Summary

Chromosomal instability (CIN) is one of the hallmarks of cancer and is found to be a characteristic property of most solid tumors. However, only little is known about the exact mechanisms leading to CIN. On the other hand, CIN is known to drive tumor cell evolution by clonal expansion leading to tumor heterogeneity, providing proliferative advantage, metastatic potential and chemoresistance to tumor cells. Hence, it is of utmost importance to identify causal mutations and delineate the mechanisms involved in CIN development in order to design targeted treatments for such notorious tumors.

In this thesis, I analyzed the NCH149 cell line derived from a primary glioblastoma tumor that is highly resistant to chemo- and radiotherapy. Cytogenetic analysis of this cell line revealed extraordinary aneuploidy, clonal heterogeneity and CIN. We could further demonstrate that mitotic chromosome segregation defects and centriole amplification were the causes of CIN in NCH149 cells.

With the aim to identify mutated genes that might contribute to the CIN phenotype of NCH149 cells whole exome sequencing was performed. This led to the identification of a novel mutation in the tumor suppressor gene LATS1. Functional characterization of LATS1 protein showed that the identified mutation (p.I615V) interferes with YAP1 binding and prevents phosphorylation of YAP1 causing its nuclear localization. Overexpression of constructs harboring the identified LATS1 mutation influenced the subcellular localization of YAP1. In addition, micronucleus formation and centriole over-duplication was induced by overexpression of mutant LATS1. In addition, we could show that hyperactive YAP1 in NCH149 cells, which is due to mutated LATS1, is an effective drug target to induce cytotoxicity to highly resistant NCH149. Verteporfin, an inhibitor of the transcriptional activity of YAP1, prevents the transcription of downstream targets and by this specifically kills LATS1-mutant NCH149 cells compared to LATS1 wild type NCH82 glioblastoma cells.

Therefore, this study demonstrates that LATS1 plays a key role in maintaining genomic integrity. Mutant LATS1 causes loss of YAP1 oncogene negative regulation and leads to the development of CIN. In addition, Verteporfin has been identified as a targeted cytotoxic agent against LATS1 mutant cells.

2 Zusammenfassung

Chromosomale Instabilität (CIN) ist ein Charakteristikum von Krebs und in den meisten soliden Tumoren zu finden. CIN beschleunigt die Tumorentwicklung durch klonale Evolution, die zu Tumorheterogenität, beschleunigter Proliferation, Metastasierung und Resistenz gegenüber Chemotherapie führt. Allerdings ist über die genauen Mechanismen, die zur Enstehung von CIN führen, wenig bekannt. Daher ist es von großer Bedeutung, ursächliche Mutationen und die an der Entwicklung von CIN beteiligten Mechanismen zu identifizieren, um eine gezielte Behandlung von Tumoren mit CIN zu ermöglichen.

In dieser Arbeit wurde die NCH149-Zelllinie, die aus einem primären Glioblastom generiert wurde und die eine ausgeprägte Resistenz gegenüber Chemo- und Strahlentherapie aufweist, untersucht. Zytogenetische Analysen zeigten, dass diese Zellen hochgradig aneuploid und sehr heterogen und somit chromosomal instabil sind. Weiter konnte gezeigt werden, dass CIN in diesen Zellen auf fehlerhafte Chromosomensegregation während der Mitose und eine Zentriolenamplifikation zurückzuführen ist.

Zur Identifikation von Mutationen, die ursächlich für den hohen Grad an CIN in diesen Zellen sein können, wurde das gesamte Exom der NCH149-Zellen sequenziert. Dabei wurde eine neue Mutation im Tumorsuppressorgen LATS1 identifiziert. Funktionelle Analysen dieser Mutation (p.I615V) zeigten, dass die Mutation die Interaktion von LATS1 und YAP1 verhindert, wodurch YAP1 nicht phosphoryliert wird und dadurch im Zellkern lokalisiert. Überexpression eines LATS1-Konstrukts, das die Mutation enthält, führt ebenfalls zu einer vermehrt nukleären YAP1-Lokalisation. Zudem führt die Überexpression von mutiertem LATS1 zur Bildung von Micronuclei und zur Zentriolenamplifikation. Weiter konnte ich diese LATS1-Mutation und die daraus resultierende YAP1-Hyperaktivität als ein therapeutisches Target identifizieren, um NCH149-Zellen, die sonst resistent gegenüber Standardbehandlungen sind, gezielt zu töten. Die Behandlung von Zellen mit Verteporfin, dass die transkriptionelle Aktivität von YAP1 inhibiert, zeigt, führte zum Absterben LATS1-mutierter NCH149-Zellen, wohingegen LATS1-Wildtyp NCH82-Glioblastomzellen durch Verteporfin nicht beeinflusst wurden.

Zusammenfassend zeigt sich, dass LATS1 für die Integrität des Genoms von Zellen von großer Bedeutung ist. Die identifizierte LATS1-Mutation hat einen Verlust der Regulation des YAP1-Onkogens und somit die Entstehung von CIN zur Folge. Zudem konnte Verteporfin als ein spezifisch gegen LATS1-mutierte Zellen wirkendes Chemotherapeutikum identifiziert werden.

3 Introduction

3.1 Chromosomal Instability

Chromosomal Instability (CIN) is defined as a persistent high rate of gain or loss of chromosomes (1). These gains and losses of chromosomes are manifested as aneuploidy; an abnormal karyotype of a cell (2). Although, aneuploidy is the ultimate consequence of CIN and could be a measure of the degree of CIN, these terms can not be used interchangeably (3). CIN is a dynamic process of changes in the cellular chromosome content over generations resulting in aneuploidy. Aneuploidy on the other hand is a description of a cellular state, it specifically describes a cell whose karyotype is not a multiple of the haploid complement (4). In contrast to CIN, aneuploidy may develop from a transient chromosomal aberration event during the development of the cell leading to the abnormal karyotype that is subsequently stably propagated and inherited. For instance, Down syndrome is caused only due to trisomy (gain of a single copy) of chromosome 21 while the rest of the chromosome content is unperturbed. Therefore it can be stated that all chromosomally instable cells are aneuploid but aneuploid cells are not necessarily chromosomally instable (5).

CIN can be broadly divided into two categories: structural and numerical CIN. Structural CIN encompasses subtle sequence instabilities represented by amplifications, inversions, translocations, deletions, and other events such as NER-associated instability (NIN) or microsatellite instability (MIN) (6). Numerical instability on the other hand includes gains and losses of whole chromosomes. This work is focused on the causes of numerical CIN and the resulting aneuploidy and its role in disease development and progression.

CIN is most often a result of defects in the machinery responsible for faithful chromosome segregation during mitosis. These defects could arise either through mutation of genes encoding mitotic proteins or by imbalances in protein levels or activities that reduce mitotic fidelity (7). To gain a better understanding of the development of CIN it is important to look into the process of cell division in greater detail.

3.2 The Cell Cycle

The cell cycle is described as the period and the sum of all biochemical processes between the emergence of a cell from a mother cell and its division into two daughter cells (8). The eukaryotic cell cycle is divided in four successive phases (M, G1, S, G2). The M-phase (division phase) includes mitosis (nuclear division) and cytokinesis (division of cytoplasm/cell). The interval between two M-phases is termed interphase which includes G1-, S- and G2-phases of the cell cycle. The term G1 (gap 1) describes the period between M-phase and S-phase. In the S-phase (synthesis phase) replication of nuclear DNA takes place. The G2-phase falls between S phase and M phase wherein the connections with neighboring cells are dissolved to prepare for mitosis.

Mitosis involves a sequence of events that culminate in the production of new (daughter) cells that are genetically identical to the original (mother) cell (9). This requires precise orchestration of three major events: entry into mitosis, chromosomal segregation, and cytokinesis which are distributed over four stages: prophase, metaphase, anaphase and telophase. In prophase chromosomes are condensed and the spindle apparatus starts to build up. With the beginning of metaphase (prometaphase) the nuclear envelope breaks down and the spindle microtubules are formed that attach to the kinetochores (protein structure on chromatids) of the chromosomes. During metaphase chromosomes are arranged at the equatorial plane of the cell and the spindle apparatus is fully formed. Anaphase marks the separation of sister chromatids leading to their segregation to the two spindle poles. In parallel, the microtubules lengthen moving the spindle poles apart. In telophase a new nuclear membrane is formed around the two sets of chromosomes at each pole and the contractile ring is formed. During cytokinesis the contractile ring ingresses forming the cleavage furrow eventually separating the daughter cells.

The cell cycle phases are subject to strict control by various control mechanisms referred to as "checkpoints", which verify whether the requirements for the cell to pass to the next phase of the cell cycle have been fulfilled (Figure 3.1) (10).

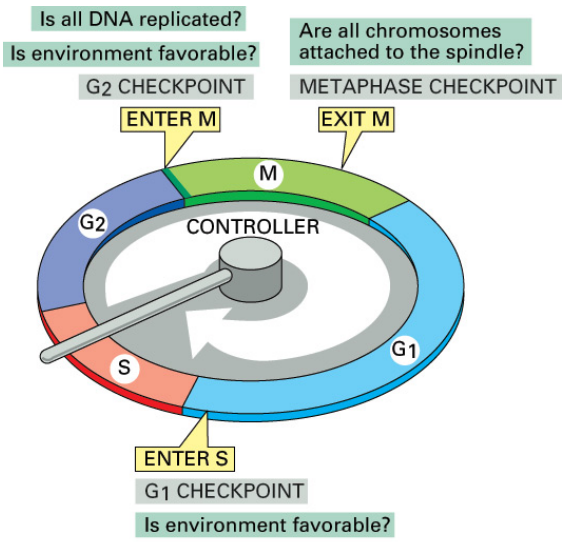

Figure 3.1 The cell cycle and its checkpoints

The cell cycle is divided into four phases: S-phase (synthesis phase), M-phase (mitosis phase), and the G1- and G2-phases (Gap-phases). Checkpoints regulating the various phases of cell cycle are indicated. Albert, B. *et al.* (2008) Molecular biology of the cell. New York, USA: Garland Science.

3.3 Cell cycle checkpoints

The first checkpoint within the course of the cell cycle is called the restriction point or G1-checkpoint, which occurs at the end of G1-phase of the cell cycle. At the G1-checkpoint decided whether or not the cell is allowed to divide depending on the environmental condition. Under unfavorable conditions cells can either delay entry intro S-phase or enter the resting G0-stage (11).

The cell encounters a second checkpoint at the G2-M boundary called the DNA damage checkpoint or S-phase checkpoint. This ensures that the cells do not enter mitosis with damaged DNA that may have accumulated during S-phase. DNA repair proteins (e.g. ATM, ATR) that localize to sites of DNA damage in G2-phase initiate a signaling cascade that regulates mitotic entry via Cdk1-cyclin B (12).

Third, the spindle assembly checkpoint (SAC) or mitotic checkpoint ensures that chromosome segregation proceeds error free thereby preventing aneuploidy. During mitosis, this checkpoint inhibits anaphase onset until all chromosomes are properly attached to the spindle and the kinetochores of the sister chromatids are correctly attached to opposite spindle poles, ensuring their proper segregation (13). A mitotic checkpoint

complex (MCC) comprising of MAD2, BUBR1/Mad3 and BUB3, assembles at unoccupied kinetochores (14). This complex negatively regulates the ability of CDC20 to activate APC/C-mediated polyubiquitinylation of cyclin B and securin, thereby preventing separation of sister chromatids and exit from mitosis, respectively. Securin is a stoichiometric inhibitor of separase which is required to cleave the cohesin complex that holds sister chromatids together, and cohesin cleavage is required to execute anaphase. On the other hand, proteolysis of cyclin B by APC/C inactivates CDK1, which promotes mitotic exit (15). Hence, by keeping CDC20 in check, the SAC prolongs metaphase until all chromosomes have become bi-orientated between separated spindle poles on the metaphase plate. Even a single unattached kinetochore is sufficient to delay anaphase onset indicating the efficiency of this checkpoint.

3.4 Causes of CIN

Deregulation of proteins involved in chromosome condensation, sister-chromatid cohesion, kinetochore structure and function, centrosome/microtubule formation and dynamics and checkpoint genes that monitor the proper progression of the cell cycle can lead to CIN (16). The pathways by which cells can gain or lose chromosomes during mitosis are described below (Figure 3.2).

3.4.1 Defects in cell cycle checkpoints

The first defect that was proposed to play a causal role in CIN was a defect in the spindle assembly checkpoint (SAC) (17). Impairment of the mitotic checkpoint due to reduction in levels of one or more checkpoint components might allow cells to enter anaphase in the presence of unattached or misaligned chromosomes. As a consequence, both copies of one or more replicated chromosomes are deposited in the same daughter cell (non-disjunction errors) causing aneuploidy (18).

Mitotic checkpoint errors can give rise to aneuploidy or lead to cell death, depending on the extent of checkpoint malfunction. Complete inactivation of the mitotic checkpoint resulting from elimination of key components such as MAD2 or BUBR1 leads to extensive aneuploidy and massive chromosome missegregation, which is lethal for cells (19). Studies in mice have shown that weakened SAC activity is associated with a high incidence of aneuploidy and tumorigenesis (20; 21). However, meanwhile it has been shown that most aneuploid

human cancer cells have a functional SAC indicating that loss of SAC function seems not to play a major role in CIN induction in human tumors. However, despite extensive search, large-scale genome sequencing has revealed very few mutations in genes that encode proteins involved in SAC have been found in human tumors (22; 23).

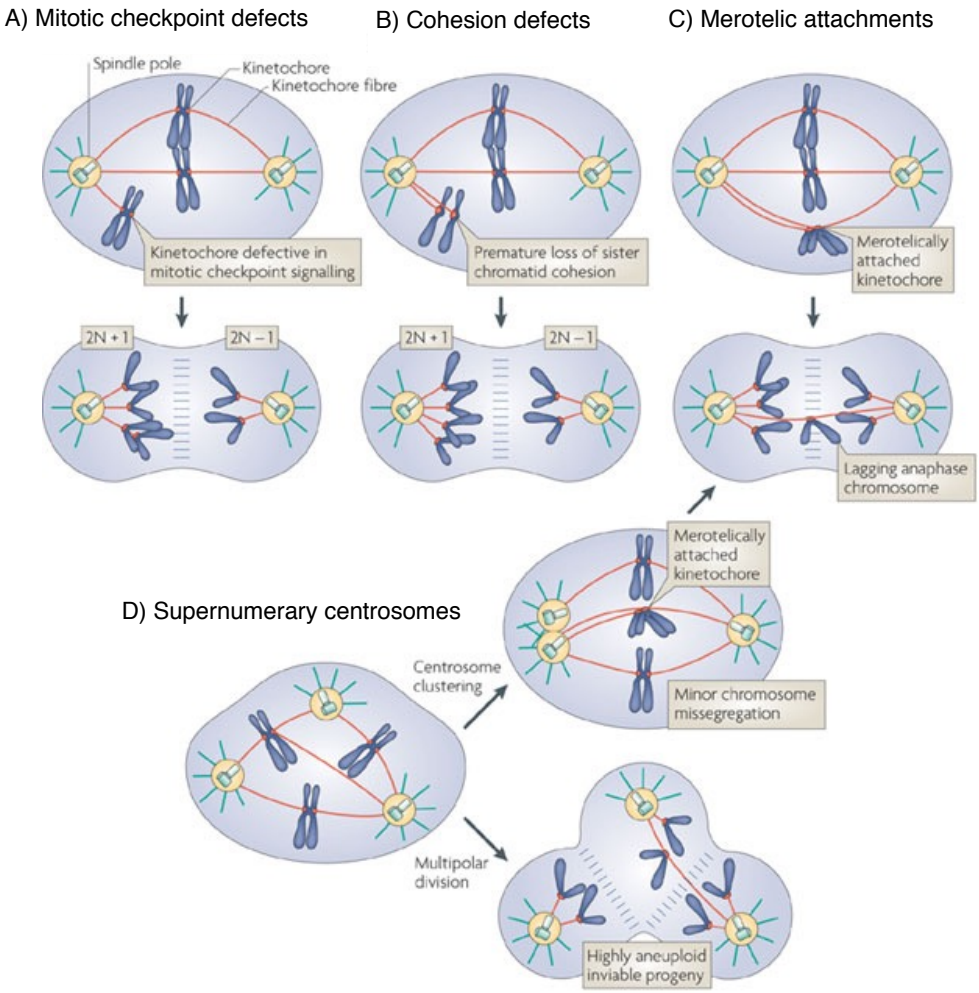

Figure 3.2 Pathways to chromosomal missegregation

Mechanisms of chromosomal missegregation include mitotic checkpoint defects (A), cohesion defects (B), merotelic microtubule-kinetochore attachments (C) and supernumerary centrosomes which, by themselves, lead to merotelic microtubule-kinetochore attachments again (D). Modified from Holland *et al*., Nature, 2009, with permission.

3.4.2 Chromosomal missegregation

Mitotic errors leading to aneuploidy can occur despite intact mitotic checkpoint signaling. During mitosis, faithful segregation of chromosomes relies on the bi-oriented attachment of kinetochores to spindle microtubules (k-MT attachments) called amphitelic attachments, meaning that each kinetochore binds to microtubules oriented toward only one spindle pole, thereby generating centromeric tension that satisfies the SAC (24). Kinetochores in human cells bind approximately 20 microtubules and errors in k-MT attachments lead to missegregation of chromosomes. In chromosomally instable cells missegregation of chromosomes is found on an average, once in every one to five cell divisions (25). Erroneous k-MT attachments frequently occur during prophase when (i) one of the sister kinetochores is left unattached (monotelic attachment), (ii) when both sister kinetochores become attached to microtubules from the same pole (syntelic attachment) or when (i) a single kinetochore attaches to microtubules arising from both spindle poles rather than just one (merotelic attachment) (Figure 3.3). Monotelic and syntelic configurations fail to satisfy the SAC because not all kinetochores are bound to microtubules or no centromeric tension is generated and are therefore detected by the spindle checkpoint. In contrast, merotely avoids detection by the SAC since kinetochores attain full occupancy by microtubules despite improper orientation and centromeric tension is generated as well (26). Therefore, undetected by the SAC, merotelic attachments can cause sister chromatids to either be pulled towards the same pole into one daughter nucleus (chromosome non-disjunction) or left behind in the spindle midzone (lagging chromosomes), thereby often excluding them from both the daughter nuclei resulting in micronucleus formation (27). Studies have shown that on average about 21% of daughter cell pairs of CIN cells have micronuclei (28). Destabilization of erroneous k-MT attachments is essential for their correction and was found to restore faithful chromosome segregation to CIN cells, indicating a causal relationship between k-MT attachment errors and CIN (29). Correspondingly, it has been shown that chromosomally instable cells often have hyperstable k-MT attachments, which impairs their ability for faulty attachment correction (30).

Another defect that contributes to chromosomal missegregation is premature loss of sister chromatid cohesion. Maintenance of cohesion between the two sister centromeres until anaphase onset is essential for proper chromosome segregation. Duplicated sister chromatids are held together until anaphase by the cohesin complex ensuring proper k-MT attachments and centromeric tension needed for proper segregation. Premature loss of sister chromatid cohesion causes the sister chromatids to separate and float in the cellular

space. Overexpression of separase, cohesin complex subunits or dysfunctional securin has been shown to cause a loss of proper sister chromatid cohesion (31). As a consequence, sister chromatids fail to segregate equally between the daughter cells leading to aneuploidy. Emerging cancer genomics studies have documented that cohesin genes are a frequent target of somatic alterations in a number of tumor types including glioblastoma, Ewing sarcoma, urothelial carcinoma and acute myeloid leukemia (32).

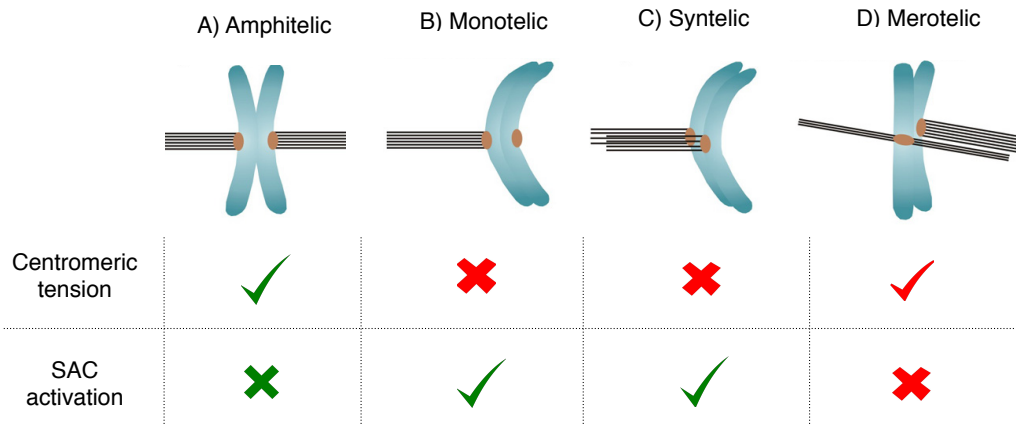

Figure 3.2 Types of k-MT attcahments

The various types of kinetochore-microtubule attachments include: A) correct amphitelic microtubule attchment to the sister kinetochores that attains the right centromeric tension (green) and therefore does not activate SAC (green). B) and C) erroneous attachments where only one (monotelic) or both sister kinetochores (syntelic) are attached to microtubules from the same spindle pole do not lead to correct centromeric tension (red), causing SAC activation (green) and subsequent correction to proper k-MT attachment. D) Merotelic attachment, where one of the kinetochores is attached aberrantly to microtubules form both spindle poles and since the kinetochores attain full occupancy of microtubules centromeric tension is falsely satisfied (red) which avoids detection by the SAC (red) causing chromosomal missegregation.

3.4.3 Supernumerary centrosomes

Centrosomes are important regulators of cell-cycle progression, serving as the main microtubule-organizing centers (MTOC) to form k-MT attachments and aid faithful segregation of chromosomes during mitosis. A centrosome is composed of a pair of centrioles and a surrounding amorphous cloud of pericentriolar material (PCM). Centrosome number is tightly regulated during the cell cycle such that a centrosome duplicates in S phase and separates at mitotic entry. However, defects in the centrosome duplication machinery lead to supernumerary centrosomes (33; 34; 35). Presence of supernumerary (extra) centrosomes leads to the formation of multiple spindle poles during mitosis followed by multipolar division. Multipolar divisions give rise to highly aneuploid daughter cells, which

are usually unviable (36). In order to generate viable daughter cells, supernumerary centrosomes are often found to be clustered together to form two groups, allowing cells to divide in a pseudo-bipolar fashion (37; 38). This mechanism is termed centrosomal clustering. The frequency of multipolar spindles is found to be higher in prometaphase than in anaphase confirming that centrosomes cluster to promote bipolar spindle formation prior to anaphase onset (39).

Interestingly, extra centrosomes are capable of driving chromosome missegregation through a mechanism independent of multipolar divisions. Studies have shown that the process of centrosomal clustering via transient multipolar spindle formation increases the propensity of merotelic k-MT attachments leading to chromosome missegregation (40). Thus, the presence of extra centrosomes accompanied by centrosomal clustering increases the rate of k-MT attachment errors leading to CIN. Notably, the presence of extra centrosomes and clustering mechanisms prolong the duration of mitosis by delaying satisfaction of the SAC (41; 42). Although a majority of the cells with extra centrosomes divide bipolarly with missegregated chromosomes, some cells die during the prolonged mitotic arrest and some others remain without undergoing cytokinesis and end up as a single tetraploid G1 cell (43).

3.5 Consequences of CIN

Mutation-induced mitotic checkpoint relaxation, defects in chromatid cohesion, merotelic attachments of microtubules to kinetochores, and supernumerary centrosomes cause chromosome missegregation resulting in aneuploid cells. Aneuploidy is marked by altered chromosome copy number leading to changes in the level of transcripts of affected genes. This in turn translates into protein dosage changes that can alter the balanced stoichiometry of various complexes or pathways leading to malfunctioning of corresponding biological processes. When proteins involved in various mitotic processes are affected, it may lead to errors causing further CIN and thus contributing to aneuploidy generation (44). Hence, chromosomally instable cells enter a vicious circle of events leading to continuous genomic instability which might be beneficial or disadvantageous to a cell.

In theory, the direct consequences of CIN should be disadvantageous for cell proliferation and survival. The lack of essential genes produced by random aneuploidy may adversely effect survival and the aberrant genome would risk detection by selection barriers (e.g. checkpoints) resulting in elimination. If the accumulated damage rises above the threshold

for viability, apoptotic pathways are activated and cell death ensues. However, CIN gives rise to heterogeneity, which might prove beneficial for survival. The heterogeneity in the population of a given cell mass arising as a result of CIN ensures that at least some of the cells contain the required genetic alteration to overcome selection barriers and continue proliferation (45). Heterogeneity allows cells to survive and adapt to changing microenvironments giving cells proliferative advantages (46).

Such adaptive interactions can provide opportunities for chromosomally instable cells to survive and evolve to suit the microenvironment, in a manner comparable to Darwinian theory of natural selection. Hence, by clonal evolution, an aberrant karyotype is established, which has optimal chances of survival, proliferation and resistance to internal and external elimination pressure, which are the characteristic features of most cancer cells. Indeed, various studies show that CIN plays a crucial role in the development of cancer (47; 48).

3.6 Role of CIN in Cancer

The presence of aneuploid chromosome contents in tumor cells has been common knowledge for over 100 years. The foundations for viewing cancer as a genetic disease were laid as early as 1890 when David von Hansemann postulated that aberrant cell divisions are responsible for the decreased or increased chromatin content found in cancer cells. Theodor Boveri found the association between aberrant mitoses, aneuploidy and malignancy – Boveri, T. *Zur Frage der Entstehung Maligner Tumoren*; Gustav Fisher, Jena, 1914. Today, it has been demonstrated that 68% of all solid tumors have numerical variations in their chromosomes number, i.e. they are aneuploid (49). In a study by Lengauer *et al.*, fluorescence *in situ* hybridization (FISH) was used to show that losses or gains of multiple chromosomes occurred as often as 10-100 times more often in aneuploid colorectal cancer cell lines than in normal cells. Karyoptypic analyses show that tumors display both intra- and intertumor heterogeneity suggesting that most tumors are not only aneuploid, but also chromosomally instable. As CIN is found to be a characteristic property of most solid tumors, it has been regarded as a hallmark of cancer. Although scientific advances in recent years have permitted more refined analysis of the types of chromosomal abnormalities in cancer, the function of numerical chromosome aberrations in the etiology of cancer is less understood. A crucial question still remains unanswered: is CIN is a cause or a consequence of tumorigenesis?

The presence of CIN in cancer cells has been interpreted in two ways. One point of view portrays CIN and aneuploidy as a consequence of general chaos that accompanies malignant cells (50). The second point of view ascribes a causal importance to aneuploidy, arguing that it fuels tumorigenic progression (51). It has been established that cells have to acquire several genetic changes to allow tumorigenesis. It has been argued that the normal rate of mutation would be insufficient to provide the amount of genetic variation that is required for tumor growth, and hence it is often proposed that mutations causing genomic instability occur as the initiating event and act as a driving force of tumorigenesis (52).

Tumors initiate as a result of one or more mutations that give a cell the selective growth advantage by means of CIN to overcome waves of clonal selection. As mentioned before CIN further drives adaptation by allowing tumors to constantly sample their microenvironment and attain the genetic changes necessary to propel tumor survival, proliferation and resistance to therapy. This model of mutation-driven genomic instability and tumorigenesis has been confirmed by numerous studies (53; 54).

3.7 Genetic basis for CIN in cancers

The concept that tumors develop through the accumulation of mutations in oncogenes and tumor suppressor genes is now a widely accepted fundamental principle of cancer biology. Although CIN aids faster accumulation of carcinogenic mutations, it still remains unclear what causes CIN itself. Mutations in genes with putative functions in guarding against chromosome missegregation and aberrant mitoses have been shown to cause CIN in rare cases (55).

In theory, hundreds of human genes can be categorized as CIN causing genes, but only a few have been identified so far (56). These genes include hBUB1 and MAD2, proteins required for the proper functioning of the spindle assembly checkpoint (57; 58). Inherent mutations in BRCA1 and BRCA2 (involved in DNA repair and recombination, checkpoint control of the cell cycle and transcription) lead to high-grade familial breast cancer and CIN (59). Cyclin-dependent kinases (CDKs), the governors of cell cycle, are often found mutated or dysregulated in cancer cells, which manifests in an increased rate of cell cycling, cellular hyperproliferation and acquired genomic and chromosomal instability (60). In addition, studies have shown that overexpression of one of the two key regulators controlling sister chromatid cohesion, separase or securin, promotes CIN and oncogenic transformation (61). Moreover, mutational inactivation of genes encoding cohesin subunits such as STAG2 and

RAD21 have also been found in various human cancers (62).

Michor and colleagues classify CIN genes based on the mutational events required to trigger instability (63). Class I CIN genes cause CIN if one allele of the gene is mutated or lost (e.g. MAD2) and class II CIN genes trigger CIN if one allele is mutated in a dominant-negative fashion (e.g. hBUB1). Thus, class I and II genes are called 'single hit' CIN genes. Class III CIN genes cause CIN only if both alleles are mutated (e.g. BRCA1 and BRCA2).

Hence, a direct connection can be drawn between mutations in cell cycle components, tumor suppressor genes, oncogenes and CIN development. This provides evidence that CIN has a mutational origin and clues to the mechanistic basis of instability in cancers.

3.8 Hippo pathway and cancer

The mammalian Hippo pathway is a kinase cascade that plays a pivotal role in organ size control and tumor suppression by restricting proliferation and promoting apoptosis (64). The Hippo pathway was first identified in *Drosophila* by genetic mosaic screens for tumor suppressor genes. It is a highly conserved pathway, which in mammals includes two sets of core kinases MST1/2 and LATS1/2, which along with their respective co-activators SAV1 and Mob1 form the backbone of the kinase cascade. The N-terminus of LATS1 contains two PPxY motifs (P, proline; X, any amino acid; Y, tyrosine), which bind to WW-domains (conserved tryptophans spaced 20-22 amino acids apart) of the transcriptional co-activators TAZ and YAP. When the pathway is active, Lats1/2 phosphorylates YAP and/or TAZ, which leads to cytoplasmic sequestration and degradation of these proteins. As consequence, TEAD 1-4 remains bound to VGL4 rendering it incapable of switching on the transcription of target genes. When the pathway is inactive, YAP/TAZ remain unphosphorylated and free to enter the nucleus and bind to TEAD1–4 resulting in context-dependent transcriptional output that mediates major physiological functions (Figure 1.3) (65). However, the regulatory mechanisms for the Hippo signaling pathway are not well understood (66). Numerous upstream regulators of the Hippo pathway have been identified recently, e.g. NF2/merlin-mediated regulation involved in cell polarity as well as G-protein-coupled receptor (GPCR)-dependent signaling for growth and proliferation. Lysophospholipid (LPA), sphingosine-1-phosphate (S1P) or protease-activated receptors (PARs) bind to their corresponding membrane GPCRs and act through Rho-GTPases to activate YAP/TAZ (67). In addition, the actin cytoskeleton or mechanical tension appears to transmit upstream signals to the core

Hippo signaling cascade. Therefore, LATS-dependent modulation of YAP/TAZ activity appears to act as a focal point for different upstream cellular signals to Hippo pathway.

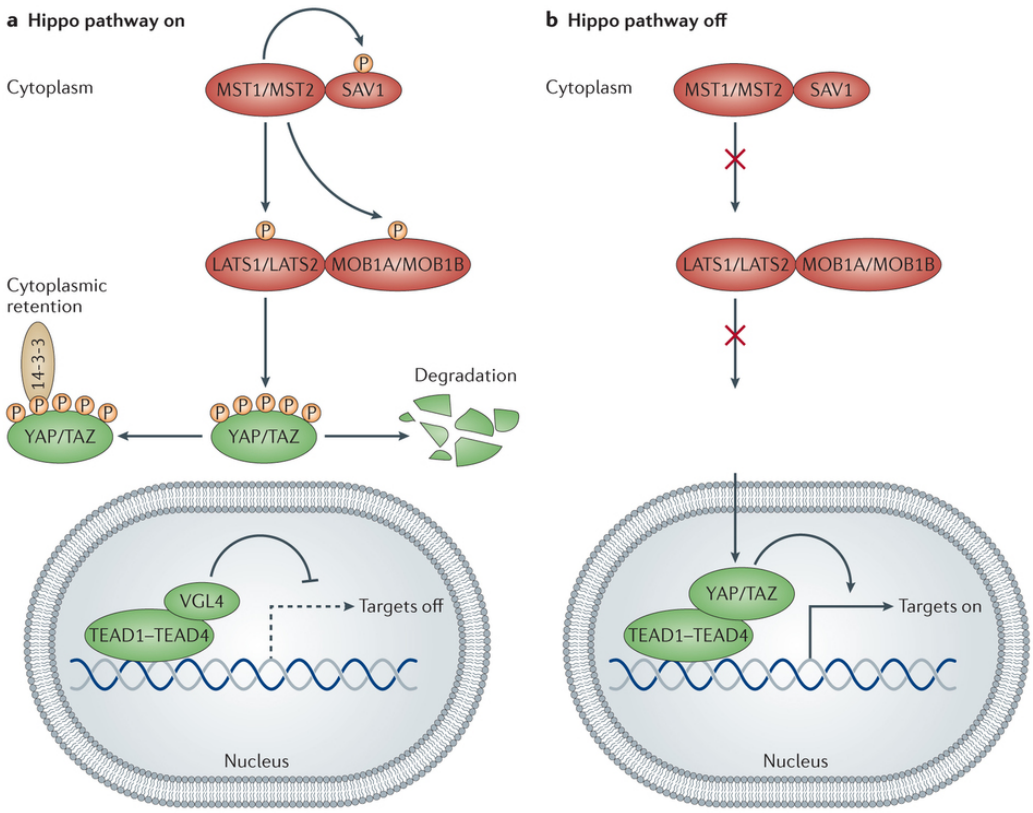

Figure 3.3 The Hippo pathway

Schematics of the core pathway components of the Hippo pathway and how they interact are depicted. A) When the pathway is on, proteins are phosphorylated resulting in cytoplasmic retention or degradation of YAP/TAZ. As a consequence TEAD1-4 remains bound to VGL4 rendering it incapable of switching on the transcription of target genes. B) When the pathway is off, un-phosphorylated YAP/TAZ translocates to the nucleus and competitively binds to co-activators TEAD1-4 to switch the transcription of target genes on. Johnson *et al.* 2014, with permission.

3.8.1 LATS1 and YAP1

LATS1 is a member of the LATS/Warts tumor suppressor family. It is a putative serine/threonine kinase that belongs to AGC group (named after protein kinase A, G and C) and acts as a negative regulator of YAP1 in the Hippo signaling pathway. YAP1 is known to be an oncogene and shown to cause CIN and radioresistance in medulloblastoma (68). LATS1 localizes in the cytoplasm and to centrosomes during interphase and during mitosis. It is known to migrate to the mitotic spindle, spindle poles as well as the midbody during mitosis indicating its role in proper mitotic progression (69). During interphase,

phosphorylated LATS1 phosphorylates YAP1 at Ser127, which leads to 14–3–3 binding and cytoplasmic sequestration followed by ubiquitination-dependent degradation of YAP1. In early mitosis LATS1 is dephosphorylated causing dephosphorylation of YAP1 and hence its nuclear localization leading to transcription of genes important for cell proliferation, cell death, and cell migration. Therefore, deregulation of LATS1-mediated sequestration of YAP1 in interphase causes YAP1 to translocate to the nucleus and prematurely activate transcription of cell growth proliferation and survival genes which is known to be associated with many cancer types (70). LATS1-mediated YAP1 phosphorylation is regulated by cell density *in vitro* in cultured cells and plays an important role in mediating cell contact inhibition. Upon reaching confluence (high density), YAP1 is found phosphorylated and localized to the cytoplasm of the cells whereas, at low density, YAP1 is predominantly localized in the nucleus (71). YAP1 expression levels and nuclear localization are found strongly elevated in some human cancers suggesting the loss of cell contact inhibition indicative of uncontrolled cell proliferation.

In addition, LATS1 also functions in non-canonical Hippo signalling and Hippo-independent pathways. It has been shown that autophosphorylation of LATS1 during the G2/M transition plays a critical role in maintenance of ploidy through its actions in mitotic progression and G1 tetraploidy checkpoint. LATS1 regulates the cell cycle by modulating CDK1/Cyclin A activity (72). LATS1 with its protein-binding domain (PBD) is also known to bind and regulate the activity of MOB1, a regulatory protein of LATS1 and component of mitotic exit network (73). LATS1 interacts with regulators of actin filament assembly, Zyxin and LIMK1 indicating that LATS1 functions in mitosis and mechano-sensing independent of YAP/TAZ as well (74) (75). During the G2/M transition, YAP1 is found to be hyper-phosphorylated due to additional positive regulation of YAP1 by CDK1-mediated phoshorylation at T119 and S289. Defects in CDK1-mediated YAP1 phosphorylation were found to play a role in neoplastic transformation as they lead to mitotic defects and increased cell motility (76). This extensive involvement of LATS1 in important cellular functions elucidates its role in tumor suppression and maintenance of genomic integrity.

Interestingly, studies of The Cancer Genome Atlas (TCGA) consortium show that LATS1 is infrequently mutated in human cancers (http://www.cbioportal.org/public-portal/) (Figure 3.4). However, in a variety of human cancers upstream components of the pathway are downregulated through deletion or epigenetic mechanisms (e.g. deletion of NF2), with silencing of upstream components of the pathway leading to increased activity of the downstream effectors of YAP and TAZ. Experimental N-terminal truncation of LATS1 in mouse embryonic fibroblasts (MEFs) was found to cause abnormal cell growth and CIN in

nude mice (77). Decreased expression of LATS1 is correlated with progression and prognosis of glioma (78). This suggests that Hippo signaling is closely linked to tumor initiation and progression.

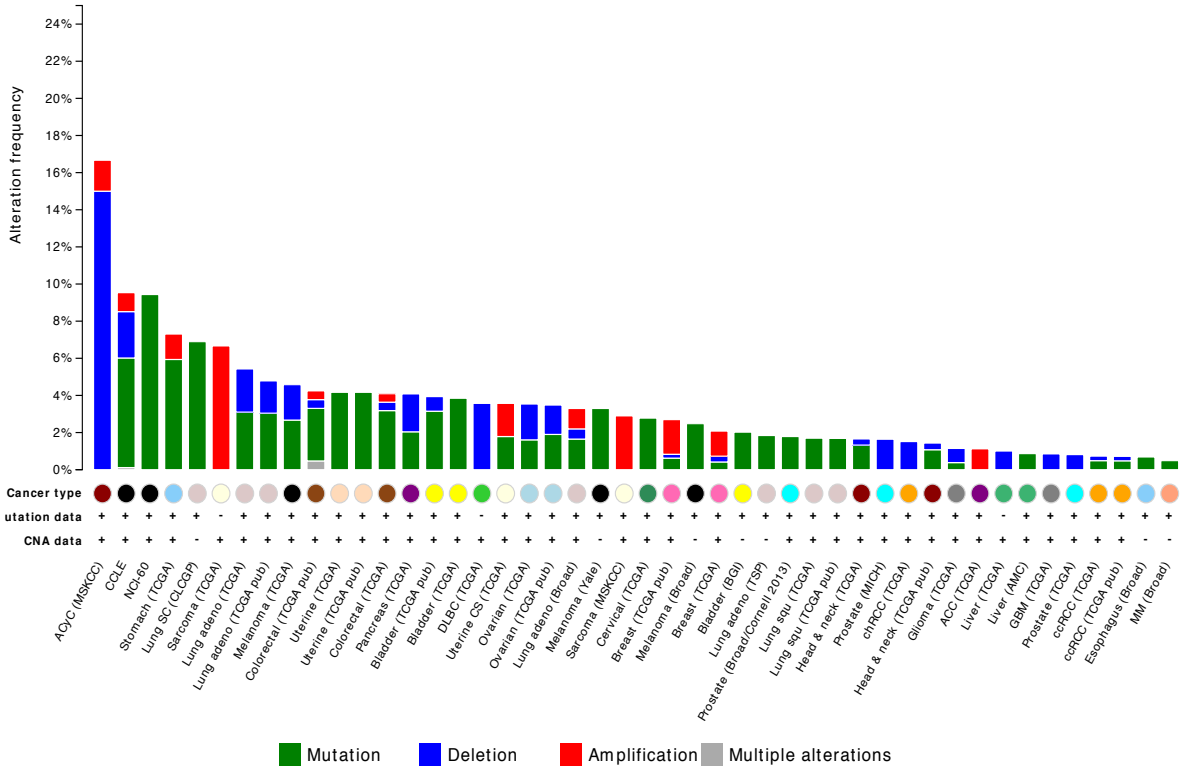

Figure 3.3 LATS1 mutations in cancers

Cross cancer histogram of LATS1 mutations obtained from cBioportal indicating a low frequency of mutations, deletions or amplifications of the LATS1 gene in patients with various cancer types. The graph includes data pooled together from 69 cancer genomics studies, from a total of 17584 cancer patient samples. Gao *et al*. 2013 & Cerami *et al.* 2012.

3.9 YAP1 inhibitors

The complex relationship between CIN and cancer and the possible causal role of the Hippo pathway in CIN induction offer previously unrecognized means to limit tumor growth by pharmacological intervention. Although kinases are effective targets for small molecules, designing inhibitors to restore loss-of-function of kinases has been found to be a challenging task. Functionally, the most attractive targets for pharmacologic intervention with the Hippo pathway are the key proteins YAP and TAZ, which are the final common conduits of the entire pathway. Also, YAP is dispensable for the growth and homeostasis of normal tissues, thus potentially limiting the likelihood of side effects on healthy tissues (79). Since YAP and TAZ are the final downstream effectors, drug resistance achieved by alternative pathways can be, in theory, ruled out. Recent progress in the search for small-molecule Hippo pathway modulators has identified Verteporfin (VP) and Dobutamine (a GPCR-beta adrenergic receptor antagonist) to be specific inhibitors of YAP1. Also, monoclonal antobodies (mAb's) against LAP and SIP (YAP1 activators) has proven to be effective against YAP1 activity. Verteporfin is a benzoporphyrine derivative, a photosensitizer used for photodynamic therapy of macular degradation of the eye. VP disrupts YAP-TEAD transcriptional activation complex formation, hence, inhibiting YAP1 activity (80). The porphyrin ring of VP disrupts the formation of the YAP–TEAD complex by binding to YAP and changing its conformation, thereby blocking the transcription of downstream targets. VP has already been be used as a chemotherapeutic agent for cancer cells overexpressing YAP1 *in vitro* (81).

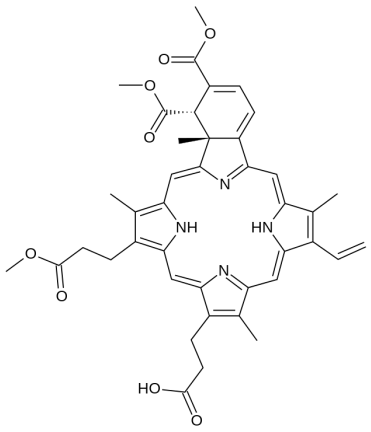

Figure 3.5 Structure of Verteporfin

Verteporfin, a benzoporphyrin derivative, with its porphyrin ring disrupts the YAP-TEAD complex inhibiting its transcriptional activity.

3.10 Glioblastoma and CIN

Gliomas are the most common primary malignant brain tumors in adults. The World Health Organization (WHO) classification distinguishes gliomas into four different grades of which Glioblastoma multiforme (GBM) is the fastest growing malignant type of brain tumor and accounts for about 15 percent of all brain tumors (82). Patients with GBM have a poor prognosis with a median survival of 15 months (83). GBM is know to be highly anaplastic and a morphologically highly heterogeneous tumor (84). Several studies showed that GBM samples harboring mutations of *p53*, or amplification of MDM2, epidermal growth factor receptor *(EGFR)* or mismatch repair (MMR) genes were typically chromosomally instable (85) (86) (87). GBM is also known to be remarkably resistant to chemotherapy and ionizing radiation. Resistance to treatment might be a consequence of CIN/aneuploidy, genetic alterations and intratumor heterogeneity, which are characteristics of these tumors. Understanding the genetic alterations, specific molecular biomarkers and proliferative pathways may promote development of effective therapeutic strategies for the management of GBM patients. Nevertheless, only little is known about patterns or exact mechanisms of CIN in GBM.

3.11 GBM cell lines

NCH149 and NCH82 are two cell lines derived form primary GBM tumors in the lab of Dr. C. Herold-Mende at the Department of Neurosurgery, University Hospital Heidelberg, Germany (88). Cytogenetic analysis of these cell lines revealed extraordinary aneuploidy in NCH149 cells with chromosome numbers ranging from 42 to 129 and a few structural chromosome aberrations were observed namely t(13;17), isochromosome 7q, deletions 11q, 16p, and 18p as well as unbalanced translocations der(13)t(11;13) and der(17)t(17;19), each of which were found in only 2 of 21 metaphase spreads analysed. NCH82 cells were found to have a near tetraploid karyotype and some recurrent unbalanced translocations like der(7)t(7;22) (observed in 14/15 metaphase spreads) and a deletion in the long arm of chromosome 22 (in 15/15 metaphase spreads) were observed (89). This data indicates that NCH149 cells are possibly chromosomally instable while NCH82 cells are stablly tetraploid.

3.12 Aim of this study

Extensive literature evidence has suggested a direct link between CIN and the pathogenesis of various human malignancies. Nevertheless, the underlying molecular mechanisms of CIN development and resulting tumorigenesis remain undefined. Among a collection of primary GBM cultures one sample, the NCH149 cell line showed extensive numerical CIN and resistance against irradiation and cytotoxic agents was identified. With the aim to study the mechanism of massive numerical CIN, a comparative analysis of chromosomally instable (NCH149) and chromosomally stable (NCH82) patient-derived glioblastoma cell lines was performed. Using FISH as well as fluorescence microscopy the extent of CIN and the underlying mechanisms were investigated.

Since it is discussed that mutation-induced aberrations in cellular mechanisms could lead to CIN, the mutation profile of the NCH149 GBM tumor cell line was assessed by whole exome sequencing. This profile was compared to the profile of cells of the associated primary tumor from which the cell line was derived as well as with healthy tissue from the patient. Dependent on the mutations detected in primary tumor and tumor cell line derived thereof, the role of the mutated genes for the development of CIN were investigated by microscopic, cell biological and biochemical techniques.

4 Materials and Methods

4.1 Materials

4.1.1 Biological materials

4.1.1.1 Eukaryotic cell lines

Table 4.: Eukaryotic cell lines

Cell Lines	Description	Source / Reference
Normal Human Astrocytes	Cell line derived from primary astrocytes of a healthy donor. Catalog number: 1800	Sciencell, CA, USA
NCH149	Human Glioblastoma	A. Régnier-Vigouroux, DKFZ, Heidelberg, Germany
NCH82	Human Glioblastoma	A. Régnier-Vigouroux, DKFZ, Heidelberg, Germany
U2OS	Human Osteosarcoma cell line	Ponten and Saksela, 1967, ATCC HTB-96
U2OS-Tet on	Human Osteosarcoma cell line expressing tetracyclin (Tet)-regulated transactivator Tet-On	Life technologies; Invitrogen, Carlsbad, USA

4.1.1.2 Patient material

Paraffin sections and DNA extracts of the parental tumor which was used to establish the NCH149 cell line as well as control brain tissue of the same patient were provided by C. Herold-Mende, University Hospital, Heidelberg (Tissue Bank of the National Center for Tumor Diseases (NCT) in Heidelberg, Germany). This material was used for fluorescence in situ hybridization (FISH) and whole exome sequencing experiments.

4.1.1.3 Bacterial Material

Table 4.1 Bacterial Material

Name	Genotype	Source / Reference
E. coli DH5 alpha	F- ϕ80*lac*ZΔM15 Δ*(lac*ZYA *arg*F) U169*rec*A1*end*A1 *hsd*R17 (rKmK+) *pho*A *sup*E44 *thi*-1*gyr*A96 *rel*A1 λ-	Stratagene, USA

4.1.1.4 Genetic material

4.1.1.4.1 DNA primers

All primers were ordered from Eurofins MWG Operon, Ebersberg, Germany.

Table 4.2: List of Primers used for GATC sequencing, mutagenesis and PCR

Nr.	Name	Use	Sequence (5'-3')
1	LATS1_Mlu1	PCR	AGTCAGCTGACGCGTATGGACTACAAAGA CGATGACGACAAG
2	LATS1_Sal1	PCR	AGAGATATCGTCGACTTAAACATATACTAGA TCGCGATTTTTAATCTCTGAG
3	LATS1_Mut_s	Mutagenesis	AAGAAACAGATTACAACTTCACCTGTTACT GTTAGGAAAAACAAGAAAG
4	LATS1_Mut_as	Mutagenesis	CTTTCTTGTTTTTCCTAACAGTAACAGGTGA AGTTGTAATCTGTTTCTT
5	LATS1_PCR	PCR	ACCGCTTCAAATGTGACTGTGATGCCACCT
6	LATS1_r_PCR	PCR	TCTACTTTTCTTGCTAGACAGACTTCACCA
7	L3	Sanger Sequencing	TGGGCATGAAATCCCTACA

4.1.1.4.2 Expression plasmids

Table 4.4: Expression Plasmids

Vector	Tag (terminus)	Antibiotic Resistance	Source
CMV-LATS1	2XFlag (N)	Ampicillin	Addgene
pTRE2hyg	-	Ampicillin	Clontech

4.1.1.4.3 Expression constructs

Table 4.5: List of expression constructs

Nr.	Name	Description	Primer	Source
1	LATS1-wt-pTRE2hyg	Wild type LATS1 cDNA in pTRE-2Hyg vector	1&2 (Table 2.4)	Produced during this work
2	LATS1-mut-pTRE2hyg	Produced by Mutagenesis of expression construct 1	1&2 (Table 2.4)	Produced during this work

4.1.1.4.4 Centromere probes

All FISH probes were received from Prof. A. Jauch, Department of Human Genetics, University of Heidelberg, Germany.

Table 4.6: Centromere probes used for FISH

Chromosome	Probe Name	Resistance
Chr 1	pUC 1.77	Ampicillin
Chr 2	pBS4D (M. Rocchi)	Ampicillin
Chr 3	pAE0.68 (M. Rocchi)	Ampicillin
Chr 8	pZ8.4	Ampicillin
Chr 17	P17H8	Ampicillin
Chr 20	pZ20 (M. Rocchi)	Ampicillin

4.1.1.4.5 Nucleotides

Table 4.7: Nucleotides and DNA

Name	Source
CY3-dUTP	Dyomics GmbH, Jena, Germany
FITC-dUTP	Dyomics GmbH, Jena, Germany
dNTPs in Lithium salt	Roche Diagnostics, Basel, Switzerland
Salmon Sperm DNA	Sigma Aldrich St. Louis, USA

4.1.1.5 Antibodies

4.1.1.5.1 Primary Antibodies

Table 4.8: List of Primary Antibodies

Antigen	Clone	Immunized species/Typ	Dilution	Fixation for IF	Source
Actin	sc-47778	Mouse (monoclonal)	1:5000	-	Santa Cruz, Dallas, USA
CP110	1278	Rabbit (ploYclonal)	1:200	MeOH/ Ac	Proteintech, Chicago, USA
CREST - Centromere	Z140228 B2	Human	1:20	MeOH	EuroImmun, Germany
IgG mouse	SC-2025	Mouse	1:200	-	Santa Cruz, Dallas, USA
IgG Rabbit	SC-2027	Rabbit	1:200	-	Santa Cruz, Dallas, USA
LATS1	C665B	Rabbit (monoclonal)	1:1000	MeOH/ Ac	Cell Signalling, MA, USA
MCM7	141.2, sc-9966	Mouse (monoclonal)	1:1000	-	Santa Cruz, Dallas, USA
Pericentrin	ab4448	Rabbit (polyclonal)	1:1000	MeOH	Abcam, Cambridge, UK
pYAP1 (S127)	EP1675 Y	Rabbit	1:10000	-	Abcam, Cambridge, UK
YAP1	EP1674 Y	Rabbit	1: 25000	MeOH	Abcam Cambridge, UK
YAP1 (63.7)	Sc-101199	Mouse	1:1000	MeOH	Santa Cruz, Dallas, USA
γ-Tubulin	TU-30	Mouse (monoclonal)	1:1000	MeOH/ Ac	EXBIO, Prag, CZ
α-Tubulin	DM1A	Mouse (monoclonal)	1:500	MeOH/ Ac	Sigma-Aldrich St. Louis, USA

4.1.1.5.2 Secondary Antibodies

Table 4.9: List of Secondary Antibodies

Antigen	Immunized species	Conjugate	Dilution	Source
Anti-MouseHRP	Goat	HRP	1:5000	Santa Cruz, Dallas, USA
Anti- rabbit HRP	Goat	HRP	1:5000	Santa Cruz, Dallas, USA
Mouse IgG	Goat	Alexa 568	1:1000	Invitrogen, Carlsbad, USA

Mouse IgG	Goat	Alexa 488	1:1000	Invitrogen, Carlsbad, USA
Rabbit IgG	Goat	Alexa 568	1:1000	Invitrogen, Carlsbad, USA
Rabbit IgG	Goat	Alexa 488	1:1000	Invitrogen, Carlsbad, USA

4.1.1.6 Enzymes

Table 4.10: List of Enzymes

Name	Source
DNAse	Roche Diagnostics, Basel, Switzerland
E.coli DNA Polymerase I	Roche Diagnostics, Basel, Switzerland
Pepsin	Sigma-Aldrich, Missouri, USA
Phusion High-Fidelity DNA Polymerase	Fermentas/Thermo Fisher Scientific, Waltham, USA
Restriction Endonucleases	New England Biolabs, Ipswich, UK
RNase	Roche Diagnostics, Basel, Switzerland
Shrimp Alkaline Phosphatase	Fermentas/Thermo Fisher Scientific, Waltham, USA
T4 DNA Ligase	New England Biolabs, Ipswich, UK
Lambda phosphatase	New England Biolabs, Ipswich, UK

4.1.2 Molecular weight markers

Table 4.11: Molecular Weight Markers

Name	Source
HighRanger DNA Ladder	Norgen Biotek Corp., Ontario, Canada
Hind III marker	Fermentas Life Science, Waltham, USA
Precision Plus Protein™ Dual Color Standards	Bio-Rad Laboratories, Hercules, USA

4.1.3 Kits

Table 4.12: Kits used in this work

Name	Source
Annexin V FITC v1.0	BD Bioscience, San Jose, USA
CellTiter-Glo® Luminescent Viability Assay	Promega, Madison, USA
Fugene® 6 Transfection Reagent	Promega, Madison, USA
In-Fusion® HD Cloning Kit	Clontech Inc., Mountain View, CA
Midi/Maxi Plasmid Purification Kit	Qiagen, Hilden, Germany
Pierce® ECL Western Blotting Substrate	Thermo Scientific, Waltham, USA
QIAprep® Spin Miniprep Kit	Qiagen, Hilden, Germany
QIAQuick® Gel Extraction Kit	Qiagen, Hilden, Germany
Quick Start™ Bradford Protein Assay	Bio-Rad Laboratories, Hercules, USA
QuikChange XL Mutagenesis Kit	Agilent Technologies, Santa Clara, USA
Vectashield®	Vector Laboratories, Burlingame, USA
Vectashield® with DAPI	Vector Laboratories, Burlingame, USA

4.1.4 Chemicals

The standard chemicals used in this work were purchased from Sigma-Aldrich (St. Louis, USA), Carl Roth GmbH (Karlsruhe, Germany), Merck (Darmstadt, Germany), Roche (Basel, CH), AppliChem (Darmstadt, Germany), Serva (Heidelberg, Germany) and GERBU Biochemicals GmbH (Gaiberg, Germany). Consumables used were purchased from GE Healthcare (Chalfont St Giles, UK), Greiner Bio-One (Kremsmuenster, Austria), Starlab (Hamburg, Germany), Sarstedt (Nuembrecht, Germany), Eppendorf (Hamburg, Germany) and Whatman (Maidstone, UK).

4.1.4.1 Media, buffers and solutions

4.1.4.1.1 Media for Bacterial culture

LB-Medium	1% (w/v) Trypton
	0,5% (w/v) Yeast extract
	1% (w/v) NaCl
	pH 7,2

LB-Agar	LB-Medium 1,5% (w/v) Agar
SOC-Medium	2% (w/v) Trypton 0,5% (w/v) Yeast Extract 0,05% (w/v) NaCl 2,5 mM KCl 10 mM $MgCl_2$ 20 mM Glucose pH 7,0

4.1.4.1.2 Media and solutions for cell culture

DMEM	Gibco®/Invitrogen, Carlsbad, USA
McCoy´s 5A	Gibco®/Invitrogen, Carlsbad, USA
OptiMEM	Gibco®/Invitrogen, Carlsbad, USA
B-Mercaptoethanol	Gibco®/Invitrogen, Carlsbad, USA
PBS/EDTA	2 mM EDTA in PBS
Poly-L-Lysine	Sigma-Aldrich St. Louis, USA
Trypsin/EDTA-Lösung	0,25% (v/v) Pig-trypsin (Gibco®/Invitrogen, Carlsbad, USA) in PBS/EDTA

4.1.4.2 Buffers and reagents

Acrylamide	Acrylamid / Bis 37.5:1 solution (30% w/v) (Serva Electrophoresis, Gremany)
APS	Carl Roth, GmbH, Germany
Blocking buffer for Immunofluorescence	10% Goat serum in PBS
Blocking buffer for Western Blot	5% Bovine serum albumin (BSA) in TBST
Borat Buffer	20 mM boric acid

	1,3 mM EDTA pH 8.8
Dilution Buffer for CoIP	10 mM Tris/HCl, pH 7.5 150 mM NaCl 0.5 mM EDTA 1 Tablet/50 ml Complete Protease inhibitor (Roche, Basel, CH)
Hoechst 33342	Trihydrocloride, trihydrate (Life Technologies)
PBS	137 mM NaCl 2,7 mM KCl 10 mM Na_2HPO_4 1,7 mM KH_2PO_4 pH 7,4
RIPA-Buffer	50 mM Tris/HCl, pH 7,5 150 mM NaCl 0.25 % (w/v) Nadeoxycholate 1 % (v/v) Nonidet P40 1 mM EDTA 1 Tablets/50 ml Complete protease inhibitor (Roche, Basel, CH) 5 Tablets/50 ml PhosSTOP Phosphatase inhibitor (Roche, Basel, Switzerland)
SDS 20%	Dissolved in water to make 20% solution (Roth)
SDS-Running buffer	380 mM glycin 50 mM Tris 0,1% (w/v) SDS
SSC 20x	3M NaCl 0.3M Trisodium citrate pH 7.0
Stop Mix	0.5% Dextran blue 0.1% NaCl 20mM EDTA 20mM Tris pH7.5, in double distilled water

TAE	40 mM Tris/HCl, pH 8,0 0,12% conc. Acetic acid 1 mM EDTA
TEMED	Serva Electrophoresis, Germany
TBS	10 mM Tris/HCl 150 mM NaCl pH 8.0
TBST	0.1% (v/v) Tween 20 in TBS
Transfer buffer 10x	50 mM Tris 40mM Glycine 3.7g SDS (For working solution add 20% of absolute methanol to 1x transfer buffer)
6x DNA-Loading Buffer	200 mM EDTA 100 mM Tris/HCl, pH 7,5 0,01% (w/v) Bromphenol blue 0,01% (w/v) Xylencyanol 30% (v/v) Glycerol
6x SDS-Protein loading buffer	240 mM Tris/HCl, pH 6,8 30% (v/v) β-Mercaptoethanol 6% (w/v) SDS 30% (v/v) Glycerol 0,002% (w/v) Bromphenolblau
Vectashield	Mounting Medium (Linaris GmBH, Germany)

4.1.4.3 Antibiotics

Carbenicillin	Serva, Heidelberg, DE, Final concentration: 100 µg/ml
Geneticin (G418)	PAA Laboratories GmbH (Austria) Final concentration: suited for the cell line
Hygromycin B	Invitrogen, Carlsbad, USA, Final concentration: suited for the cell line

Penicillin/Streptomycin	Gibco®/Invitrogen, Carlsbad, USA, Final concentration: 100 µg/ml
Puromycin	Merck, Darmstadt, DE, Final concentration: suited for the cell line

4.1.4.4 Drugs

Nocodazole	Sigma-Aldrich, Missouri, USA
Thymidine	Sigma-Aldrich, Missouri, USA
Verteporfin	Sigma-Aldrich, Missouri, USA

4.1.4.5 Laboratory equipment

BD Accuri C6 Flow cytometer	Becton Dickinson, San Jose, USA
Centrifuge 5417R	Eppendorf, Hamburg, Germany
Fluorescence microscope Axiovert 200M equipped with AxioCam MRm	Carl Zeiss, Göttingen, Germany
Fluorescence microscope Axioskop equipped with AxioCam MRc	Carl Zeiss, Göttingen, Germany
Axio Observer.Z1, Live cell observer	Carl Zeiss, Göttingen, Germany
Confocal Microscope Leica TCS SP5	Leica, Wetzlar, Germany
Mini-PROTEAN® Tetra Cell	Bio-Rad Laboratories, Hercules, USA
Mini Trans-Blot® Electrophoretic Transfer Cell	Bio-Rad Laboratories, Hercules, USA
PCR-Maschine „Mastercycler gradient“	Eppendorf, Hamburg, Germany
PCR-Maschine „Mastercycler personal“	Eppendorf, Hamburg, Germany
pH-Meter SevenMulti	Mettler Toledo, Giessen, Germany
Photometer	Eppendorf, Hamburg, Germany
Shandon Cytospin III	Thermo electron corporation, Pittsburg, USA
Spectrophotometer “NanoDrop”	PeqLab Biotechnologie,

	Erlangen, Germany
UV Table	Konra Benda, Wiesloch, Germany
Zentrifuge Megafuge 1.0R	Heraeus, Hanau, Germany
Zentrifuge Sorvall RC6Plus	Thermo Scientific, Waltham, USA

4.1.4.6 Software

ApE- A plasmid editor	M. Davis Wayne, Utah, USA
AxioVision Version 4.7.2	Carl Zeiss, Göttingen, Germany
BD Accuri C6	Becton Dickinson, San Jose, USA
ImageJ	Wayne Rasband, USA
Microsoft Office 2010	Microsoft Corporation, Redmond, USA
QuickChange Primer Design	Stratagene, LaJolla, USA

4.2 Methods

4.2.1 Cell biology methods

4.2.1.1 Cell culture

The cell lines listed in Table 4.1 were cultured at 37 °C under 5% CO_2 in tissue culture flasks or dishes. To passage, adherent cells were washed once with PBS/EDTA, trypsin/EDTA was added and the cells were incubated for 2-4 min at 37 °C. The cells were then collected in fresh medium, and seeded into new cell culture flasks or dishes. The following media were used:

Normal Human Astrocytes	HA medium + 10% (v/v) FCS + 1% Pen/Strep
NCH149	DMEM + 10% (v/v) FCS + 1% Pen/Strep
NCH82	DMEM + 10% (v/v) FCS + 1% Pen/Strep
U2OS	DMEM + 10% (v/v) FCS + 1% Pen/Strep

U2OS-Tet on	DMEM + 10% (v/v) FCS + 1% Pen/Strep + 4mM Glutamine + Geneticine (End concentration 200ug/ml)

4.2.1.2 Synchronization of human cell lines

In order to study cell cycle duration and progression, cells were synchronized using one of the following methods:

4.2.1.2.1 Nocodazole

Cells were incubated for about 16 h with 100 ng/ml nocodazole to block asynchronously growing cells in early mitosis. After this incubation, cells were gently washed twice with nocodazole-free medium and mitotic cells were collected by mitotic “shake off”, i.e., strongly tapping the flasks to detach rounded mitotic cells from the bottom. If mitotic cells were needed, these cells were washed (5 minutes, 200 g, RT) and then fixed for FACS (ice cold 100% methanol) or lysates were prepared for Western blot or CoIP experiments (see 4.2.6). To analyze later cell cycle stages, mitotic cells were seeded in medium without nocodazole and incubated for the appropriate time.

4.2.1.2.2 Synchronization by double thymidine block

200,000 cells were seeded in 14 cell culture dishes (60 mm). At the next day the first thymidine block was performed by incubating the cells with medium containing 2 mM thymidine for 16 hours leading to S-phase arrest of the cells. After washing three times with PBS, medium containing 24 uM 2'-deoxycytidine was added to the cells and they were incubated at 37 °C for additional 12 hours. Then, the cells were subjected to the second S-phase arrest by re-addition of 2 mM thymidine containing medium for 12 hours. After washing three times with PBS, 2'-deoxycytidine-containing medium was added to the cells and processed every hour to obtain lysates upto 8 hours.

4.2.1.3 Poly-l-lysine coating

Sterile glass slides and cover slips were coated with poly-l-lysine solution under sterile conditions, incubated for 20 minutes at 37°C and then washed twice with 1x PBS. Coated

slides and coverslips were used for culturing cells in order to enhance the attachment of cells, especially mitotic cells, to glass slides or cover slips.

4.2.2 Immunofluorescence

To stain eukaryotic cells by indirect immunofluorescence, cells were cultured on coverslips. The cells were washed with PBS and fixed in accordance with the requirements of the primary antibodies used for staining (see Table 4.8). For methanol-acetone fixation the cells were incubated with a 1:1 methanol-acetone mixture for 7 minutes and the coverslips were then air dried. For methanol fixation, cells were incubated for 10 minutes with ice-cold 100% methanol followed by air drying. The dried coverslips were stored at -20 °C. After fixation, the cells were blocked for 30 minutes with 10% goat serum in PBS and then incubated with the primary antibody for 1-1.5 hours. The cells were washed 3 times with PBS to remove excess primary antobody and then incubated for 30 minutes with the secondary antibody. Both primary and secondary antibodies were diluted in 10% goat serum in PBS (see Tables 4.8 and 4.9). To stain the nuclei, cells were then incubated with 10 ug/ml Hoechst 33342 in 10% goat serum in PBS and incubated for 5 min. After washing three times with PBS and washing once with ddH_2O, the coverslips were immersed in 100% ethanol, dried on filter paper and coated with Vectashield. The analysis of stained cells was done by fluorescence microscopy.

4.2.3 Flow cytometry

The distribution of cells from a cell population in different cell cycle phases was determined using flow cytometry. For this, cells were collected by trypsinization or mitotic shake off and washed with PBS. Subsequently, the cell pellet was resuspended in 250 ul PBS. The cells were fixed by dropwise addition of 700 ul of 100% ice-cold methanol and vortexing. After incubation at 4°C for at least 1 hour the cells were washed once with PBS and 200 ul of a propidium iodide solution (10 ug/ml propidium iodide + 0.25 mg/ml RNase A in PBS) was added to the cells. Cells were then incubated for 30 min at 37 °C and analyzed by a BD Accuri flow cytometer using C6 software. Since propidium iodide is a DNA intercalating substance, DNA content and the cell cycle stages can be determined.

4.2.4 Live cell imaging

In order to observe the behavior of cells in real time, live cell imaging was performed. For this purpose, cells were seeded in 35 mm dishes (µ-dish, Ibidi, Martinsried) and allowed to adhere for 24 hours. Cells were syncronized overnight (see 4.2.1.2), released and placed into the incubation chamber (37°C and 5% CO_2) of an Axio Observer. To determine the duration of mitosis, bright field images were taken every 10 minutes at various dish positions using a 20x objective.

4.2.5 Protein biochemistry methods

4.2.5.1 Preparation of cell lysates

The preparation of cell lysates was carried out using RIPA buffer. Adherent cells were scraped from the bottom of the cell culture dishes, washed with PBS. Cells were pelleted by centrifugation. The pellet was resuspended in RIPA buffer and incubated on ice for at least 30 minutes. Cell clumps were removed by repeated pipetting up and down or vortexing during the incubation period. The mixture was then subjected to centrifugation for 10 minutes at 18000 g and 4 °C, the supernatant was transferred to a new tube and the protein concentration was determined (see 4.2.5.2.) and analyzed either by SDS-PAGE (see 4.2.5.3.) or used for co-immunoprecipitation (see 4.2.6).

4.2.5.2 Determination of protein concentration

To determine the protein concentration of cell lysates the "Quick START Bradford Protein Assay" was used according to the manufacturers protocol. To create a calibration curve a BSA standard was used.

4.2.5.3 SDS-polyacrylamide gel electrophoresis (SDS-PAGE)

The electrophoretic separation of proteins was performed by SDS polyacrylamide gel electrophoresis under denaturing conditions (90). Gels were prepared with 6-12% acrylamide depending on the size of the proteins to be detected. Cell lysates were mixed with 1x SDS protein loading buffer, boiled for 5 min at 95 °C and 50-100 ug protein was

loaded per well. Separation was performed in the stacking gel at 80 V and in the separating gel at 110-120 V.

4.2.5.4 Western Blot

Proteins separated by SDS-PAGE (see 4.2.5.3.) were transferred to a PVDF membrane (GE Healthcare, Chalfont St Giles, UK) by wet transfer methodology using "Mini Trans-Blot Electrophoretic Transfer Cell". The membrane was activated in 100% methanol for 1 minute, and sandwiched with the gel between 3 layers of filter paper and fiber pads on each side. The protein transfer was performed for 2.5 hours at 4 °C and 450 mA in either borate buffer or methanol transfer buffer. The proteins were then detected by immunodetection (see 4.2.5.5).

4.2.5.5 Immunodetection

For the detection of proteins by means of immunodetection the membrane was blocked for one hour with 5% (w/v) milk powder in 1x TBST at room temperature and then incubated with the primary antibodies overnight at 4 °C with gentle shaking. After three 5 minutes washes with 1 x TBST, the membrane was incubated with secondary antibody for 1 hour at room temperature and then again washed 3 times for 5 minutes each with 1 x TBST. Both primary and secondary antibodies were diluted in 5% (w/v) milk powder or 5% (w/v) BSA in 1 × TBST (see Tables 4.8 and 4.9). Detection was done by treating the membrane with "Pierce ECL Western Blotting Substrates" according to the manufacturer's instructions followed by exposure to X-ray films (Amersham HyperfilmTM ECL, GE Healthcare, Chalfont St Giles, UK). The films were then developed in a dark room.

4.2.6 Co-Immunoprecipitation

To detect protein-protein interactions, co-immunoprecipitation (Co-IP) was performed in which an antibody against the target protein was used. By adding this antibody to whole cell lysates, proteins binding to the target protein or proteins present in the same complex, can be co-immunoprecipitated with the target protein. For this purpose, cell lysates were prepared (see 4.2.5.1.) and diluted with 500 ul of dilution buffer. For the co-immunoprecipitation of endogenous proteins the antibodies were bound to protein A/G agarose beads. For this, 25 µl of each, protein A and protein G agarose beads (Roche, Basel, Switzerland), were mixed and washed three times with 500 µl dilution buffer

(centrifugation at 500 g, 4 °C for 5 min) and incubated with 1 µg antibody for one hour under constant rotation at 4 °C. The IgG antibodies are used as control. The cell lysates were incubated with the antibody-coupled agarose beads overnight at 4 °C with continuous rotation. The agarose were again washed three times with dilution buffer, mixed with 2x SDS protein loading buffer and boiled for 10 minutes at 95 °C. The analysis was performed by SDS-PAGE (see 4.2.5.3.), Western blot (see 4.2.5.4.) and immunodetection (see 4.2.5.5.).

4.2.7 Molecular Biology Methods

4.2.7.1 PCR

Polymerase chain reaction (PCR) was performed to enzymatically amplify specific DNA sequences using suitable primers (Table 4.3) (91). To this end, a PCR approach was established, as follows:

CloneAmp HiFi PCR Premix	10 µl
Forward primer (100pmol/µl)	1 µl
Reverse primer (100pmol/µl)	1 µl
dNTP mix (10 mM each)	1 µl
Template DNA	10 ng
Nuclease free water	make up to 50 µl

The PCR program was set as follows; denaturation, annealing and elongation were repeated for 35 cycles:

Initial denaturation of DNA	98 °C	10 s
Denaturation and Annealing	55 °C	15 s
Elongation	72 °C	5 s per kb of template

The PCR product was treated with DpnI enzyme in Super Cut buffer for 1 hour at 37 °C to remove the template DNA, followed by heat treatment at 80 °C for 15 minutes to inactivate the enzyme. The purification of amplified DNA fragments was carried out using the "QIAQuick Gel Extraction Kit" according to the manufacturer's protocol.

4.2.7.2 Agarose gel electrophoresis

DNA fragments were separated according to their size using agarose gel electrophoresis. The DNA samples were mixed with 1x DNA loading buffer and loaded on to 1% agarose gels containing ethidium bromide (0.1 µl/ml of a 1% ethidium bromide solution). The electrophoresis was carried out in 1x TAE buffer for 1 hour at 120 V.

4.2.7.3 DNA digestion by restriction endonucleases

Plasmid DNA was cut by type II restriction endonucleases at specific sites. Two batches of 50 ul reactions were prepared containing the following components:

10x reaction buffer	5 µl
Restriction enzymes	20 U per enzyme
Purified PCR fragment or plasmid DNA	5 ng / 5 µg
nuclease-free water	make up to 50 µl

The mixtures were incubated for 1-3 h at 37 °C. The linearized plasmid DNA was dephosphorylated by the addition of 1 U "Shrimp Alkaline Phosphatase" for 30 min at 37 °C. Purification of cleaved DNA was performed by "QIAQuick Gel Extraction Kit" according to the maufacturer's protocol.

4.2.7.4 Ligation

After determination of the concentration of the PCR amplified DNA and the target plasmid, the ligation was carried out using the manufacturer's protocol (In-Fusion HD Cloning Kit). Ligation mixture was prepared along with negative control (without PCR amplified DNA) as follows:

5x HD enzyme mix	2 µl
Vector (54 ng)	2 µl
PCR amplified DNA (50 ng)	4 µl
Nuclease free water	2 µl (to make up to 10 µl)

The ligation was performed for 15 minutes at 50 °C.

4.2.7.5 Transformation of chemically competent bacteria

To transform chemically competent bacteria (see Table 4.2), 50 ul of competent bacteria provided with the In-Fusion HD Cloning Kit were thawed and incubated with 2.5 ul of ligation mixture for 30 minutes on ice. This was followed by a heat shock for 45 s at 42 °C. After incubation for 2 minutes on ice, 500 ul of SOC medium was added and the bacteria were allowed to grow for 1 hour at 37 °C while shaking. Then, bacteria were centrifuged (5 minutes, 1300 g), resuspended in 100 ul of SOC medium and streaked on LB plates containing the respective antibiotic. Incubation was carried out overnight at 37 °C.

4.2.7.6 Mutagenesis

Site-directed mutagenesis was carried out using mutagenesis primers listed in Table 4.3 and the "QuikChange II XL Site-Directed Mutagenesis Kit" according to the manufacturer's instructions. The mutagenesis was performed using the following PCR program. Denaturation, annealing and elongation were repeated for 35 cycles:

Initial denaturation	95°C	2mins
Denaturation	95°C	20 s
Annealing	60°C	10 s
Elongation	68°C	30 s per kb
Final Elongation	68°C	5 mins

The PCR product obtained was treated with Dpn I enzyme and transformed into chemically competent bacteria (see 4.2.7.5). These bacteria were plated on ampicillin agar plates and resistant colonies were picked. The DNA was extracted using miniprep kit (see 4.2.7.7) and the presence of the mutation was verified by sequencing (GATC Biotech AG, Konstanz, Germany).

4.2.7.7 Plasmid isolation

For the extraction of plasmid DNA, single colonies were picked and placed in 2 ml LB medium containing the appropriate antibiotic and incubated overnight at 37 °C while shaking. The next day, plasmid DNA was purified using the "QIAprep Spin Miniprep Kit" according to manufacturer's instructions. Verification of successful cloning was carried out by sequencing (GATC Biotech AG, Konstanz, Germany). For purification of larger amounts of plasmid DNA, the positive clones were expanded into 100 ml of LB medium with

antibiotic and subsequent DNA purification by the "Midi/Maxi Plasmid Purification Kit" according to the manufacturer's protocol.

4.2.8 Transfection of human cell lines

4.2.8.1 Transient transfection

To study phenotypes after overexpression of a protein, plasmid DNA was transfected into human cells. For transfection of plasmid DNA Fugene 6 was used according to the manufacturer's instructions. The ratio of transfection reagent (µl): plasmid (µg) used was either 3:1. The cells were seeded one day before transfection so that 60% confluency was attained on the day of transfection.

4.2.8.2 Stable transfection

For the preparation of stably transfected cell lines, the cells were transfected with the appropriate expression construct (Table 4.5) and incubated at 5% CO_2 for 48 hours at 37 °C. For selection and isolation of the transfected cells, these were re-plated at various dilutions in larger cell culture dishes and the antibiotic whose resistance gene was included in the plasmid DNA, was added to the culture medium. The cells were cultured for two to three weeks and the medium with antibiotic was changed every two days. During this selection period, single colonies were scraped off carefully using a pipette tip and put into a 24-well plate, seeding only one colony per well. The cells were expanded and the success of the stable transfection was determined by indirect immunofluorescence (see 4.2.2) and Western blotting (see 4.2.5).

4.2.9 Cytogenetic methods

4.2.9.1 Multicolour FISH and karyotyping

Multiplex fluorescence in situ hybridization (M-FISH) on fixed metaphase spreads of the GBM cell lines NCH82 and NCH149 were carried out as described (92). For this, DOP-PCR amplified probe pools were labeled in combination with seven different fluorochromes (DEAC, FITC, Cy3, Cy3.5, Cy5, Cy5.5, and Cy7) and hybridized together in the presence of cot-1 DNA. Twenty-one metaphase spreads were captured using a DM RXA

epifluorescence microscope (Leica Microsystems, Bensheim, Germany) equipped with a Sensys CCD camera (Photometrics, Tucson, AZ, USA). Images were processed on the basis of the Leica MCK software (Leica Microsystems Imaging solutions, Cambridge, UK) and presented as multicolor karyograms. These experiments were performed by Brigitte Scholer in the laboratory of Prof. A Jauch, Department of Human Genetics, University of Heidelberg.

4.2.9.2 Interphase FISH

Two color FISH experiments were carried out according to previously reported standard protocols (93) using repetitive DNA probe sets for the centromeric regions of chromosomes (see Table 4.6) and atleast 300 nuclei per experiment were analyzed for each chromosome.

4.2.9.2.1 Nick translation

For direct labeling of centromere repetitive probes, a nick translation reaction was performed as follows:

B-mercaptoethanol	5 µl
NT-Buffer (10x)	5 µl
dNTP mix (mM)	5 µl
Probe DNA	1 µg
dUTP (Spectrum green/orange)	1 µl
DNAse 1mg/ml (1:50 in water)	3 µl
DNA polymerase (50 U/µl)	1 µl
Nuclease free water	up to 50 µl

The reaction mixture was incubated for 90 minutes at 15 °C. A stop mix was added to the tubes to block the polymerase and stop the reaction. The size of the probes was checked by agarose gel electrophoresis (see 4.2.7.2) using Hind III marker as molecular weight marker.

4.2.9.2.2 Precipitation of probes and preparation of the hybridization mix

The labeled probes were precipitated by spinning at 10000 g for 30 minutes at 4 °C. To make the hybridization mix ready to use, the pellet was re-suspended in 6.5 ul of deionized formamide by shaking at 37 °C followed by addition of 3.5 ul of 20% dextran sulphate.

4.2.9.2.3 Hybridization

The desired cells were collected, washed, put on glass slides using a cytospin centrifuge (400 g, 5 minutes) and fixed using methanol-acetic acid (3:1). The slides were be stored at -20 °C up to several days. For hybridization, the slides were equilibrated briefly in a coplin jar with 2x SSC at 37 °C. Then, the slides were incubated for 1 hour with 100 mg/ml (1:200 ul 2x SSC) RNase in a moist chamber at 37 °C. Slides were washed three times with 2x SSC for 5 minutes and then treated with pepsin HCL working solution in a coplin jar for 12 minutes. The slides were subsequently washed with 1x PBS and fixed with 1% formaldehyde at RT for 10 minutes under a fume hood. For denaturation, the slides were immersed in 70%, 90% and 100% ethanol sequentially for 3 minutes each. For hybridization, 3 µl of hybridization mix (see 4.2.9.2.2) was added to each cytospin and covered with a coverslip. Then, slides were placed in a metal box and incubated in a water bath for 5 minutes at 75 °C. The coverslips were sealed to prevent them from drying and incubated overnight at 37 °C. At the next morning coverslips were removed and the slides were washed twice with 0.2x SSC and once with 4x SSC/1% Tween 20. DAPI was added to the cytospins to stain the DNA and cells were mounted using Anti-Fade. Analysis was performed using fluorescence microscopy.

4.2.10 Whole exome sequencing

Dr. Balca Mardin, a member of Jan Korbel's group (Genome biology) at EMBL, Heidelberg, Germany performed whole exome sequencing of the NCH149 cell line as well as of the control and tumor DNA from the patient of whom the cell line was established.

4.2.11 Sanger sequencing

LATS1 mutation in genomic DNA of cell lines were confirmed by Sanger sequencing. For this, mRNA was isolated and cDNA was synthesized followed by PCR amplification of LATS1 mutation containing region using the primers 5 and 6 in table 4.3. The PCR products along with primer 7 (table 4.3) were then sent for Sanger sequencing to GATC.

4.2.12 Viability assay

Viability assay was performed to calculate the number of viable cells in culture with and with out verteporfin treatment. For this assay, the cells were seeded in 6-well plates (1x10E6 cells per well) and allowed to adhere over night. The next day, desired concentrations of the drug to be analyzed were prepared and added to the cells. At desired time points after addition of the drug, cells were harvested and the number of live cells were counted.

4.2.13 Annexin staining

FITC Annexin V is used to quantitatively determine the percentage of cells within a population that are undergoing apoptosis. Annexin V is a calcium-dependent phospholipid-binding protein that has a high affinity for phosphatidylserine (PS), which is found exposed in apoptotic cells. Propidium Iodide (PI) is a standard flow cytometric viability probe and is used to distinguish viable from nonviable cells. Viable cells with intact membranes exclude PI, whereas the membranes of dead and damaged cells are permeable to PI. Cells that stain positive for FITC Annexin V and negative for PI are currently undergoing apoptosis. Cells that stain positive for both FITC Annexin V and PI are either in the end stages of apoptosis, are undergoing necrosis, or are already dead. Cells that stain negative for both FITC Annexin V and PI are alive and not undergoing measurable apoptosis. Treated and untreated cells were harvested, washed twice with ice cold PBS and then resuspend in 1× binding buffer at a concentration of 1×10^6 cells/ml). Then 100 µl of this solution (1×10^5 cells) was transfered to a 5 ml culture tube followed by addition of 5 µl of FITC Annexin V and 10 µl PI, vortexed and incubated for 15 minutes at 25 °C in the dark. Unstained and single stained controls for each sample were also prepared for flow cytometric analysis. Flow cytometric analysis was performed using a BD Accuri flow cytometer and analysed using B6 software.

4.2.14 Statistical Analysis

All results are presented as mean ± standard deviation (SD). Differences between experimental groups were analyzed by unpaired Student's t-test for unpaired groups and values of $p < 0.05$ were considered as statistically significant. The asterisks represent significantly different values. *: $p<0.05$; **: $p<0.01$; ***: $p<0.001$.

5 Results

5.1 Identification of CIN in glioblastoma cell lines

5.1.1 Karyoptypic profiling of NCH149 and NCH82 cell

Cellular genome integrity at the chromosomal level is reflected through cellular ploidy levels and intercellular heterogeneity. In order to characterize genome integrity of the two glioblastoma (GBM) cell lines NCH149 and NCH82, cytogenetic analysis was performed in the laboratory of Prof. Dr. Anna Jauch using multiplex FISH (M-FISH; Figure 5.1) as well as classical karyotyping. By M-FISH analysis both numerical and structural chromosomal aberrations were observed in these cell lines. Metaphase spreads of the NCH149 cell line (n=21) revealed that these cells display extraordinary CIN with a variety of clones having different metaphase chromosome numbers ranging from 42 to 129. In contrast to NCH149 cells, the chromosome number of NCH82 cells has been almost equal within the metaphases analyzed showing a tetraploid karyotype in 15 evaluated metaphases. This was indicative for a more stable karyotype of NCH82 cells compared to NCH149 cells as observed by Dokic *et. al.* 2014.

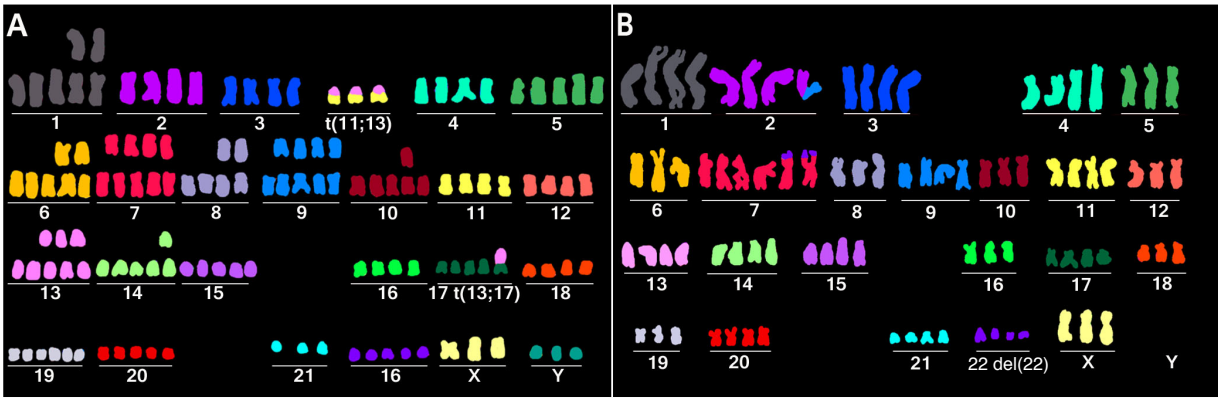

Figure 5.1 M-FISH karyoptypes of GBM cell lines

M-FISH images of NCH149 (A) showing extreme aneuploidy and NCH82 (B) showing a near tetraploid karyotype. Modified from Dokic *et. al.* International Journal of Radiation Biology, 2014, with permission.

5.1.2 Confirming CIN in NCH149 cells

In order to verify the M-FISH data I performed interphase-FISH for chromosomes 2 and 20 and at least 300 interphase cells were scored for each chromosome by Dr. Tilmann Bochtler. Analyzing considerably more cells as compared to M-FISH analysis allowed to ensure that NCH82 have a more stable karyotype than NCH149 cells. As expected, high intercellular variation in chromosome number was observed in NCH149 cells. Quantification showed that up to 10 copies of the analyzed chromosomes were present in single cells. In addition, grouping the cells according to the chromosome number revealed that each group does not comprise of more than 25% of the cells indicating the presence of CIN (Figure 5.2A). In contrast, In contrast, NCH82 cells were found to have a stable tetraploid karyotype with little intercellular variation. In the NCH82 cell line 68% and 79% of cells were tetraploid for chromosme 2 and 20, respectively, and the rest mainly diploid meaning that a major fraction of the cells were tetraploid at least for these two chromosomes but not chromosomaly instable (Figure 5.2 B).Together this shows that, although both cell lines harbor numerically aberrant karyotypes, NCH82 cells have a stable near tetraploid karyotype while NCH149 cells are chromosomally instable.

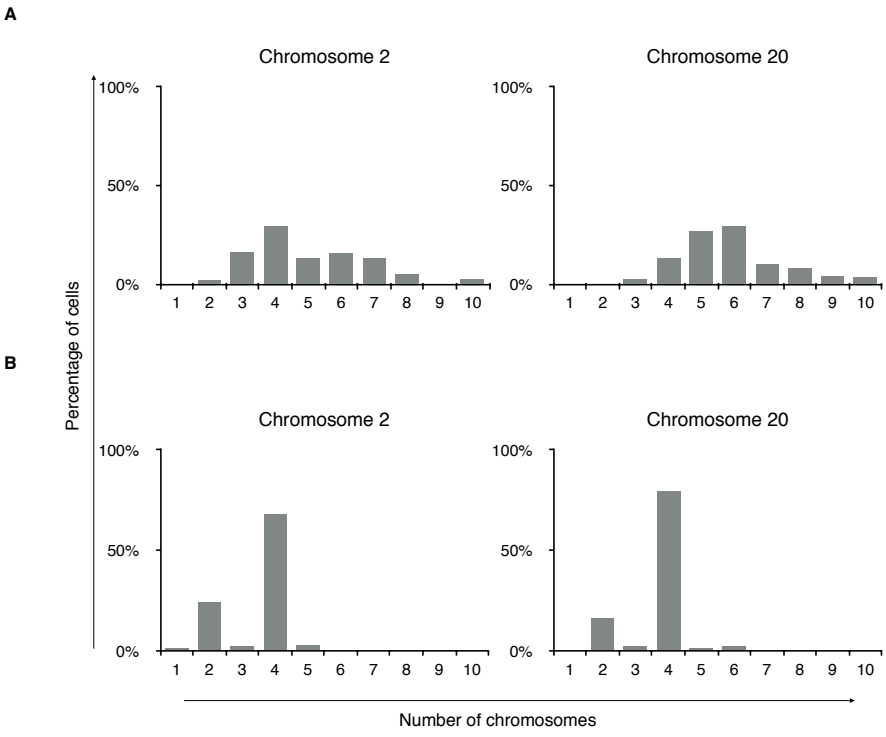

Figure 5.2 Interphase FISH score for chromosmes 2 and 20

Interphase FISH with centromere probes for chromosmes 2 and 20 of the NCH149 cell line showing excessive cell-to-cell variation in chromosome numbers (A). NCH82 cells seem to have a major tetraploid subclone and a minor subclone which is diploid for chromosomes 2 and 20 (B).

5.2 CIN phenotype of NCH149 cells

Next, I studied the phenotype of NCH149 cells using immunofluorescence microscopy and live cell imaging. To further assess the CIN phenotype, we performed immunofluoresence and live cell imging experiments to evaluate parameters such as presence of micronuclei, lagging chromosmes, centriole amplification and aberrant mitosis that indicate extent of CIN in the NCH149 cell line compared to the NCH82 cell line with out CIN.

5.2.1 Presence of micronuclei

Firstly, the two cell lines were stained for DNA (Hoechst) and centromeres (CREST) to check for the presence of micronuclei (Figure 5.3). For each cell line 300 cells were counted in 3 independent experiments. Upon microscopic analysis it was found that 25 ± 1% (mean ± SD) of NCH149 cells show micronucleus formation. On the other hand, only 2% ± 1% (mean ± SD) of NCH82 cells harbor micronuclei ($p < 0.001$) (Figure 5.3).

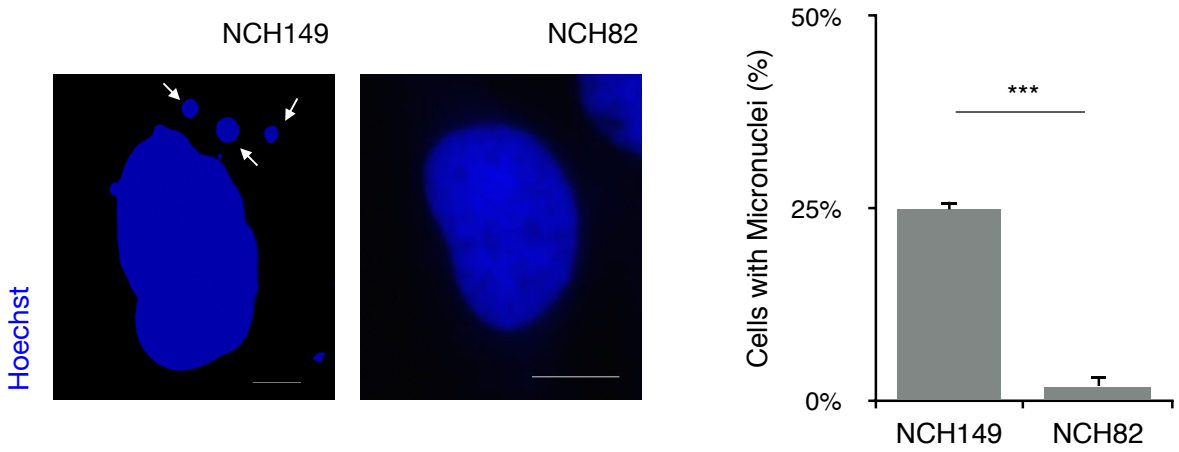

Figure 5.3 Extensive micronucleus formation in NCH149 cells

NCH149 and NCH82 cells were stained with DNA dye, Hoechst (blue) and scored for micronuclei (indicated by arrows) by fluoresence microscopy showing that NCH149 cells, in contrast to NCH82 cells, possess micronuclei. Scale bar, 10 µm.

5.2.2 Occurrence of whole chromosomes in micronuclei

Further, to determine the contents of micronuclei I stained the NCH149 cells with the nuclear lamina marker lamin A in this experiment to investigate whether the DNA is surrounded by a nuclear envelop. In addition I again used the CREST-antibody against centromeres. The presence of a CREST signal in micronuclei indicates the presence of whole chromosomes. Quantification of 300 cells in 3 independent experiments revealed that amongst the cells containing micronuclei, 75.15 ± 2.7% (mean ± SD) of micronuclei harbor 1 or 2 centromere (CREST) signals in NCH149 cells (Figure 5.4). Incontrast, in NCH82 cells, however, had only 1.33 ± 0.5% (mean ± SD) of micronuclei with CREST signals ($p < 0.001$). This suggests that NCH149 cells missegregate whole chromosomes at significantly higher rates as compared to the NCH82 cell line.

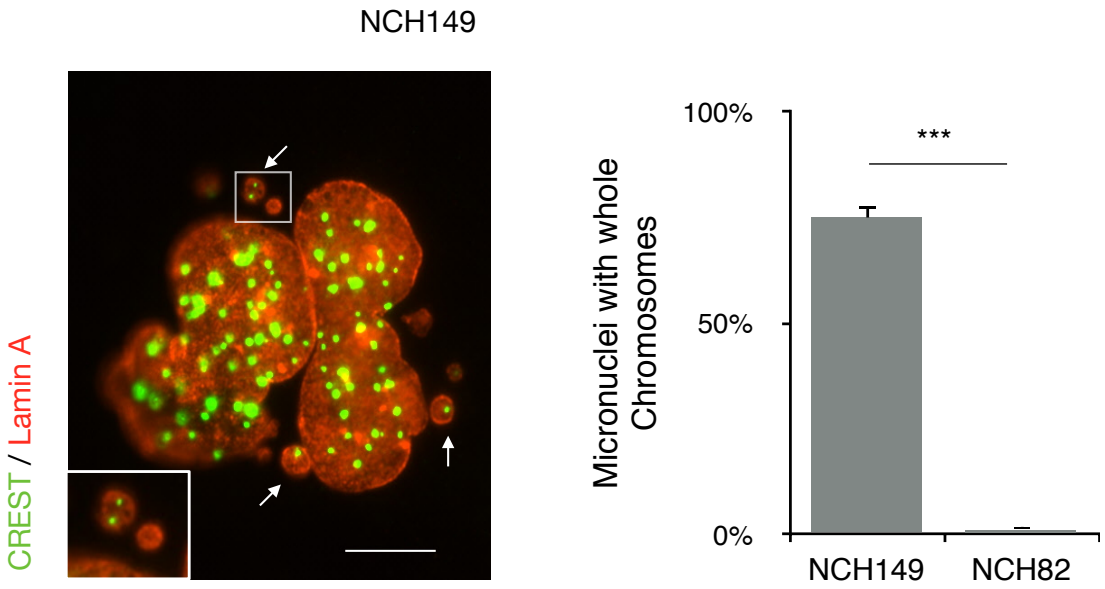

Figure 5.4 Presence of whole chromorsomes in micronuclei of NCH149 cells

Immunofluoresence staining of NCH149 cells with an antibody to lamin A (red) and CREST antibodies (green). Most of micronuclei in NCH149 cells were found to contain one or more CREST signals confirming the presence of whole chromosomes (indicated by arrows). Inset shows micrunucleus with and without CREST signal. Scale bar, 10 µm.

5.2.3 Chromosome missegregation in NCH149 cells

It has been shown that micronucleus formation occurs due to missegregation of chromosomes during late mitosis leading to lagging chromosomes resulting in aneuploidy and chromosomal instability (94). Hence, we further analysed mitotic missegregation of chromosomes in NCH149 and NCH82 cell lines. For this, we synchronized the cells by thymidine block and collected mitotic cells by fixing after release (see 4.2.1.2.2). Mitotic cells were stained with CREST antibodies and an antibody to α-tubulin and 100 mitotic cells were scored and quantified from 3 different experiments. Interestingly, in 30 ± 2.2% (mean ± SD) of mitotic NCH149 cells lagging chromosomes were found (Figure 5.5). In NCH82 cells only very few cells 0.6 ± 0.57% (mean ± SD) containing lagging chromosomes are observed ($p < 0.001$).

The lagging chromosome score correlates with the micronuclei score in both the cell lines (see 5.2.1). This suggests that the presence of micronuclei is indeed a result of chromosomal missegregation events which is more pronounced in NCH149 cells when compared to NCH82 cells.

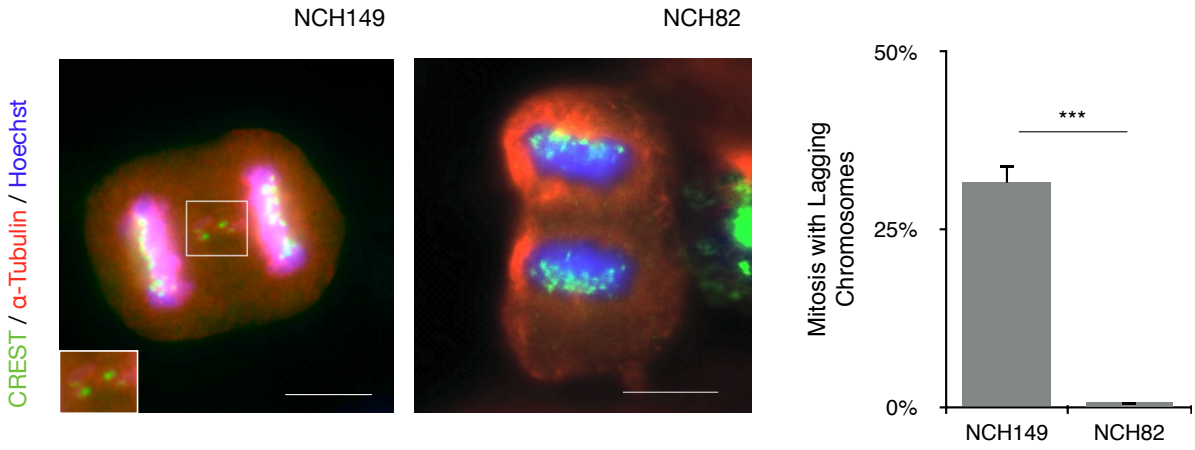

Figure 5.5 Chromosomal missegregation

Scoring mitotic cells immunostained with α-tubulin (red) and CREST (green) antibodies as well as Hoechst (blue) showed lagging chromosomes in 30% of mitotic NCH149 cells. In NCH82 <1% of mitotc cells showed lagging chromosomes. Scale bar, 10 µm.

5.2.4 Centriole amplification

CIN is often associated with and caused by amplified centrosomes/centrioles. Therefore, we next determined the centriole content of NCH149 as well as NCH82 cells by immunostaining with antibodies against the centriolar proteins centrin and CP110. Counting both centrin and CP110 signals in 100 interphase cells in 3 independent experiments revealed that 44.3 ± 2.36 % of NCH149 cells possess supernumerary centrioles while this is true for only 8 ± 0.82 % (mean ± SD) of NCH82 cells ($p < 0.001$) (Figure 5.6). Both immunostaining and analysis were performed by Anna Cazzola.

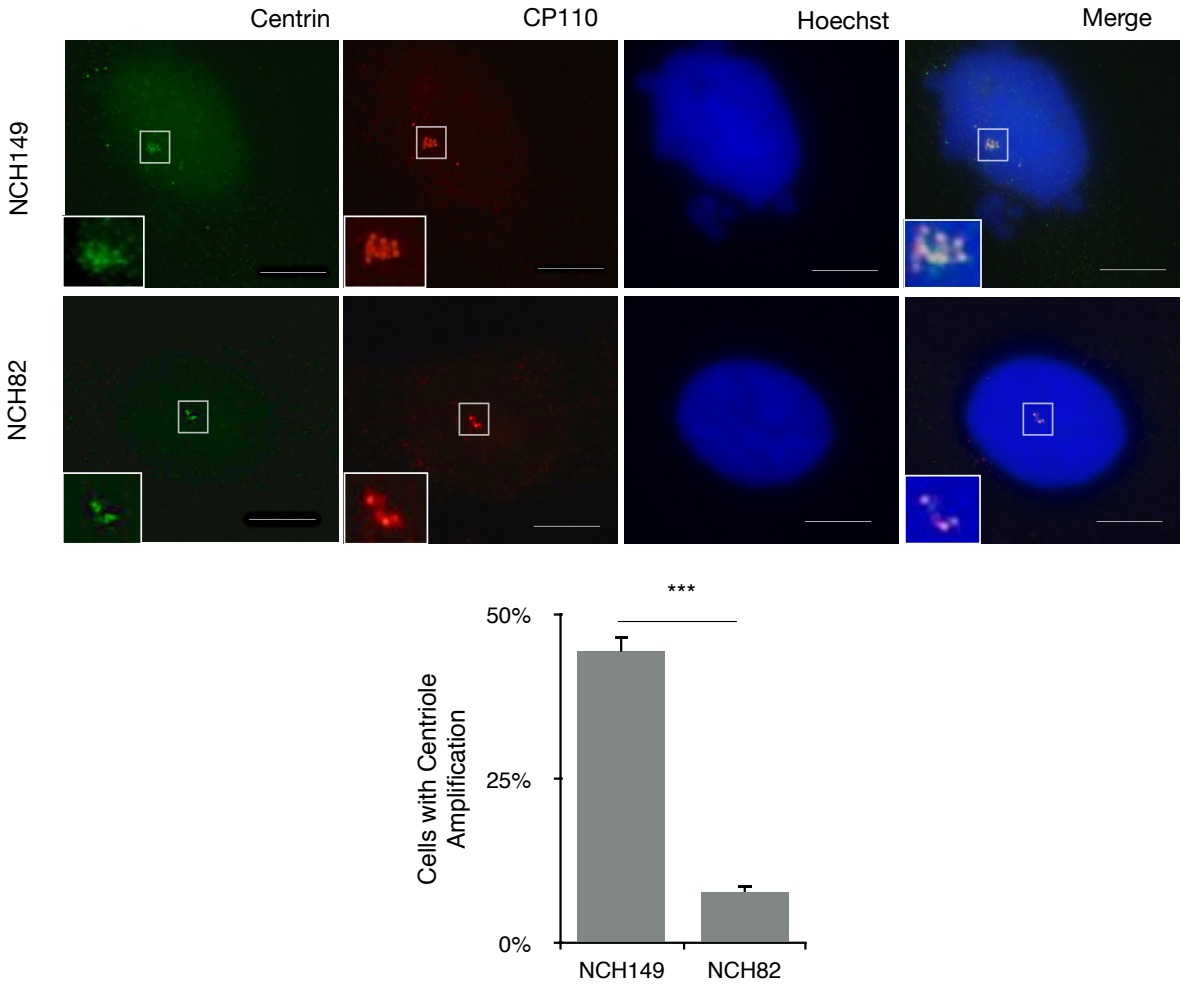

Figure 5.6 Centriole amplification in NCH149 cells

Cells were stained with antibodies to centrin (green) and CP110 (red) and Hoechst. Cells with > 4 centrin signals were considered to have centriole amplification. Centriole amplification was observed in 44.3 % of NCH149 cells whereas NCH82 cells show amplified centrioles in only 8% of the cells. Scale bar, 10 µm.

5.2.5 Mitotic phenotype

Aberrant multipolar mitoses or evasion from cytokinesis after nuclear division is one of the main mechanisms leading to aneuploidy or CIN especially in the presence of supernumerary centrosomes. Often in cancer cells the extra chromosomes cluster together to force the cell into pseudo-bipolar division. However, despite clustering, extra centrosomes prolong mitosis by delaying the satisfaction of the SAC due to merotelic attachment of kinetochores to microtubules. To investigate the mitotic phenotype of NCH149 and NCH82 cells immunofluorescence microscopy and live cell imaging techniques were used.

For immunofluorescence microsopy mitotic cells were stained with the centrosomal marker pericentrin (PCNT) and α-tubulin to visualise mitotic spindles. Given the aberrant number of centrioles, the majority of NCH149 cells surprisingly undergoes bipolar mitosis. Only less than 1 of 100 mitoses scored in three independent experiments show abnormal multipolar divisions (Figure 5.7A). Also most of the NCH82 cells also undergo bipolar division.

Further, to analyse the duration of mitosis of NCH149 and NCH82 cells I performed live cell imaging. The duration of mitosis was calculated from cell rounding to cytokinesis; n=300; (Figure 5.7B). 79% of NCH149 underwent mitosis within 80 minutes compared to 75% of NCH82 cells within 40 minutes indicating prolonged mitosis duration in NCH149 cells. In addition to the prolonged mitosis, 13 % of mitotic NCH149 cells failed to undergo cytokinesis after nuclear division during the 24 hours of observation period.

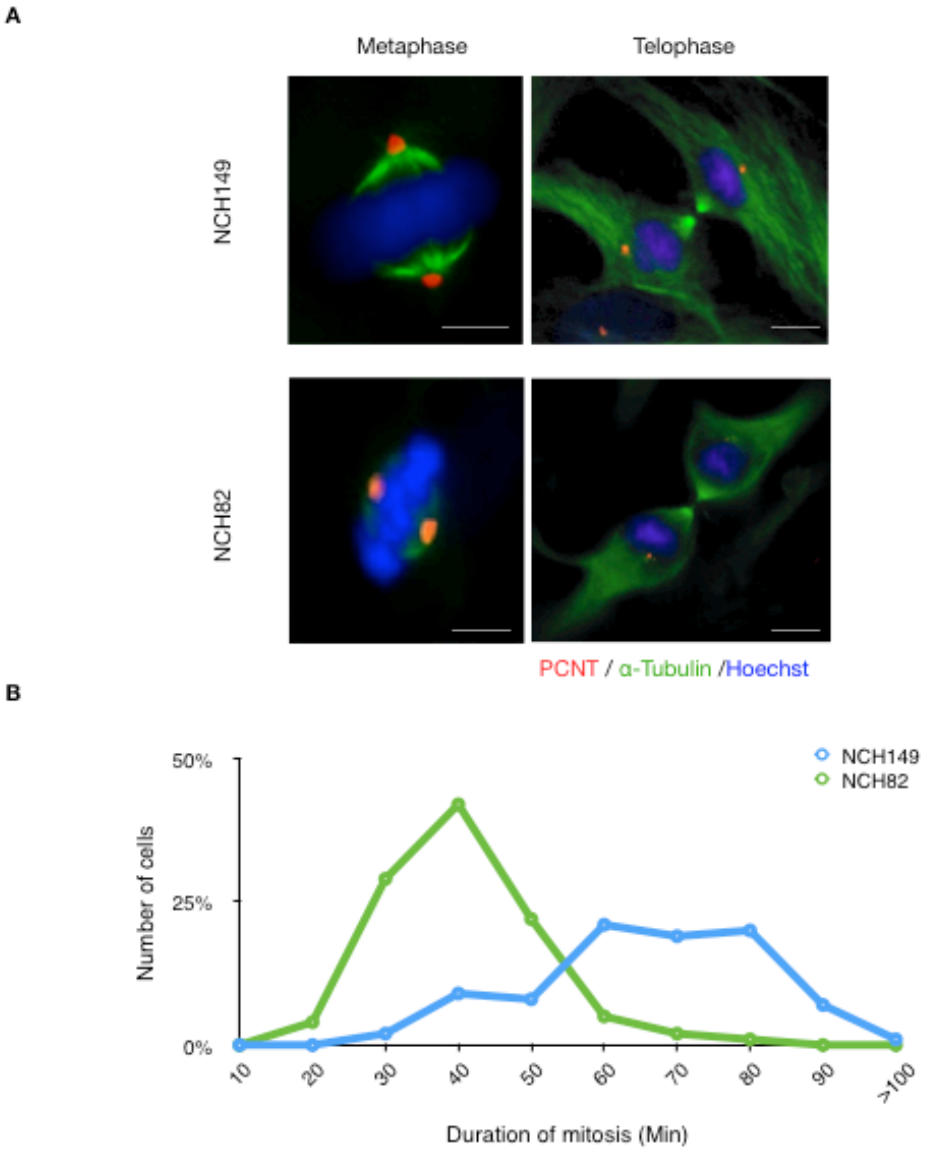

Figure 5.7 Mitotic phenotype

(A) Immunofluorescence staining of NCH149 and NCH82 cells with antibodies against pericentrin (PCNT) (red), α-tubulin (green) and Hoechst shows normal bipolar mitosis in both cell lines. Scale bar, 10 µm. (B) Duration of mitosis from cell rounding to cytokinesis was calculated from live cell imaging data (n=300).

Together, these results demonstrate that NCH149 cells missegregate whole chromosomes at a high frequency indicated by the presence of whole chromosomes in micronuclei, centriole amplification and prolonged mitosis, pointing towards a CIN phenotype of NCH149 cells. On the other hand NCH82 cells have a stable aneuploid/tetraploid karyotype as they show minimal chromosomal missegregation, centriole amplification and normal mitotic phenotype.

5.3 Mutation profile of NCH149 cells

To gain insight into the cause of the CIN phenotype of NCH149 cells we performed whole exome sequencing of the NCH149 cell line as well as the primary tumor from which the cell line was derived, compared to healthy brain tissue (control) of the same patient. Sequencing and data analysis was performed by Dr. Balca Mardin form the Korbel group, EMBL, Heidleberg.

5.3.1 Whole exome sequencing

The read depth plots show massive gains and losses of chromosomes in tumor tissue and the cell line derived thereof when compared to control tissue supporting the finding of extensive aneuploidy in NCH149 cells (Figure 5.8).

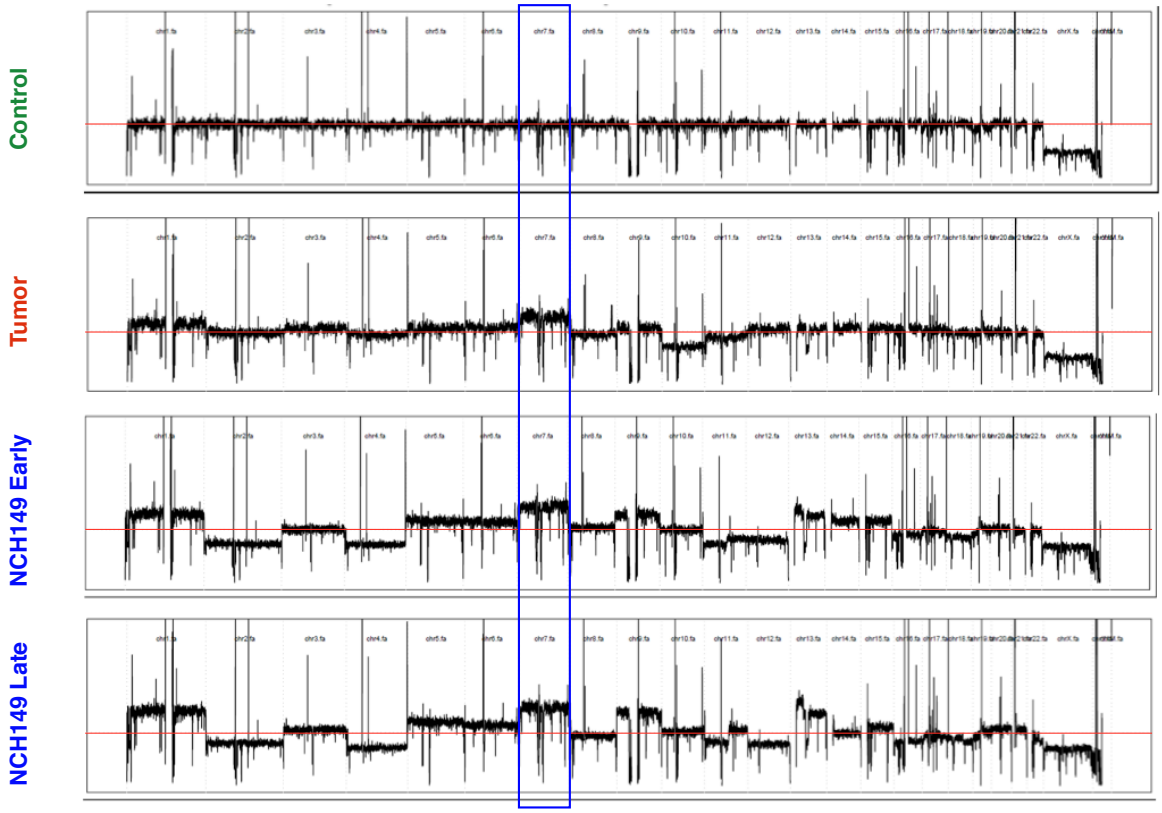

Figure 5.8 Read Deapth plots

Comparative read depth plots of all chromosoms for control, tumor as well as early and late passage of the cell line. The red line indicates normal 2n number of chromosmes, copy number gains or losses are shown as a shift above or below the red line, respectively. An example for a whole chromosome gain of chromosome 7 is highlighted in the blue box.

5.3.2 Mutations in NCH149 cells

Besides gains or losses of whole chromosomes, the whole exome sequencing also led to the identification of 24 novel, non-synonymous mutations, found in the primary tumor and the derived cell line NCH149 but not in the control healthy brain tissue (Table 5.1).

Table 5.1 List of Mutant genes in NCH149

Gene	Mutations	Zygosity
ALPK1	exon4:c.184G>A:p.V62M	Heterozygous
C6orf118	exon2:c.158G>A:p.R53Q	Heterozygous
DLGAP3	exon9:c.2618C>T:p.A873V	Heterozygous
DOCK11	exon27:c.2885G>T:p.W962L	Homozygous
DFNB31	exon3:c.863G>A:p.R288Q	Heterozygous
DYRK2	exon3:c.586G>T:p.G196C	Heterozygous
EPHB3	exon4:c.879G>C:p.K293N	Heterozygous
GIPC1	exon3:c.170G>T:p.R57L	Heterozygous
KCNJ12, 18	exon3:c.242G>A:p.R81Q	Heterozygous
KHNYN	exon3:c.1262A>C:p.Q421P	Heterozygous
LAMA5	exon69:c.9385G>A:p.G3129S	Heterozygous
LATS1	exon4:c.1843A>G:p.I615V	Heterozygous
LASS3	exon12:c.860C>T:p.T287M	Heterozygous
LILRA3	exon5:c.557C>T:p.A186V exon5:c.749C>T:p.A250V	Heterozygous Heterozygous
LRP2	exon27:c.4493C>T:p.T1498M	Heterozygous
MUC6	exon31:c.4711C>A:p.P1571T	Heterozygous
MMP1	exon7:c.911G>A:p.R304H	Homozygous
OR52K1	exon1:c.59C>G:p.P20R	Homozygous
PIK3R1	exon10:c.1126G>A:p.G376R	Heterozygous
PUM1	exon5:c.720T>A:p.F240L	Heterozygous
PPL	exon22:c.4186C>T:p.R1396C	Heterozygous
RANBP17	exon20:c.2144G>A:p.R715H	Heterozygous
SLA	exon8:c.602G>T:p.W201L	Heterozygous
SYF2	exon3:c.233A>G:p.E78G exon3:c.229T>G:p.W77G exon3:c.254A>G:p.K85R	Heterozygous Heterozygous Heterozygous

These mutations are all novel and are predicted to affect protein function. Among the genes harboring mutations, LATS1 (highlighted in red) has been chosen for further investigation with regard to CIN and tumorigenesis of NCH149 cells since mutations in LATS1 have been implicated in tumorigenesis and found to be associated with CIN and resistance to therapy. The LATS1 mutation was further verified using Sanger sequencing (Figure 5.9).

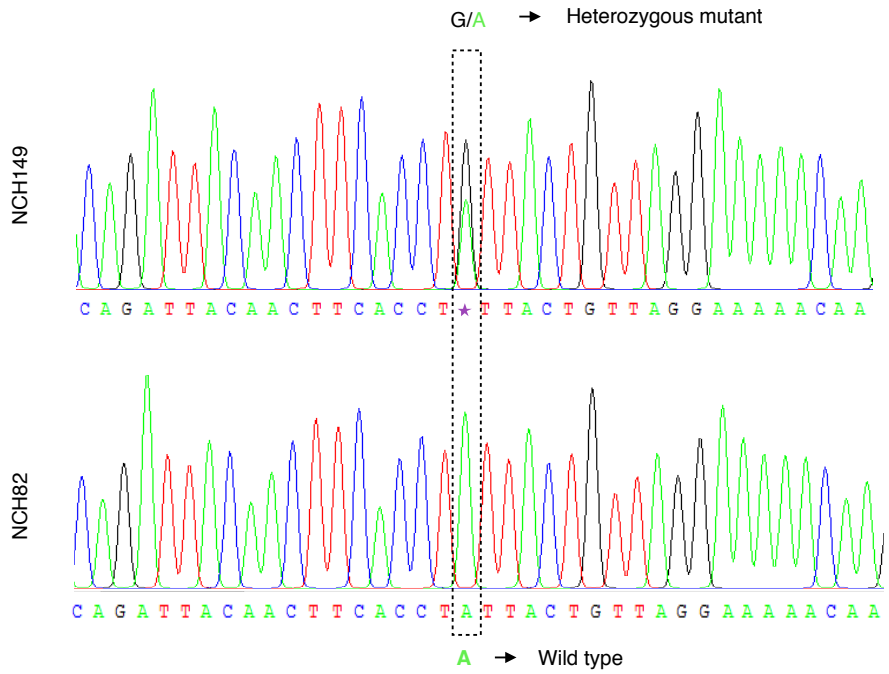

Figure 5.9 Sanger sequencing of LATS1 in NCH149 and NCH82 cells

Verification of a LATS1 gene mutation in NCH149 cells compared with wildtype LATS1 in NCH82 cells by Sanger sequencing, confirming a point mutation at base 1843 A>G leading to an amino acid change from isoleucine (GTT) to valine (ATT) (p.I615V).

5.3.3 LATS1 mutation

The novel, heterozygous LATS1 mutation identified here is a point mutation (exon 4: base 1843 A>G) leading to an amino acid exchange p.I615V. This mutation was found to localize in the YAP1 binding domain (p.526-p.655) of LATS1 and might therefore might impair LATS1 binding to YAP1 (Figure 5.10A). Absence of binding may affect the ability of LATS1 to phosphorylate YAP1 preventing its cytoplasmic sequestration and subsequent degradation.

To determine the frequency of LATS1 mutations in human cancers we used the online database cBioportal (http://www.cbioportal.org/public-portal/). Among all cancers, 10% (21/214) of the LATS1 mutations registered in this database were found to be in the YAP1 binding domain of LATS1 (Figure 5.9B) (95)(96). Also, this data base currently contains genomic data from 596 GBM samples. Mutations of LATS1 have been identified in only 1% GBM patient samples. The functional significance of the LATS1 mutations in various cancer types including GBM is largely unclear. Since LATS1 is part of the Hippo pathway, we further investigated the impact of the identified mutation on Hippo pathway signalling. For this, we next analyzed expression, localization and interactions of mutated LATS1 and YAP1 in NCH149 cells.

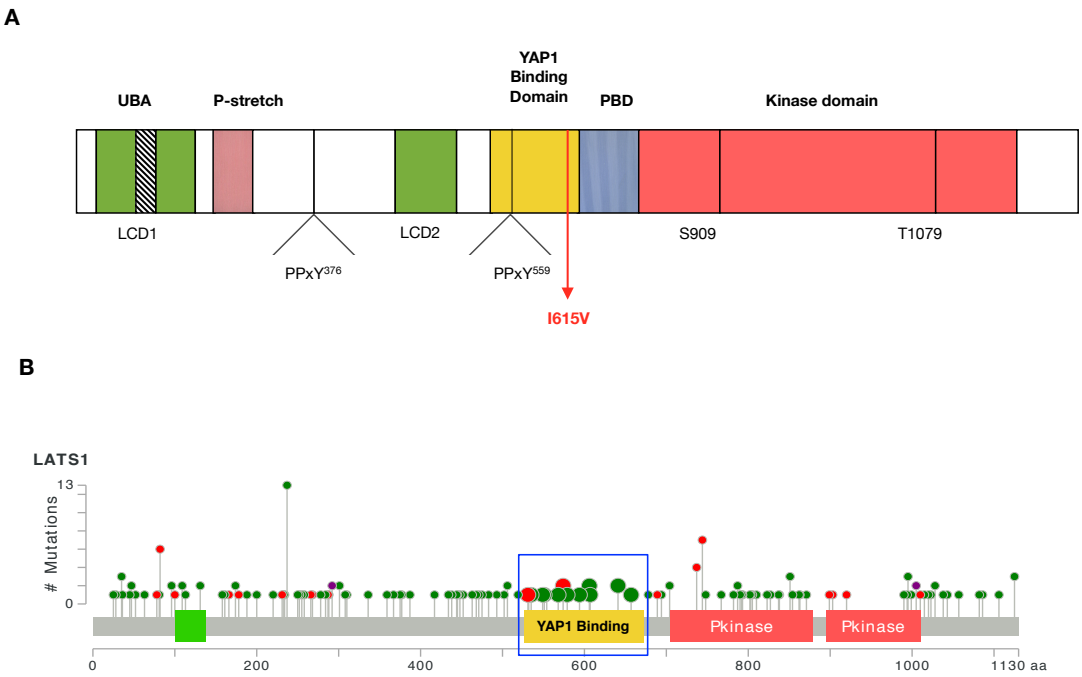

Figure 5.10 Domain structure of LATS1 and LATS1 mutations described up to date

LATS1 protein domain structure, showing the localization of the I615V mutation in the YAP1 binding domain (A). Mutations found in various regions of the LATS1 protein among the GBM data set in cBioportal. The pins indicate the positions of mutations and the height of pins their frequency of occurance (cBioportal, B).

5.4 Hippo pathway signalling dysfunction due to LATS1 mutation

5.4.1 LATS1 and YAP1 protein expression

Firstly, we checked whether the p.I615V mutation within LATS1 influences the expression level of LATS1. Cell lysates of normal human astrocytes (NHA) as a healthy control, chromosomally instable U2OS osteosarcoma cell line, NCH149 and NCH82 were prepared and the expression level of endogenous LATS1 was analyzed by Western blot. For this, the bands corresponding to LATS1 as well as ß-Actin, which served as loading control, were quantified (n=3). From these values a ratio was determined for each cell line analyzed. In order to normalize the expression levels, the expression level of NHA lysates were set to 1. As shown in Figure 5.11A the mutation does not lead to a significant change in LATS1 expression in NCH149 cells as compared to the other cell lines. The same is true for YAP1 expression levels (Fig. 5.11B). Hence, the p.I615V mutation does not seem to significantly alter the expression level of LATS1 and YAP1 in NCH149 cells compared to wild type NCH82 and NHA control.

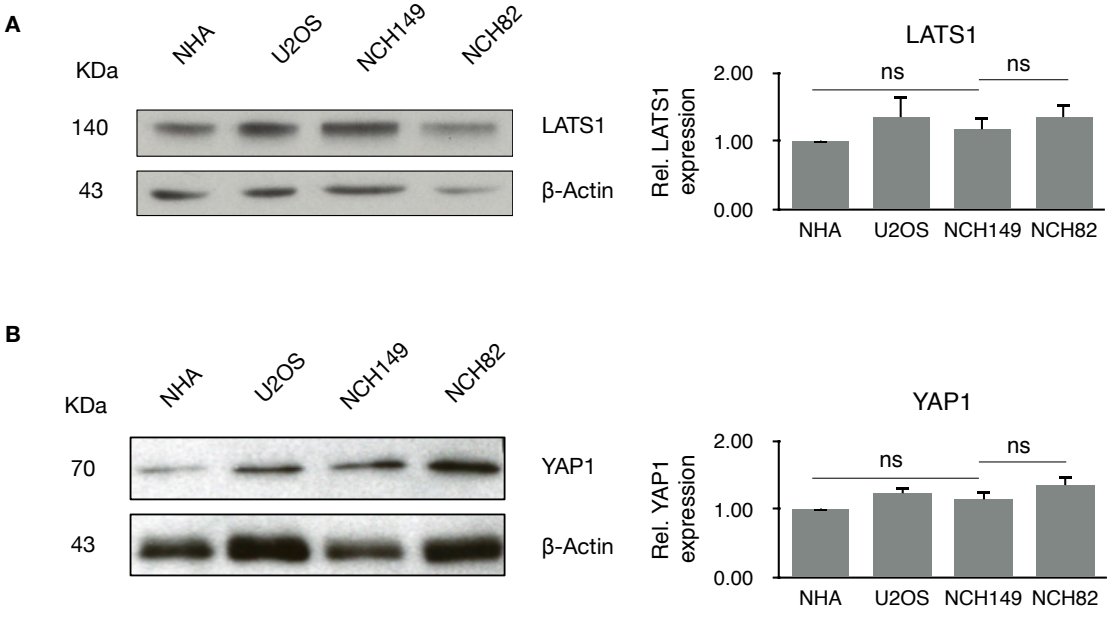

Figure 5.11 LATS1 and YAP1 protein expression levels

Representative blots of LATS1 (A) and YAP1 (B) are shown. Densitometric quantification of the bands normalized to the ß-actin control reveals that the mutation in NCH149 cells has no influence on the expression of LATS1 and YAP1 compared to normal NHA control cells.

5.4.2 LATS1 localization

Next, cellular localization of LATS1 and YAP1 was investigated using immunofluorescence microscopy. Cells were immunostained with a LATS1 antibody that detects both phosphorylated and non-phosphorylated LATS1. LATS1 in interphase cells is present in the cytoplasm in NCH149, NCH82 and NHA cell lines (Figure 5.12). This indicates that the p.I615V muation does not influence the cellular localization of LATS1 in NCH149 cells which is comparable to NCH82 and NHA cells wildtype for LATS1.

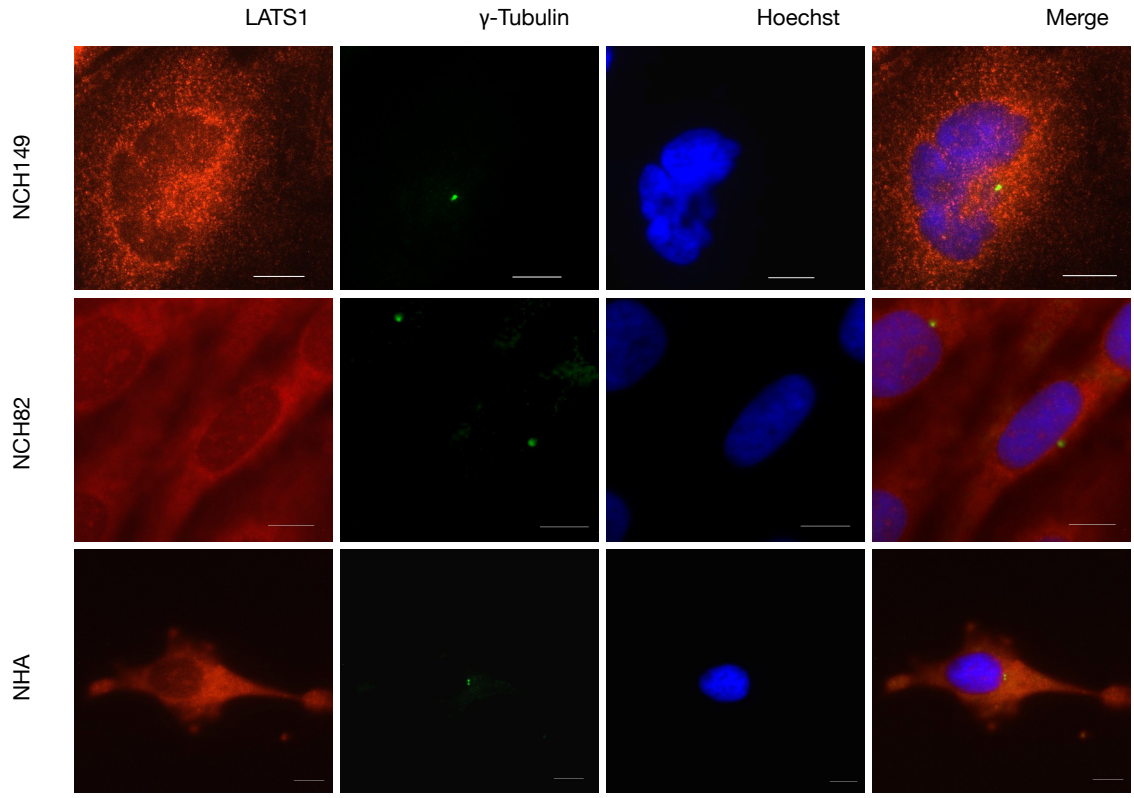

Figure 5.12 Cellular localization of LATS1

NCH149 and NCH82 cells were stained with antibodies against LATS1 and γ-tubulin. LATS1 localised in the cytoplasm during interphase in all the cell lines. Scale bar, 10 µm.

5.4.3 Density-dependent localization of YAP1

YAP1 is one of the downstream Hippo pathway targets of LATS1. In proliferating cells YAP1 translocates to the nucleus and acts as a transcriptional co-activator while in resting cells, LATS1 is known to phosphorylate YAP1 causing its cytoplasmic retention and further degradation.

To study the localization of YAP1 in LATS1 mutant NCH149 compared to LATS1 wildtype NCH82 cells and NHA cells, non-confluent (low density) and confluent (densely packed) cells were fixed and stained with an antibody to YAP1. At low density YAP1 is found localised in the nucleus in all three cell types which is normal for proliferating cells (Figure 5.13 A). Interestingly, at high density, YAP1 localizes to the nucleus in NCH149 cells while in NCH82 cells and normal NHA cells the signal is restricted to the cytoplasm (Figure 5.13 B). This indicates that although the cells are confluent the negative regulation of YAP1 by LATS1 is inactive leading to its uncontrolled translocation to the nucelus.

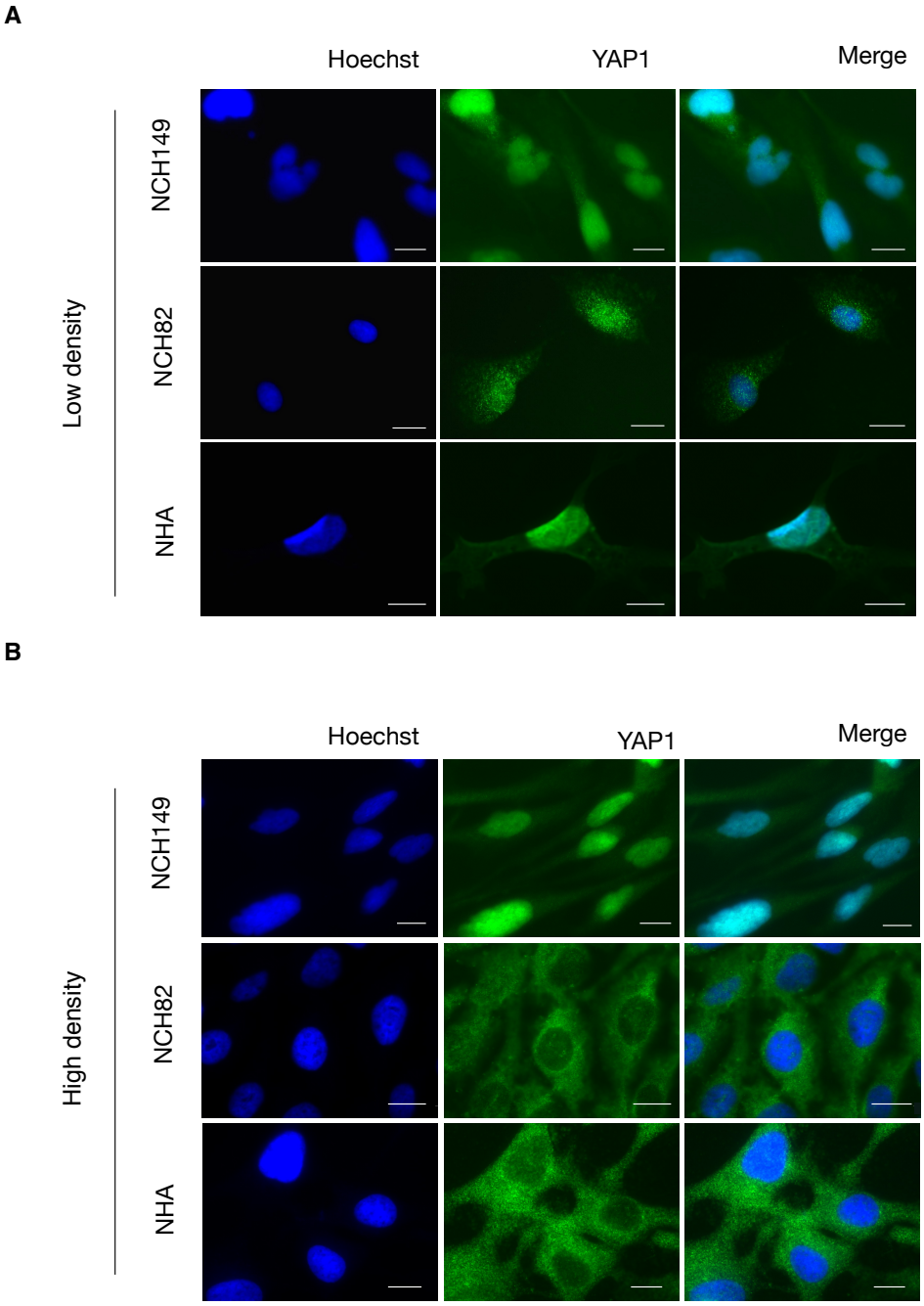

Figure 5.13 Density-dependent intracellular localization of YAP1

Immunofluoresence microscopy after immunostaining with an antibody against YAP1 (green) and DNA stained with Hoechst (blue). (A) Under low density conditions YAP1 localized to the nucleus in all three cell lines. (B) At high density normal cytoplasmic localization of YAP1 is observed in normal human astrocytes (NHA) and NCH82 cells and abnormal nuclear localization in NCH149 cells. Scale bar, 10 µm.

5.4.4 YAP1 phosphorylation

In order to investigate whether a loss of YAP1 phosphorylation by I615V-mutant LATS1 causes the altered localization of YAP1 in NCH149 cells at high density, the extent of LATS1-specific phosphorylation of YAP1 at Ser127 was determined by Western blot analysis. The pYAP1 levels in NCH149 and NCH82 cells were compared at low density and high density. The phosphorylation of YAP1 at Ser127 was significantly lower in NCH149 compared to NCH82 cells at both high and low density. Mainly, at high density the levels of phosphorylated YAP1 (Ser127) were found to be greatly reduced in NCH149 cells when compared to NCH82 cells ($P < 0.005$) (Figure 5.14).

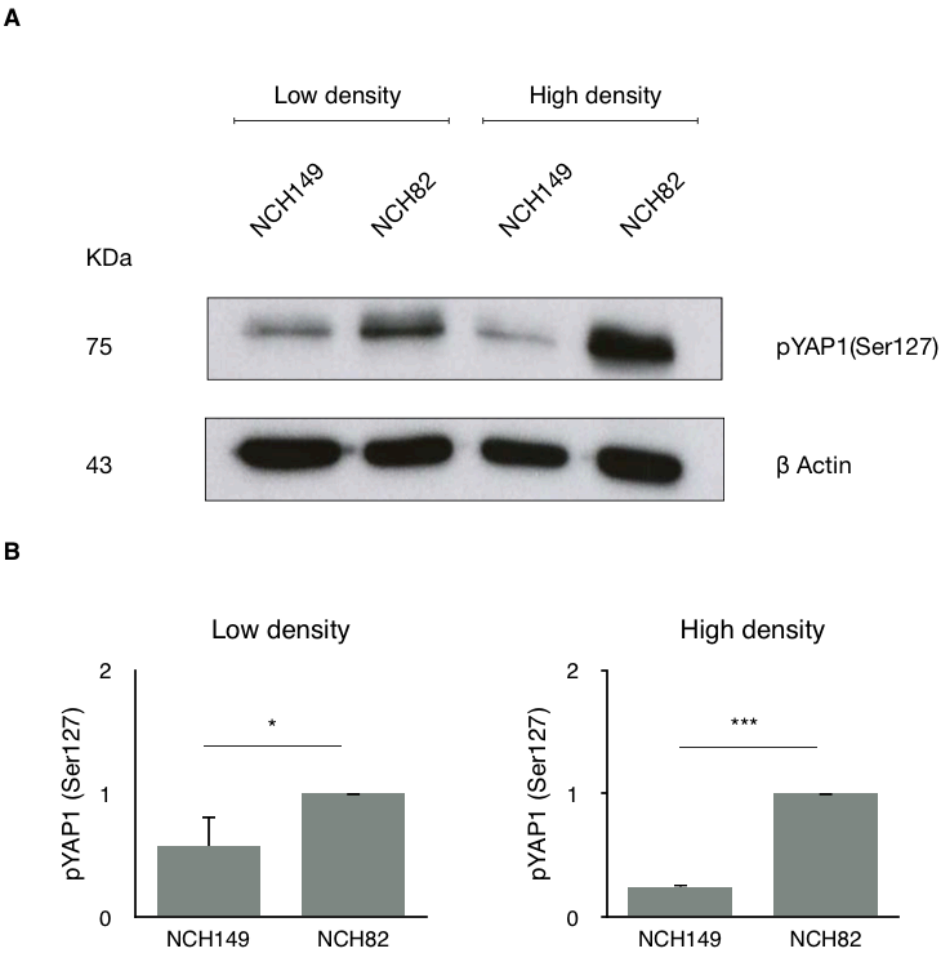

Figure 5.14 pYAP1 (Ser127) Western Blot

Western blot detection of pYAP1 using a phospho (Ser127) YAP1 specific antibody showed lower pYAP1 levels in NCH149 compared to NCH82 at both high and low density (A). Quantification of bands normalized to ß-actin confirmed significant decrease in phosphorylation of YAP1 at Ser127 in NCH149 compared to NCH82 at both high and low density (B).

5.4.5 Interaction of LATS1 and YAP1

To confirm that the reduced phosphorylation of YAP1 at Ser127 by LATS1 was due to a failure of YAP1 binding to LATS1, I performed co-immunoprecipitation experiments. For this, I immunoprecipitated YAP1 and analysed for co-immunoprecipitation of LATS1 by Western blotting and vice versa. It was observed that in NCH149 cells YAP1 does not co-immunoprecipitate with LATS1 confirming the lack of interaction between the two proteins and hence explaining reduced YAP1 phosphorylation and localization of YAP1 to the nucleus. In contrast, the interaction between YAP1 and LATS1 was intact in NCH82 cells, as these proteins co-immunoprecipitated in these cells (Figure 5.15). This result confirms that the p.I615V mutation impairs the binding of YAP1 to LATS1, hence preventing the phosphorylation of YAP1 by LATS1.

This leads to a conclusion that in NCH149 cells YAP1 binding to LATS1 is impaired due to the p.I615V mutation causing reduced phosphorylation of the YAP1. Unphoshorylated YAP1 then translocates to the nucleus in NCH149 cells.

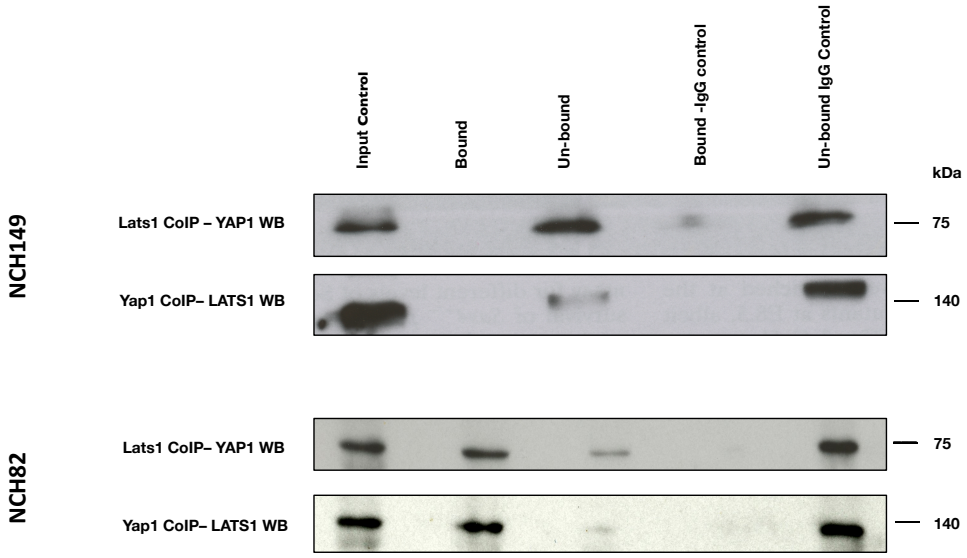

Figure 5.15 Co-immunoprecipitation of LATS1 and YAP1

Western blots showing absence of bound fraction of LATS1 and YAP1 in NCH149 cells while LATS1 and YAP1 were found to co-immunoprecipitate in NCH82 cells.

5.5 Chemotherapeutic intervention of Hippo pathway

Final downstream effectors of Hippo pathway YAP and TAZ are attractive targets for chemotherapeutic interventions. Various inhibitors have been identified to target YAP directly or indirectly. YAP is dispensable for growth and homeostasis of normal tissues and is the final common conduit of upstream signals thus, potentially limiting side effects and drug resistance achieved by alternative pathways. Verteporfin is one such small molecule that disrupts the YAP-TEAD transcriptional activation complex formation, thereby specifically inhibiting YAP1 activity. Since verteporfin has been shown to act *in vitro* as an effective chemotherapeutic agent for cancer cells overexpressing YAP1, this inhibitor was chosen for further experiments.

5.5.1 Dose-dependent toxicity of VP on NCH149 cells

To analyze the impact of VP on cell viability, the NCH149 and NCH82 cells were treated with VP (2 µg/ml and 10 µg/ml) and cell numbers were determined by scoring live cells every day for a total of three days (n=3). NCH149 cells which are known to be resistant to most chemotheraputic agents as well as radiation, started to die already 24 hours after initiation of VP treatment with all NCH149 cells being dead by day 3 (Figure 5.16A). In contrast, NCH82 cells, after showing some initial toxicity to VP at day 1, recovered and grew almost normally on days 2-3 (Figure 5.16B).

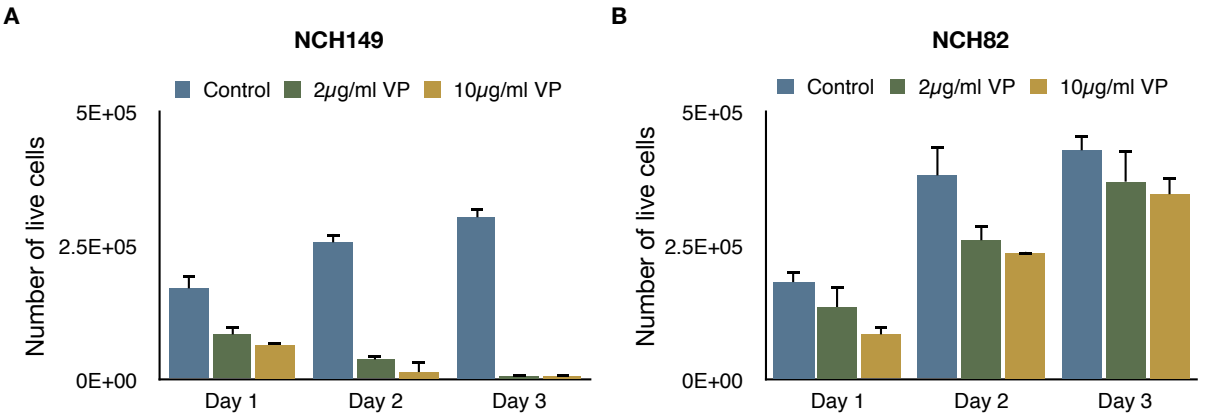

Figure 5.16 Dose-dependent toxicity of verteporfin on NCH149 cells.

NCH149 and NCH82 cells were incubated with VP for 3 days and cytotoxicity was determined by scoring the number of living cells each day. (A) Dose dependent cytotoxicity was induced by VP treatment of NCH149 which on day 3 were completely dead. NCH82 cells show initial toxicity on Day 1 but on day 2 and 3 recover to grow normally.

5.5.2 Apoptosis measurement

In addition, we performed annexin V staining to determine whether the decrease in live NCH149 cells is due to apoptosis induced by VP. For this, NCH149 as well as NCH82 cells were treated with VP for 1, 2 or 3 days with either 2 or 10 µg/ml. After the respective incubation times the cells were stained with FITC-labelled Annexin V and PI. The cells were then subjected to flow cytometric analysis and the cells were considered apoptotic when they were double positive for Annexin V and PI whereas pre-apoptotic cells were only Annexin V-positive (Figure 5.17A). The total sum of apoptotic and pre-apoptotic populations was considered for quantification of apoptosis in both the cell lines after VP treatment (green boxes in Figure 5.17A).

In NCH149 cells a dose-dependent increase in the apoptotic cell fraction was observed over the period of treatment and almost all the cells were dead by day 3 of VP treatment. In contrast, in NCH82 cells an increase of the apoptotic cell fraction related to initial toxicity was observed on day 1 but on days 2 and 3 the apoptosis level was comparable to untreated controls (Figure 5.17B). Together, this shows that VP specifically kills LATS1-mutant NCH149 cells but not NCH82 cells which are wildtype for LATS1.

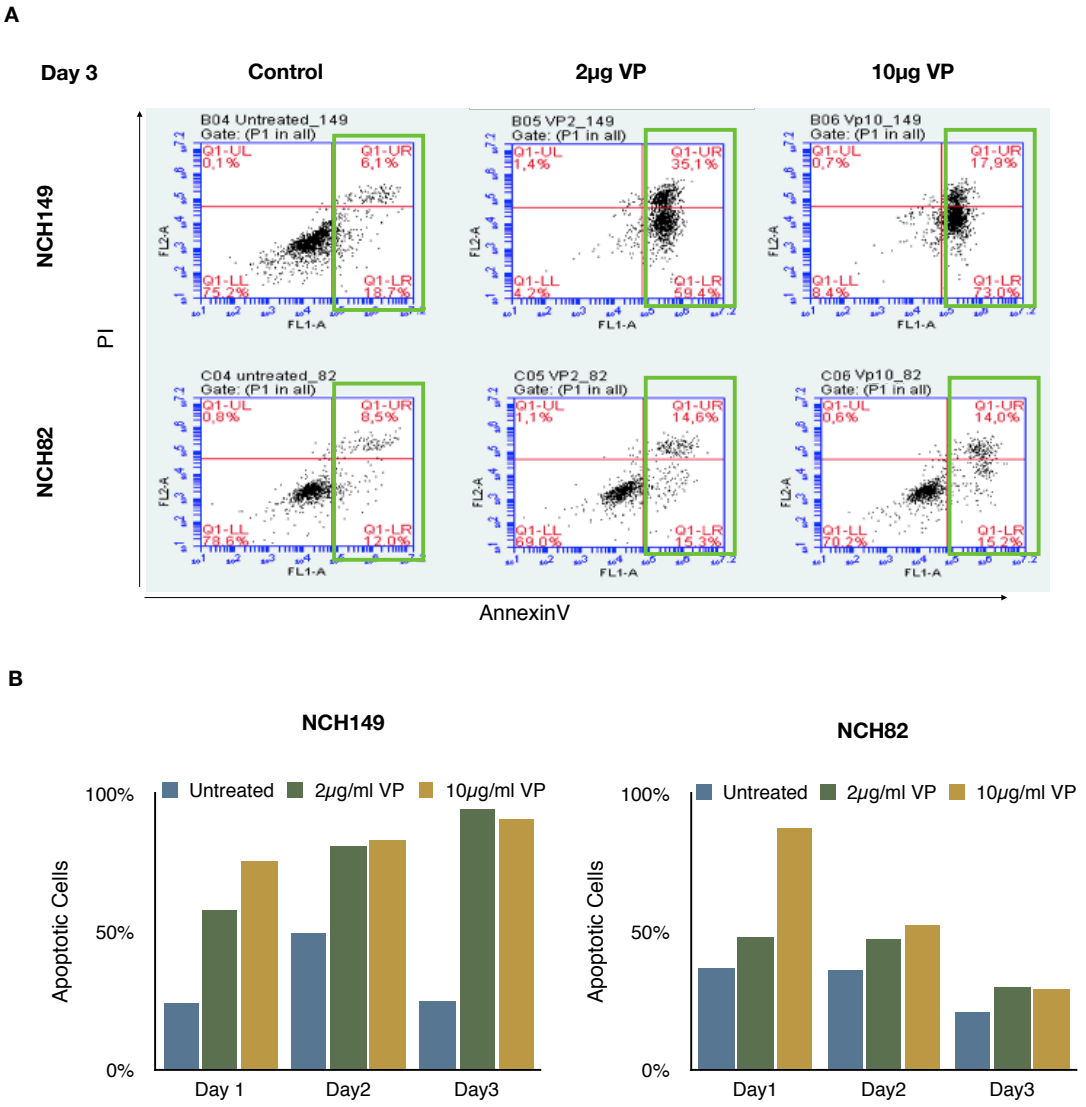

Figure 5.17 Measurement of apoptosis after VP treatment

NCH149 and NCH82 cells were treated with VP and after day 1, 2 and 3 apoptosis induction was analysed by staining cells with Annexin V and PI followed by flow cytometric analysis. (A) Examples of dot blots at day 3 are shown. Apoptotic (Annexin V / PI double-positive) and pre-apoptotic (Annexin V-positive) cells are shown demonstrating the induction of apoptosis by VP in NCH149 cells. The percentages of apotic and pre-apoptotic cells were calculated together to compare apoptosis in NCH149 and NCH82 cells during the 3 day treatment period (B). Dose-dependent increase in apoptosis was induced by VP treatment of NCH149 which on day 3 were all dead. NCH82 cells show initial toxicity on day 1 but on day 2 and 3 recover to grow normally.

5.6 Inducible expression of wildtype and mutant LATS1 in the U2OS-tet-on system

With the goal to verify the impact of the LATS1 p.I615V mutation on cell proliferation and CIN in an isogenic system, I generated stable U2OS-Tet-on cell lines that inducibly express wild type or mutant (p.I615V) LATS1 (Figure 5.18) each fused to a double Flag-tag (2xFlag). I performed immunofluorescence at various time points after induction by doxycyclin to study the effects of mutant LATS1.

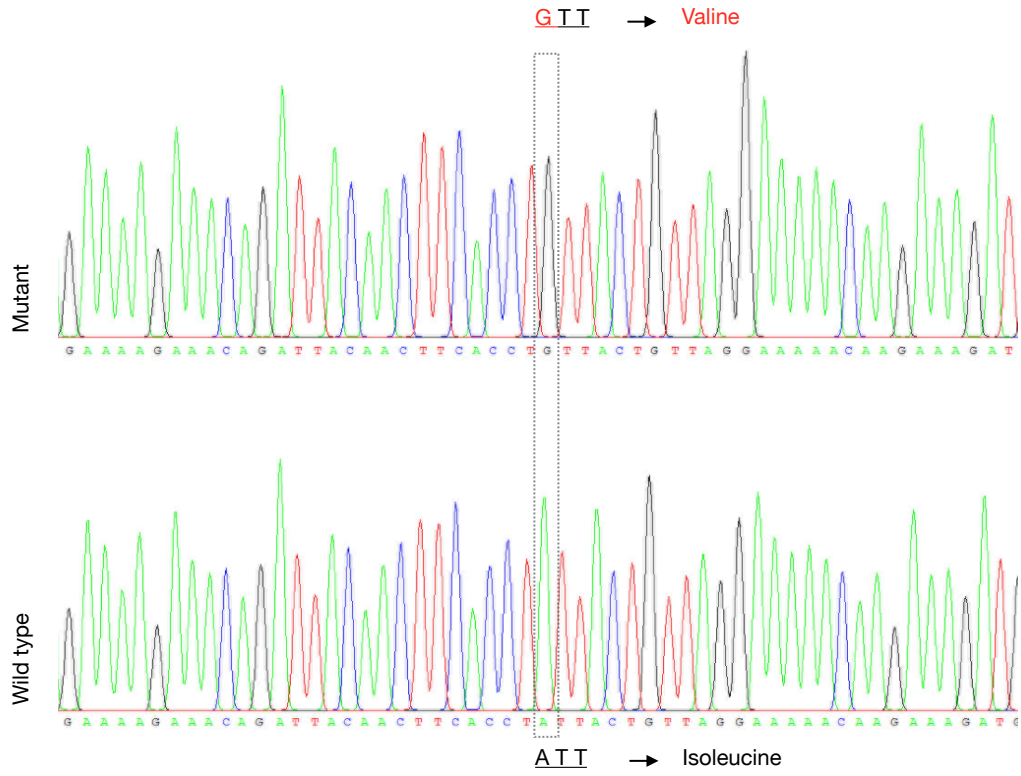

Figure 5.18 Sanger sequencing of wildtype and mutant LATS1 plasmids

Verification of LATS1 mutation by Sanger squencing in pTER2hyg plasmids generated for stable transfection of U2OS-tet-on cells, confirms a point mutation A>G at 1843.

Firstly, I analyzed the localization of wildtype and mutant LATS1 after overexpression in order to demonstrate that overexpressed Flag-tagged LATS1 (either wildtype or mutated) behaves like their endogeneous counterparts. For this, U2OS-Tet-on cells with wildtype and mutant were grown in medium with (+Dox) or without (-Dox) doxycyclin for 6 days. On day 2 after induction with doxycyclin the expression levels of wildtype and mutated LATS1 were analyzed by Western blotting using an antibody against Flag-tag. Both wild type and mutant LATS1 are expressed after induction (Figure 5.19 A). In addition, coverslips were collected and fixed every second day after induction and immunofluoresence staining was performed with antibody against Flag-tag to detect the presence of induced LATS1. Cellular localization of Flag-LATS1 in interphase cells of both wildtype and mutant LATS1 seems to be cytoplasmic similar to endogenous LATS1 in interphase cells (Figure 5.19 B). This shows that the overexpressed LATS1-versions behave like the endogeneous proteins making the cell lines suitable for further experiments.

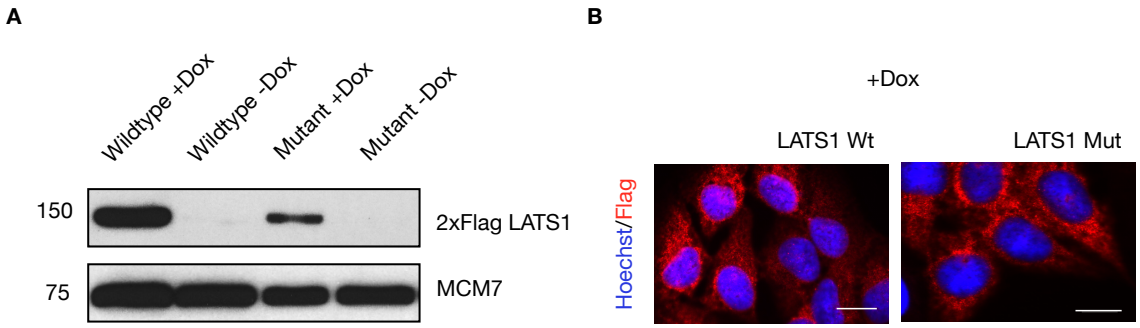

Figure 5.19 Inducible expression of 2xFlag LATS1 in U2OS-Tet-on cells

U2OS-Tet-on cells transfected with 2 x Flag wildtype (wt) or mutant (mut) LATS1 were induced by doxycyclin. Expression of wildtype or mutant LATS1 was confirmed by Western blotting (A). Immunofluorescence shows that overexpressed wildtype and mutant LATS1 localize to the cytoplasm during interphase (A). Scale bar, 10 µm.

Next, the cells were stained with an antibody against YAP1 to observe whether YAP1 localizes to the nucleus after overexpression of mutant LATS1. Indeed, already two days after induction nuclear localization of YAP1 was observed in confluent LATS1-mutant cells but not in non-induced or LATS1-wildtype cells (Figure 5.19).

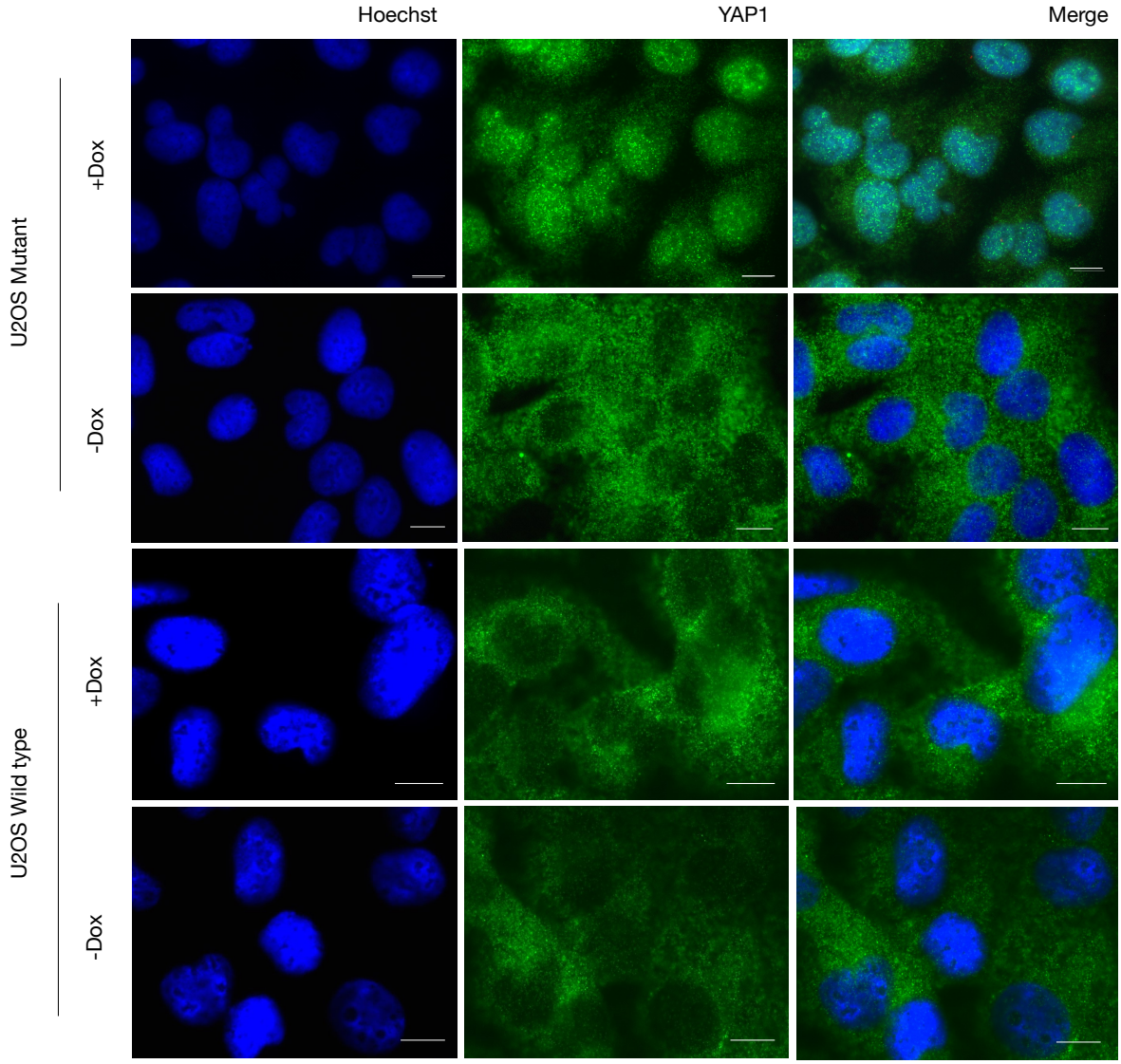

Figure 5.20 YAP1 nuclear localization in mutant-LATS1-expressing cells

Immunofluorescence staining of induced U2OS-Tet-on cells with an antibody against YAP1 (green) and Hoechst shows normal cytoplasmic localization of YAP1 in wild type and un-induced mutant cells and nuclear localization in induced mutant LATS1-expressing U2OS cells. Scale bar, 10µm.

Finally, I analyzed the impact of overexpression of wildtype and mutant LATS1, respectively, on the formation of micronuclei and centriole amplification. For this, cells were fixed 6 days after induction of either wildtype or mutant LATS1 (+Dox and –Dox). Preliminary experiments upon scoring three times 100 cells show an increase in micronucleus formation in induced LATS1-mutant as compared to non-induced LATS1-mutant cells as well as to cells expressing wildtype LATS1 (Figure 5.21A). Also, a significant increase in centriole amplification in induced LATS1-mutant over both non-induced and wildtype-LATS1 expressing cells was observed (Figure 5.21B).

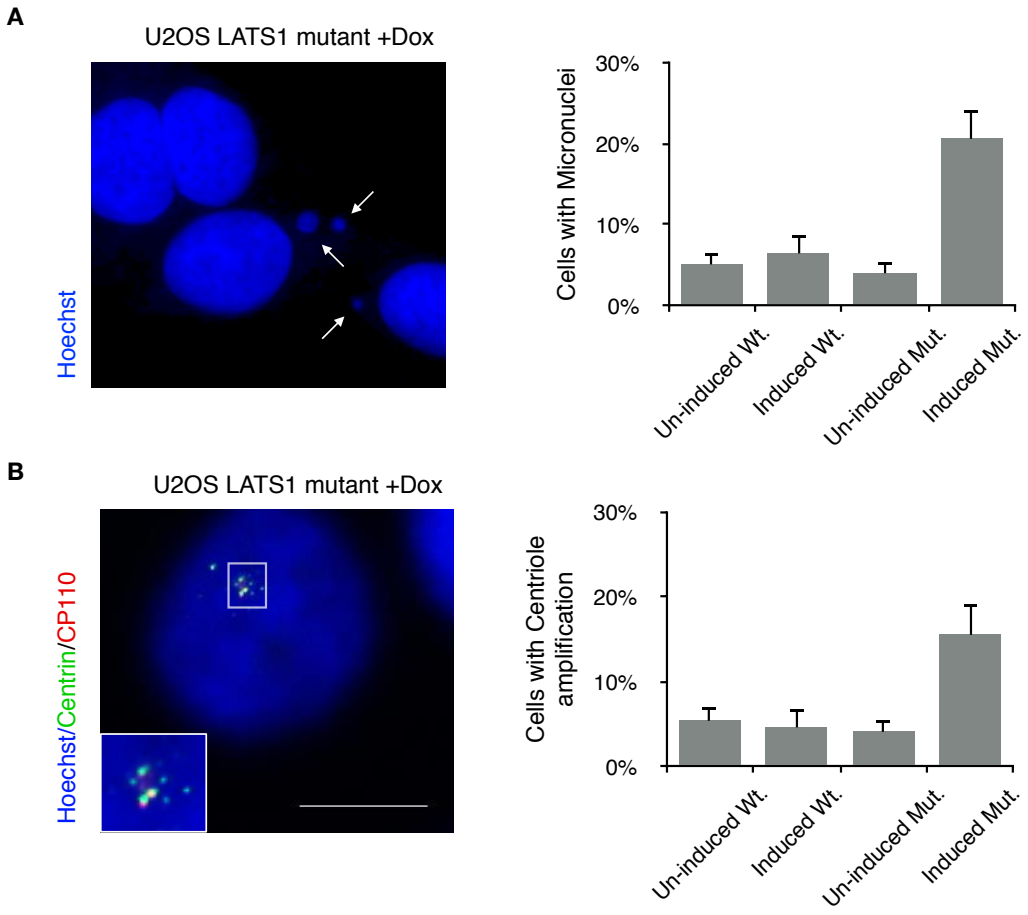

Figure 5.21 Micronucleus formation and centriole amplification in mutant-LATS1-expressing cells

An increase in the number of cells with micronuclei stained with hoechst (blue) (A) and amplified centrioles stained with centrin (green) and CP110 (red) (B) was observed in induced mutant LATS1-expressing U2OS cells when compared to un-induced mutant and wildtype LATS1 expressing U2OS cells (B). Scale bar, 10 µm.

These findings lead to the conclusion that the p.I615V LATS1 mutation impairs binding and phosphorylation of YAP1 that results in its nuclear localization. This deregulation of the Hippo pathway also seems to contribute to the CIN phenotype by increased micronucleus and centriole amplification upon overexpression of mutant LATS1.

6 Discussion

Since Hansemann's work in the late 19th century, abnormal chromosome numbers have been recognized as a nearly ubiquitous feature of human cancers (97). Today numerical CIN is an established characteristic feature of most human malignancies. For example, a current study shows that most late stage cancers contain an average of 60 to 90 chromosomes (98). Despite its long history and clinical relevance, the study of CIN has yet to prove Boveri's postulate that abnormal chromosome numbers are a cause rather than a consequence of the cancerous state (99). Although it has been shown that gains and losses of whole chromosomes have anti-proliferative effects in untransformed diploid cells, tumors exhibiting a large number of gains and losses of chromosomes seem to have a proliferative advantage (100; 101).

Normally, cells that have an abnormal DNA content are prevented from further proliferation by a number of cell cycle checkpoints, however, continuous accumulation of chromosome changes in a cell population increases the chance of mutations in oncogenes, tumor suppressor genes and cell cycle checkpoint genes decreasing the tendency for self-elimination of aberrant cells (102). Therefore, extreme CIN provides a survival advantage to cells by overcoming the protective mechanisms. It is well known that neoplastic transformation requires a set of mutations that can be achieved by having abnormally high rate of mutations and CIN provides a platform for such a high mutation rate (54). This phenomenon is explained by the “mutator hypothesis” that suggests that an initial mutation, which creates the "mutator phenotype", allows the accumulation of further mutations and the evasion of the normal checks on the cells growth (103; 47). For example, in the extreme case of human colorectal cancers that arise from the mismatch repair defect were found to have 100,000 genetic mutations and are presumed to have an ability to overcome a wide variety of negative controls on proliferation also exhibit significant CIN (104). Although, some studies challenge the idea that CIN is important for tumorigenesis (105), its prevalence in malignant solid tumors and its contribution to development and sustaining ability’s of tumor growth has brought forth the suggestion that CIN plays a causal role in tumorigenesis.

6.1 Occurance and causes of CIN in Glioblastoma

Glioblastomas are known to have high levels of CIN making them heterogeneous and difficult to treat. Although mechanisms of CIN are comparatively well understood in colorectal cancers, there have not been many studies investigating the cause and affect of CIN in GBM. In a recent study inactivating mutations in STAG2, a gene coding for subunit of cohesin complex that regulates the separation of sister chromatids was shown to cause aneuploidy in 5 % of GBM's (106). In another study oncogenic chromosomal translocation event causing fusion of FGFR and centrosomal proteins TACC was shown to induces mitotic and chromosomal segregation defects and trigger aneuploidy in 3.1 % of GBM tumors (107). The presence of intratumor hererogeneity and chemoresistance and the lack of knowledge makes GBM a suitable model to study CIN.

In the present study, the patient-derived GBM cell line NCH149 was identified in the laboratory of Dr. Anne Régnier-Vigouroux that show excessive numerical chromosome gains and loses. This cell line was also found to have extreme chemo- and radioresistance. Upon further cytogenetic analysis of NCH149 cells and comparing it to another GBM cell line NCH82 using M-FISH, it was observed that NCH149 cells exibited extreme aneuploidy and cell-to-cell heterogeneity among 24 M-FISH metaphase spreads analysed, while NCH82 cells were stably tetraploid (89). It is known that aneuploid cells may or may not be chromosomally instable. Numerical CIN is defined by a high rate of continuous gains and losses of whole chromosomes therefore; cytogenetic complexity *per se* cannot be used as evidence of CIN. In practice, instability is assessed by following the evolution of cytogenetic abnormalities in a tumor cell population over time and by comparing the rate of chromosome mutations with that in a normal cell population (108). Alternatively, CIN is monitored indirectly by quantifying the incidence of chromosomal losses, gains and resulting heterogeneity in a given population of cells. Hence, CIN cells are distinguished form merely aneuploid cells by the presence of cell-to-cell heterogeneity. Consequently, in this study, interphase FISH experiments were performed for two chromosomes, namely chromosomes 2 (large) and 20 (small) of both the cell lines. NCH149 cells were found to exibit high clonal heterogeneity confirming the presence of CIN while NCH82 have a major tetraploid subclone, this correlates with the M-FISH data. CIN causes a step-wise accumulation of cytogenetic changes during tumor growth, which is manifested as clonal heterogeneity (45). Heterogeneous tumors are known to generate a larger variety of genetic variants to be tested by selection providing a wider adaptive landscape increasing the probability of clones reaching fitness for microenvironmental challenges (109). CIN therefore also allows

cells to better adapt to changes following exposure to DNA damage encountered during radiotherapy protocols, thereby contributing to radioresistant in tumors both before and after radiotherapy (110). It has also been previously shown that CIN confers intrinsic resistance to chemotherapeutic agents in colorectal cancer cell lines and that presence of stable tertraploidy was found incapable of such resistance (111). This implies that karyotypic heterogeneity rather than increased ploidy is responsible for increased treatment resistance compared to karyotypically stable cells. Indeed, the high variation of chromosome numbers within the population of NCH149 cells strongly indicating the presence of CIN could be the cause of resistance to X-ray irradiation and carbon ion therapy as observed by Dokic *et. al*. In contrast, NCH82 cells lower resistant to these radiation treatments which can be attributed to the presence of a stable karyotype. Due to the observed differences within the population, NCH149 cells are confirmed to be chromosomally instable whereas the NCH82 cell line is stably aneuploid (tetraploid). For this reason we further examined NCH149 cells in order to determine one of the mechanisms leading to CIN in GBM. Chromosomal gains or losses in CIN are known to be a result of chromosome missegregation caused by abnormal mitotic spindle assembly, impaired microtubule–kinetochore attachment or a weakened spindle assembly checkpoint (112). When NCH149 cells were stained with Hoechst, 25% of cells were found to have one or more micronuclei per cell. In contrast, in NCH82 cells only about 2% of the cells had micronuclei. Micronuclei mainly originate when chromosome fragments or whole chromosomes fail to be included in the daughter nuclei after mitosis. These displaced chromosomes or chromosome fragments are enclosed by a nuclear membrane and appear as micronuclei. Micronuclei are smaller but morphologically similar to the nuclei and can be observed by conventional nuclear staining. Presence of micronuclei is an indicator of chromosomal missegregation (113). The frequency of micronuclei is used as a biomarker of chromosomal damage, genome stability and predicts increased risk of cancer development in human populations (114). However, only whole chromosome gains or losses indicate numerical CIN hence, we further investigate the presence of whole chromosomes by immunofluorescence staining with CREST. In NCH149 cells, 75 % of the micronuclei had whole chromosomes with CREST signals meaning that there was high incidence chromosomal missegregation. This process of missegregation in NCH149 was clearly visualized by staining fixed mitotic cells with CREST, α-tubulin and Hoechst where about 30% of mitotic NCH149 cells had lagging chromosomes during anaphase and as opposed to less than 1 % of anaphases in NCH82 cell line (Figure 5.5).

Chromosome missegregation is associated with supernumerary chromosomes for over 100 years. Today, it is well known that regulation of centrosome number and function underlies bipolar mitotic spindle formation and genetic integrity (115). Here we found that NCH149 have higher centriole amplification compared to NCH82 cells. Deregulation of the centriole duplication machinery and resulting centriole amplificaton is an obvious source of centrosome amplification and aneuploidy in tumors (35). The extent of centrosomal aberrations is often correlated with chromosomal instability (CIN) and malignant behavior in tumor cell lines, mouse tumor models, and human tumors (116; 117). Hence, the observed CIN in NCH149 cells could be a result of supernumerary centrosomes. Centrosome amplification, is often associated with multipolar mitosis that lead to aberrant chromosome segregation (43; 118). Interestingly, immunofluorescence studies of mitotic cells stained with β-actin and γ-tubulin showed that both cell lines NCH149 and NCH82 underwent normal bipolar mitosis despite centriole amplification. Comparable to this study the frequent occurrence of supernumerary centrosomes in human breast cancer samples was associated with surprisingly rare abnormal mitoses (119). Extra centrosomes to bypass the SAC by centrosome clustering to undergo bipolar mitosis. However, no signs of centrosomal clustering was observed in NCH149 or NCH82 cells. Whether or not supernumerary centrosomes undergo clustering to undergo bipolar mitosis is yet to be studied in NCH149 cells. Interestingly, by live cell imaging it was observed that NCH149 cells, on an average took ~30 minutes longer to under go mitosis when compared to NCH82 cells (Figure 5.7 B). It is has been recently shown that extra centrosomes or chromosomes delay satisfaction of the spindle assembly checkpoint leading to prolonged mitosis. Cancer cells having normal number of chromosomes and centrosome can divide in less than 20 minutes while doubling the chromosome number adds ~10 minutes while doubling the number of centrosomes adds ~30 minutes (120). Therefore, the prolonged mitosis duration could be attributed to the higher chromosome number and high centriole amplification in NCH149 cells. Prolonged mitosis due to delay in SAC checkpoint has been reported to cause missegregation of chromosomes, mitotic slippage causing aneuploidy (21). Several other causes of prolonged activation of the mitotic checkpoint in human cancer cells have been described such as inactivation of Rb and abnormal MAD2 expression, abnormal accumulation of cyclinE due to inactivation of the hCDC4 and activation of oncogenes such as c-Myc (121). The above phenotypic observations demonstrate that NCH149 is chromosomally instable indicated by presence of cell-to-cell heterogeneity, chromosomal missegregation and centriole amplification but the causal factor for these abnormalities was unknown. NCH149 cells therefore provide a suitable

system to investigate connection between CIN and genetic mutations and hence whole exome sequencing of NCH149 cells was performed to identify mutations that might cause CIN. Analysis of the whole exome sequencing data identified mutations in 24 different genes found in the tumor and in the cell line but absent in healthy tissue (Table 5.1). Of these LATS1 p.I615V mutation was most interesting with regard to tumorigenesis and CIN. Mutation induced defects in mitotic spindle assembly, mitotic check point, sister chromatid cohesion and centrosome amplification have been shown to cause chromosomal missegregation leading to CIN (29). So far, mutations in genes regulating these processes such as STAG2 and MAD2 have been identified to be possible causes of CIN. Other genes such as BRCA1, BLM and ATM that are known keep genetic alterations to a minimum, and thus when they are inactivated, mutations in other genes occur at a higher rate (122). However, LATS1 mutations are rare in cancer tissues in general and especially in GBM. Interestingly, a recent study has uncovered LATS1 p.I615T mutation by silico analysis provides evidence that LATS1 mutations in this region may play a role in CIN and drive human tumor development (123).

6.2 LATS1 mutation mediated deregulation of Hippo pathway and its role in CIN

In the present work I have attempted to deliniate the effect of the identified LATS1 p.I615V mutation on Hippo pathway function in NCH149 GBM cells. Classically identified within the Hippo signaling pathway, LATS1 also acts independently of this pathway, possessing multiple functions including regulation of cell proliferation, cell death and cell migration, and plays a governing role in mitosis and maintenance of genetic stability. LATS1 is a tumor suppressor gene. This was initially recognized by genetic studies in *Drosophila* demonstrating that heterozygous loss of LATS1 produced a wart-like phenotype characterized by excessive overproliferation of imaginal disc epithelial cells of *Drosophila* (124). Complete loss of LATS1 causes embryonic lethality in flies, which highlights the importance of LATS1 function (125). Downregulated *LATS1* gene expression was found in a variety of tumor types including soft tissue sarcomas, breast, myxoid liposarcoma, leiomyosarcomas and malignant fibrous histiocytoma (126). In one study, LATS1 downregulation was correlated with poor prognosis in glioma patients (78). In contrast there was no significant difference in the protein expression levels of LATS1 or YAP1 in LATS1-mutant NCH149 cells when compared to LATS1 wild type NCH82 cells and normal human astrocytes.

YAP1 overexpression was observed in many cancers such as mesotheliomas, non-small-cell lung carcinoma and brain tumors like GBM (127; 128). In spite of the high frequency of YAP1 overexpression, a relatively low incidence (5 –15 %) of amplification of the human chromosome 11q22 amplicon containing YAP1 gene has been reported in human tumors (129). This led to the speculation that elevation of YAP1 protein levels in cancer may not only due to gene amplification, but a result of deregulation of the Hippo pathway. The direct upstream controller of YAP1 activity is LATS1 and mutations in LATS1 could affect YAP1 negative regulation. Therefore, immunfluoresence staining of NCH149, NCH82 and NHA cells was performed which shows normal nuclear localization of YAP1 in all cell types at low density. Interestingly, YAP1 immunofluoresence staining of NCH149 cells at high density showed nuclear localization while in NHA and NCH82 cells YAP1 was found localized in the cytoplasm. It is known that in response to cell contact inhibition the Hippo pathway is activated leading to LATS1-mediated YAP1 phosphorylation with subsequent cytoplasmic retention and degradation of YAP1 (71). When cells proliferate at low density the Hippo pathway is inactive thereby facilitating the translocation of YAP1 into the nucleus to initiate trasciption of various growth promoting genes. Nuclear localization of YAP1 has been identified before during immunohistochemical survey of YAP1 expression in meningioma tumors (130). This suggests that the negative regulation of YAP1 by the Hippo pathway is not functional in p.I615V LATS1-mutant NCH149 cells. To further investigate the extent of YAP1 phosphorylation at Ser127 by LATS1, Western blot analysis was performed and compared in high and low density cells. Accordingly, pSer127-YAP1 levels were significantly lower in NCH149 cells with mutant LATS1 compared to NCH82 cells which are wildtype for LATS1. These results strongly argue that the phoshoprylation of YAP1 by LATS1 is impaired in NCH149 cells due to the presence of a mutation in the YAP1-binding domain of LATS1. This finding is supported by co-immunoprecipitation experiments, which showed that LATS1 and YAP1 did not co-immunoprecipitate in LATS1-mutant NCH149 cells. Mutations in YAP1 that lead to decreased phosphorylation by LATS1 or decreased 14–3–3 binding have been reported earlier (131; 132). In YAP1 S381 mutant cells YAP1 overexpression and nuclear localization was observed due to loss of S318 phosphorylation and subsequent degradation (133). The correlation between LATS1 dysfunction due to downregulation or mutations and its involvement in cancer development has been widely discussed. However, LATS1 mutations preventing binding and phosphorylation of YAP1 have not been identified up to now in human cells.

There have been some studies that describe the involvement of the Hippo pathway in maintenance of genetic integrity. LATS1 dynamically localizes to centrosomes and the mitotic spindle apparatus, including the central spindle, and contributes to the regulation of

proper chromosome segregation during mitotic progression and cytokinesis (74; 134). Cells expressing N-terminally truncated LATS1 show supernumerary centrosomes as well mitotic defects including chromosomal missegregation and cytokinesis failure. Also, overexpression of YAP1 has been shown to cause genomic instability in medulloblastoma (68). To determine if Hippo pathway deregulation by p.I615V-mutant LATS1 plays a role in CIN development, we established U2OS cell lines inducibly expressing wildtype and p.I615V-mutant LATS1. Upon induction of mutant LATS1, YAP1 was found localized in the nucleus even at high density while YAP1 was cytoplasmic in induced wildtype and non-induced cells. Preliminary experiments also indicated an increase in micronucleus formation and centriole amplification when compared to the induced wildtype and non-induced cells. There are various theories on how CIN could develop as a result of LATS1 mutation and resulting Hippo pathway deregulation. First, enforced expression of NDR1, a LATS1-related kinase, is known to enhances centrosomal overduplication in a kinase activity-dependent manner (135). The p.I615V mutation lies within the protein binding domain (PBD; aa.656–758) with is known to be important form MOB1 binding. Therfore mutation mediated loss of LATS1-MOB1 could in theory increase MOB1-NDR1 complex leading to centrosomal overduplication. Second, YAP1 overactivation due to LATS1 mutation may cause Akt phoshorylation and activation through IGF2 causing downregulation of ATM-Chk2-p53 pathway leading to radioresistance and genomic instability (68). During mitosis CDC2 is known to form a complex with LATS1 at the centrosome and phosphorylation of Ser613 occurs. The LATS1 p.I615V may interfere with phosphorylation at this site leading to CIN (136). These effects of LATS1 mutation on the above pathways leading to CIN development remain to be explored in NCH149 cells.

6.3 VP a specific cytotoxic agent for LATS1 mutant YAP1 hyperactive cells

An intriguing aspect of the Hippo pathway is that its components interact through well characterized structures such as WW-domain and PPxY motifs. These properties of the Hippo pathway impart significant potential and advantages to be an attractive target for drug development (137). However, to date, few small-molecule inhibitors have been discovered that target the Hippo pathway.

Recent progress in the search for small-molecule Hippo pathway modulators has identified Verteporfin (VP) to be a specific inhibitor of YAP1 (81). VP has been shown to act as an effective chemotherapeutic agent *in vitro* for mainly those cells overexpressing YAP1. Since

in this study NCH149 was shown to have YAP1 hyperactivity VP was chosen for targeting YAP1-TEAD in NCH149 cells. As mentioned before NCH149 cells are highly resistant to standard chemotherapeutic drugs and radiation. Nevertheless VP did induce dose-dependent toxicity in NCH149 but not in NCH82 cells. This toxicity observed is attributed to apoptosis induced by VP specifically in NCH149 and not in NCH82 cells. This appears to be due to a dependency of NCH149 cells on YAP1 activity for growth and proliferation. The recent discovery of G-protein coupled receptors (GPCRs) as regulators of the Hippo-YAP/TAZ pathway has broadened the scope of upstream drug targets including a wide variety of extracellular ligands and receptors. Dobutamine (a GPCR β-adrenergic receptor antagonist) was recently recognized as an inhibitor of the Hippo pathway (79). However, targeting the downstream YAP1-TEAD interaction directly has proven to be more successful. YAP and TAZ are transcriptional co-activators with no known catalytic activity. Thus, inhibiting the function of YAP1 and TAZ require targeting protein-protein interactions (138). VP was found to be effective in inhibition of growth and proliferation of retinoblastoma cells in vitro (80). In vivo experiments in inducible YAP1 transgenic mouse model showed that VP treatment suppressed YAP1-induced hepatomegaly and more importantly showed no effect on wild-type non-transgenic controls (81). As YAP1 is the final effectors of the Hippo pathway, direct inhibition of YAP1–TEAD may reduce possible side effects that might be caused by targeting upstream components that probably affect multiple intracellular signalling pathways. Also, YAP1-TEAD pathway is not active in normal tissues, drugs disrupting this interaction have the potential for increased cancer specificity and minimal healthy tissue toxicity making it a suitable drug target. Therefore, this study provides additional proof that VP could be an effective targeted therapy against LATS1-mutant or YAP1-hyperactive tumors.

In summary, the findings presented here establish for the first time a model wherein a LATS1 mutation (p.I615V) in the YAP1 binding domain hinders the interaction of the two proteins resulting in significantly decreased YAP1-Ser127 phosphorylation. YAP1, an oncogene, as a result localizes to the nucleus and binds to TEAD to activate transcription of tumor promoting genes (Figure 6.1). This deregulation of the Hippo pathway as a result of a LATS1 mutation also seems to increase chromosomal instability in cells expressing mutant LATS1.

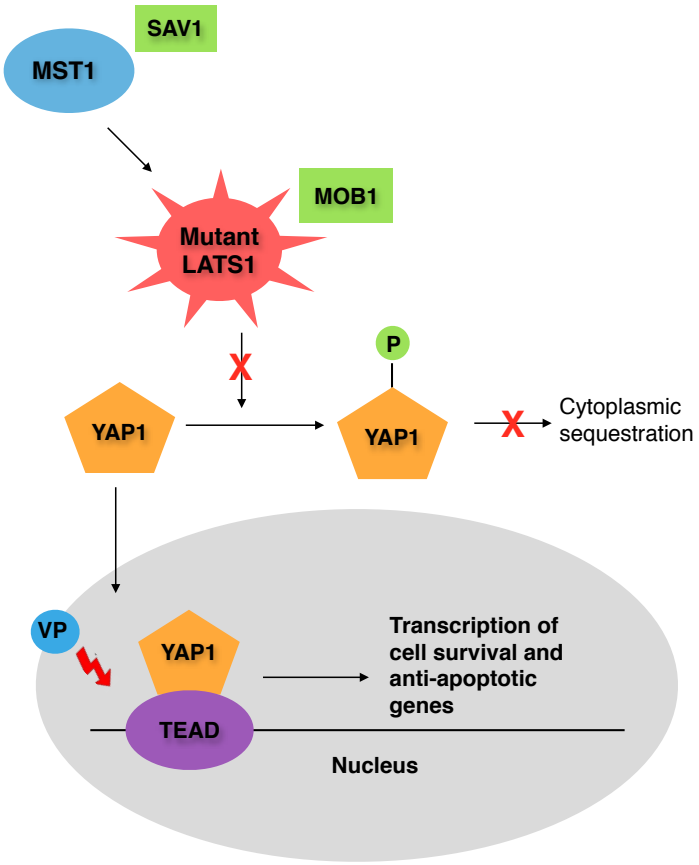

Figure 6.1: Deregulation of the Hippo pathway due to LATS1 mutation

Schematic illustration of the proposed model wherein the LATS1 p.I615V mutation leads to cancelling of YAP1 phosphorylation causing its nuclear translocation. This leads to YAP1-TEAD binding and transcriptional activation of tumor promoting genes and chromosomal instability. VP, known to disrupt the YAP1-TEAD interaction, selectively kills cells with such YAP1 hyperactivity.

6.4 Outlook

In the present work first evidence could be found that muations in the YAP1-binding domain of LATS1 deregulate the Hippo pathway by preventing negative regulation of YAP1. However, the clinical significance of this finding must be estimated possibly by immunohistochemical staining of GBM tumor sections to look for YAP1 nuclear localization along with screen to identify single nucleotide changes using derived cleaved amplified polymeric sequence (dCAPS) method (139).

To analyze whether the CIN phenotype can be reset, "rescue" experiments are necessary by siRNA-mediated "knock down" of mutant LATS specifically and the overexpression of wild type LATS. Moreover, to verify the effect of an amino acid substitution in LATS1 on the

protein itself, *in silico* studies could be performed to observe why the mutation affects YAP1 binding. Furthermore, it may be analyzed whether this mutation affects interactions of LATS1 with other proteins including MOB1, NDR kinase, TAZ and CDK1 which may have an impact on mitotic processes as well. Furthermore, experiments should be carried out to delineate mechanistically how mutant LATS1 leads to the development of CIN. One possibilty is overactivation of the NDR1 kinase that is known to cause CIN mediated by MOB1. Another is YAP1-mediated Akt activation and cell cycle checkpoint suppression or IGF2 activation to inhibit the DNA repair machinery (68).

Preliminary experiments in U2OS cells expressing wildtype and mutant LATS1 suggested that the identified mutation caused an increase in micronucleus formation and centriole amplification. To determine whether this leads to CIN in these cell lines, M-FISH analysis or interphase FISH could be performed to analyze for increased rates of chromosomal gains or losses. Furthermore, U2OS cells are known to be chromosomally aberrant from the beginning (140). Therefore, inducible diploid, chromosomally stable cells expressing wildtype and mutant LATS1 should be generated using for example the HCT116 colon cancer cell line, so that the development of CIN can be clearly monitored. In addition microarray analysis of RNA isolated from wildtype and mutant LATS1 expressing cells could be performed to identify changes in transcription of genes involved in tumor progression and CIN.

Verteporfin treatment showed that the cytotoxicity was specific to LATS1-mutant cells with YAP1 hyperactivity as in NCH149 cells. VP toxicity experiments must be performed in cell lines inducibly expressing mutant LATS1 along with healthy controls to specifically allocate this effect to the I615V-LATS1 mutation.

References

1. McGranahan N, Burrell RA, Endesfelder D, Novelli MR, Swanton C. Cancer chromosomal instability: therapeutic and diagnostic challenges. EMBO Rep. 2012 Jun;13(6):528–38.

2. Boveri T. Concerning the origin of malignant tumours by Theodor Boveri. Translated and annotated by Henry Harris. J Cell Sci. 2008 Jan;121 Suppl 1:1–84.

3. Lengauer C, Kinzler KW, Vogelstein B. Genetic instabilities in human cancers. Nature. 1998 Dec 17;396(6712):643–9.

4. Sheltzer JM. A transcriptional and metabolic signature of primary aneuploidy is present in chromosomally unstable cancer cells and informs clinical prognosis. Cancer Res. 2013 Nov 1;73(21):6401–12.

5. Manning AL, Dyson NJ. pRB, a Tumor Suppressor with a Stabilizing Presence. Trends Cell Biol. 2011 Aug;21(8):433–41.

6. Rao CV, Yamada HY. Genomic Instability and Colon Carcinogenesis: From the Perspective of Genes. Front Oncol [Internet]. 2013 May 21 [cited 2014 Nov 20];3. Available from: http://www.ncbi.nlm.nih.gov/pmc/articles/PMC3659308/

7. Nicholson JM, Cimini D. How mitotic errors contribute to karyotypic diversity in cancer. Adv Cancer Res. 2011;112:43–75.

8. Vermeulen K, Van Bockstaele DR, Berneman ZN. The cell cycle: a review of regulation, deregulation and therapeutic targets in cancer. Cell Prolif. 2003 Jun;36(3):131–49.

9. Alberts B, Johnson A, Lewis J, Raff M, Roberts K, Walter P. Molecular Biology of the Cell. 4th ed. Garland Science; 2002.

10. Rhind N, Russell P. Signaling Pathways that Regulate Cell Division. Cold Spring Harb Perspect Biol [Internet]. 2012 Oct [cited 2014 Nov 20];4(10). Available from: http://www.ncbi.nlm.nih.gov/pmc/articles/PMC3475169/

11. Foster DA, Yellen P, Xu L, Saqcena M. Regulation of G1 Cell Cycle Progression. Genes Cancer. 2010 Nov;1(11):1124–31.

12. Shiloh Y. ATM and related protein kinases: safeguarding genome integrity. Nat Rev Cancer. 2003 Mar;3(3):155–68.

13. Musacchio A, Salmon ED. The spindle-assembly checkpoint in space and time. Nat Rev Mol Cell Biol. 2007 May;8(5):379–93.

14. Nicklas RB, Ward SC, Gorbsky GJ. Kinetochore chemistry is sensitive to tension and may link mitotic forces to a cell cycle checkpoint. J Cell Biol. 1995 Aug 15;130(4):929–39.

15. Murray AW, Solomon MJ, Kirschner MW. The role of cyclin synthesis and degradation in the control of maturation promoting factor activity. Nature. 1989 May 25;339(6222):280–6.

16. Gollin SM. Mechanisms leading to chromosomal instability. Semin Cancer Biol. 2005 Feb;15(1):33–42.

17. Cahill DP, Lengauer C, Yu J, Riggins GJ, Willson JK, Markowitz SD, et al. Mutations of mitotic checkpoint genes in human cancers. Nature. 1998 Mar 19;392(6673):300–3.

18. Weaver BAA, Silk AD, Cleveland DW. Cell biology: Nondisjunction, aneuploidy and tetraploidy. Nature. 2006 Aug 17;442(7104):E9–10.

19. Kops GJPL, Weaver BAA, Cleveland DW. On the road to cancer: aneuploidy and the mitotic checkpoint. Nat Rev Cancer. 2005 Oct;5(10):773–85.

20. Iwanaga Y, Chi Y-H, Miyazato A, Sheleg S, Haller K, Peloponese J-M, et al. Heterozygous deletion of mitotic arrest-deficient protein 1 (MAD1) increases the incidence of tumors in mice. Cancer Res. 2007 Jan 1;67(1):160–6.

21. Rieder CL, Maiato H. Stuck in Division or Passing through: What Happens When Cells Cannot Satisfy the Spindle Assembly Checkpoint. Dev Cell. 2004 Nov;7(5):637–51.

22. Cancer Genome Atlas Research Network. Comprehensive genomic characterization defines human glioblastoma genes and core pathways. Nature. 2008 Oct 23;455(7216):1061–8.

23. Network TCGA. Comprehensive molecular characterization of human colon and rectal cancer. Nature. 2012 Jul 19;487(7407):330–7.

24. Cimini D, Moree B, Canman JC, Salmon ED. Merotelic kinetochore orientation occurs frequently during early mitosis in mammalian tissue cells and error correction is achieved by two different mechanisms. J Cell Sci. 2003 Oct 15;116(Pt 20):4213–25.

25. Thompson SL, Bakhoum SF, Compton DA. Mechanisms of Chromosomal Instability. Curr Biol CB. 2010 Mar 23;20(6):R285–95.

26. Orr B, Compton DA. A double-edged sword: how oncogenes and tumor suppressor genes can contribute to chromosomal instability. Front Oncol. 2013;3:164.

27. Weaver BA, Cleveland DW. Does aneuploidy cause cancer? Curr Opin Cell Biol. 2006 Dec;18(6):658–67.

28. Thompson SL, Compton DA. Chromosome missegregation in human cells arises through specific types of kinetochore–microtubule attachment errors. Proc Natl Acad Sci. 2011 Nov 1;108(44):17974–8.

29. Bakhoum SF, Genovese G, Compton DA. Deviant kinetochore-microtubule dynamics underlie chromosomal instability. Curr Biol CB. 2009 Dec 1;19(22):1937–42.

30. Kabeche L, Compton DA. Checkpoint-independent stabilization of kinetochore-microtubule attachments by Mad2 in human cells. Curr Biol CB. 2012 Apr 10;22(7):638–44.

31. Zhang N, Ge G, Meyer R, Sethi S, Basu D, Pradhan S, et al. Overexpression of Separase induces aneuploidy and mammary tumorigenesis. Proc Natl Acad Sci U S A. 2008 Sep 2;105(35):13033–8.

32. Solomon DA, Kim J-S, Waldman T. Cohesin gene mutations in tumorigenesis: from discovery to clinical significance. BMB Rep. 2014 Jun;47(6):299–310.

33. Duensing A, Liu Y, Tseng M, Malumbres M, Barbacid M, Duensing S. Cyclin-dependent kinase 2 is dispensable for normal centrosome duplication but required for oncogene-induced centrosome overduplication. Oncogene. 2006 May 11;25(20):2943–9.

34. Löffler H, Fechter A, Matuszewska M, Saffrich R, Mistrik M, Marhold J, et al. Cep63 recruits Cdk1 to the centrosome: implications for regulation of mitotic entry, centrosome amplification, and genome maintenance. Cancer Res. 2011 Mar 15;71(6):2129–39.

35. Anderhub SJ, Krämer A, Maier B. Centrosome amplification in tumorigenesis. Cancer Lett. 2012 Sep;322(1):8–17.

36. Ganem NJ, Godinho SA, Pellman D. A mechanism linking extra centrosomes to chromosomal instability. Nature. 2009 Jul 9;460(7252):278–82.

37. Nigg EA. Centrosome aberrations: cause or consequence of cancer progression? Nat Rev Cancer. 2002 Nov;2(11):815–25.

38. Krämer A, Maier B, Bartek J. Centrosome clustering and chromosomal (in)stability: A matter of life and death. Mol Oncol. 2011 Aug;5(4):324–35.

39. Quintyne NJ, Reing JE, Hoffelder DR, Gollin SM, Saunders WS. Spindle Multipolarity Is Prevented by Centrosomal Clustering. Science. 2005 Jan 7;307(5706):127–9.

40. Silkworth WT, Nardi IK, Scholl LM, Cimini D. Multipolar spindle pole coalescence is a major source of kinetochore mis-attachment and chromosome mis-segregation in cancer cells. PloS One. 2009;4(8):e6564.

41. Kwon M, Godinho SA, Chandhok NS, Ganem NJ, Azioune A, Thery M, et al. Mechanisms to suppress multipolar divisions in cancer cells with extra centrosomes. Genes Dev. 2008 Aug 15;22(16):2189–203.

42. Basto R, Brunk K, Vinadogrova T, Peel N, Franz A, Khodjakov A, et al. Centrosome Amplification Can Initiate Tumorigenesis in Flies. Cell. 2008 Jun 13;133(6):1032–42.

43. Brinkley BR. Managing the centrosome numbers game: from chaos to stability in cancer cell division. Trends Cell Biol. 2001 Jan;11(1):18–21.

44. Potapova TA, Zhu J, Li R. Aneuploidy and chromosomal instability: a vicious cycle driving cellular evolution and cancer genome chaos. Cancer Metastasis Rev. 2013 Dec 1;32(3-4):377–89.

45. Cahill DP, Kinzler KW, Vogelstein B, Lengauer C. Genetic instability and darwinian selection in tumours. Trends Cell Biol. 1999 Dec 1;9(12):M57–60.

46. Roschke AV, Rozenblum E. Multi-layered cancer chromosomal instability phenotype. Mol Cell Oncol. 2013;3:302.

47. Nowak MA, Komarova NL, Sengupta A, Jallepalli PV, Shih I-M, Vogelstein B, et al. The role of chromosomal instability in tumor initiation. Proc Natl Acad Sci. 2002 Dec 10;99(25):16226–31.

48. Jefford CE, Irminger-Finger I. Mechanisms of chromosome instability in cancers. Crit Rev Oncol Hematol. 2006 Jul 1;59(1):1–14.

49. Duijf PHG, Schultz N, Benezra R. Cancer cells preferentially lose small chromosomes. Int J Cancer J Int Cancer. 2013 May 15;132(10):2316–26.

50. Zimonjic D, Brooks MW, Popescu N, Weinberg RA, Hahn WC. Derivation of human tumor cells in vitro without widespread genomic instability. Cancer Res. 2001 Dec 15;61(24):8838–44.

51. Duesberg P, Rausch C, Rasnick D, Hehlmann R. Genetic instability of cancer cells is proportional to their degree of aneuploidy. Proc Natl Acad Sci U S A. 1998 Nov 10;95(23):13692–7.

52. Sieber OM, Heinimann K, Tomlinson IPM. Genomic instability — the engine of tumorigenesis? Nat Rev Cancer. 2003 Sep;3(9):701–8.

53. Loeb LA. Mutator phenotype may be required for multistage carcinogenesis. Cancer Res. 1991 Jun 15;51(12):3075–9.

54. Nowell PC. The clonal evolution of tumor cell populations. Science. 1976 Oct 1;194(4260):23–8.

55. Holland AJ, Cleveland DW. Boveri revisited: chromosomal instability, aneuploidy and tumorigenesis. Nat Rev Mol Cell Biol. 2009 Jul;10(7):478–87.

56. Michor F. Chromosomal instability and human cancer. Philos Trans R Soc B Biol Sci. 2005 Mar 29;360(1455):631–5.

57. Pangilinan F, Li Q, Weaver T, Lewis BC, Dang CV, Spencer F. Mammalian BUB1 protein kinases: map positions and in vivo expression. Genomics. 1997 Dec 15;46(3):379–88.

58. Schvartzman J-M, Duijf PHG, Sotillo R, Coker C, Benezra R. Mad2 is a critical mediator of the chromosome instability observed upon Rb and p53 pathway inhibition. Cancer Cell. 2011 Jun 14;19(6):701–14.

59. Gudmundsdottir K, Ashworth A. The roles of BRCA1 and BRCA2 and associated proteins in the maintenance of genomic stability. Oncogene. 2006;25(43):5864–74.

60. Choi YJ, Anders L. Signaling through cyclin D-dependent kinases. Oncogene. 2014 Apr 10;33(15):1890–903.

61. Shepard JL, Amatruda JF, Finkelstein D, Ziai J, Finley KR, Stern HM, et al. A mutation in separase causes genome instability and increased susceptibility to epithelial cancer. Genes Dev. 2007 Jan 1;21(1):55–9.

62. Eichinger CS, Kurze A, Oliveira RA, Nasmyth K. Disengaging the Smc3/kleisin interface releases cohesin from Drosophila chromosomes during interphase and mitosis. EMBO J. 2013 Mar 6;32(5):656–65.

63. Michor F, Iwasa Y, Nowak MA. Dynamics of cancer progression. Nat Rev Cancer. 2004 Mar;4(3):197–205.

64. Zhao B, Li L, Lei Q, Guan K-L. The Hippo-YAP pathway in organ size control and tumorigenesis: an updated version. Genes Dev. 2010 May;24(9):862–74.

65. Zhao B, Ye X, Yu J, Li L, Li W, Li S, et al. TEAD mediates YAP-dependent gene induction and growth control. Genes Dev. 2008 Jul 15;22(14):1962–71.

66. Yu F-X, Guan K-L. The Hippo pathway: regulators and regulations. Genes Dev. 2013 Feb 15;27(4):355–71.

67. Yu F-X, Zhao B, Panupinthu N, Jewell JL, Lian I, Wang LH, et al. Regulation of the Hippo-YAP pathway by G-protein coupled receptor signaling. Cell. 2012 Aug 17;150(4):780–91.

68. Fernandez-L A, Squatrito M, Northcott P, Awan A, Holland EC, Taylor MD, et al. Oncogenic YAP promotes radioresistance and genomic instability in medulloblastoma through IGF2-mediated Akt activation. Oncogene. 2012 Apr 12;31(15):1923–37.

69. Nishiyama Y, Hirota T, Morisaki T, Hara T, Marumoto T, Iida S, et al. A human homolog of Drosophila warts tumor suppressor, h-warts, localized to mitotic apparatus and specifically phosphorylated during mitosis. FEBS Lett. 1999 Oct 8;459(2):159–65.

70. Vlug EJ, van de Ven RAH, Vermeulen JF, Bult P, van Diest PJ, Derksen PWB. Nuclear localization of the transcriptional coactivator YAP is associated with invasive lobular breast cancer. Cell Oncol Dordr. 2013 Oct;36(5):375–84.

71. Zhao B, Wei X, Li W, Udan RS, Yang Q, Kim J, et al. Inactivation of YAP oncoprotein by the Hippo pathway is involved in cell contact inhibition and tissue growth control. Genes Dev. 2007 Nov 1;21(21):2747–61.

72. Tao W, Zhang S, Turenchalk GS, Stewart RA, St John MA, Chen W, et al. Human homologue of the Drosophila melanogaster lats tumour suppressor modulates CDC2 activity. Nat Genet. 1999 Feb;21(2):177–81.

73. Hergovich A. Regulation and functions of mammalian LATS/NDR kinases: looking beyond canonical Hippo signalling. Cell Biosci. 2013;3(1):32.

74. Hirota T, Morisaki T, Nishiyama Y, Marumoto T, Tada K, Hara T, et al. Zyxin, a regulator of actin filament assembly, targets the mitotic apparatus by interacting with h-warts/LATS1 tumor suppressor. J Cell Biol. 2000 May 29;149(5):1073–86.

75. Yang X, Yu K, Hao Y, Li D, Stewart R, Insogna KL, et al. LATS1 tumour suppressor affects cytokinesis by inhibiting LIMK1. Nat Cell Biol. 2004 Jul;6(7):609–17.

76. Yang S, Zhang L, Liu M, Chong R, Ding S-J, Chen Y, et al. CDK1 Phosphorylation of YAP Promotes Mitotic Defects and Cell Motility and Is Essential for Neoplastic Transformation. Cancer Res [Internet]. 2013 Nov 15 [cited 2014 Nov 30];73(22). Available from: http://www.ncbi.nlm.nih.gov/pmc/articles/PMC3861241/

77. Yabuta N, Mukai S, Okamoto A, Okuzaki D, Suzuki H, Torigata K, et al. N-terminal truncation of Lats1 causes abnormal cell growth control and chromosomal instability. J Cell Sci. 2013 Jan 15;126(Pt 2):508–20.

78. Ji T, Liu D, Shao W, Yang W, Wu H, Bian X. Decreased expression of LATS1 is correlated with the progression and prognosis of glioma. J Exp Clin Cancer Res CR. 2012;31:67.

79. Bao Y, Nakagawa K, Yang Z, Ikeda M, Withanage K, Ishigami-Yuasa M, et al. A cell-based assay to screen stimulators of the Hippo pathway reveals the inhibitory effect of dobutamine on the YAP-dependent gene transcription. J Biochem (Tokyo). 2011 Aug;150(2):199–208.

80. Brodowska K, Al-Moujahed A, Marmalidou A, Meyer Zu Horste M, Cichy J, Miller JW, et al. The clinically used photosensitizer Verteporfin (VP) inhibits YAP-TEAD and human retinoblastoma cell growth in vitro without light activation. Exp Eye Res. 2014 Jul;124:67–73.

81. Liu-Chittenden Y, Huang B, Shim JS, Chen Q, Lee S-J, Anders RA, et al. Genetic and pharmacological disruption of the TEAD–YAP complex suppresses the oncogenic activity of YAP. Genes Dev. 2012 Jun 15;26(12):1300–5.

82. Kleihues P, Louis DN, Scheithauer BW, Rorke LB, Reifenberger G, Burger PC, et al. The WHO classification of tumors of the nervous system. J Neuropathol Exp Neurol. 2002 Mar;61(3):215–25; discussion 226–9.

83. Johnson DR, O'Neill BP. Glioblastoma survival in the United States before and during the temozolomide era. J Neurooncol. 2012 Apr;107(2):359–64.

84. ZHANG X, ZHANG W, CAO W-D, CHENG G, ZHANG Y-Q. Glioblastoma multiforme: Molecular characterization and current treatment strategy (Review). Exp Ther Med. 2012 Jan;3(1):9–14.

85. Martinez R, Schackert H-K, Plaschke J, Baretton G, Appelt H, Schackert G. Molecular mechanisms associated with chromosomal and microsatellite instability in sporadic glioblastoma multiforme. Oncology. 2004;66(5):395–403.

86. Von Deimling A, von Ammon K, Schoenfeld D, Wiestler OD, Seizinger BR, Louis DN. Subsets of glioblastoma multiforme defined by molecular genetic analysis. Brain Pathol Zurich Switz. 1993 Jan;3(1):19–26.

87. Reifenberger G, Liu L, Ichimura K, Schmidt EE, Collins VP. Amplification and Overexpression of the MDM2 Gene in a Subset of Human Malignant Gliomas without p53 Mutations. Cancer Res. 1993 Jun 15;53(12):2736–9.

88. Karcher S, Steiner H-H, Ahmadi R, Zoubaa S, Vasvari G, Bauer H, et al. Different angiogenic phenotypes in primary and secondary glioblastomas. Int J Cancer. 2006;118(9):2182–9.

89. Dokic I, Mairani A, Brons S, Schoell B, Jauch A, Krunic D, et al. High resistance to X-rays and therapeutic carbon ions in glioblastoma cells bearing dysfunctional ATM associates with intrinsic chromosomal instability. Int J Radiat Biol. 2014 Sep 8;1–9.

90. Laemmli UK. Cleavage of structural proteins during the assembly of the head of bacteriophage T4. Nature. 1970 Aug 15;227(5259):680–5.

91. Mullis K, Faloona F, Scharf S, Saiki R, Horn G, Erlich H. Specific enzymatic amplification of DNA in vitro: the polymerase chain reaction. Cold Spring Harb Symp Quant Biol. 1986;51 Pt 1:263–73.

92. Geigl JB, Obenauf AC, Waldispuehl-Geigl J, Hoffmann EM, Auer M, Hörmann M, et al. Identification of small gains and losses in single cells after whole genome amplification on tiling oligo arrays. Nucleic Acids Res. 2009 Aug;37(15):e105.

93. Cremer M, Grasser F, Lanctôt C, Müller S, Neusser M, Zinner R, et al. Multicolor 3D Fluorescence In Situ Hybridization for Imaging Interphase Chromosomes. In: Hancock R, editor. The Nucleus [Internet]. Humana Press; 2008 [cited 2015 Jan 1]. p. 205–39. Available from: http://link.springer.com/protocol/10.1007/978-1-59745-406-3_15

94. Fenech M, Kirsch-Volders M, Natarajan AT, Surralles J, Crott JW, Parry J, et al. Molecular mechanisms of micronucleus, nucleoplasmic bridge and nuclear bud formation in mammalian and human cells. Mutagenesis. 2011 Jan 1;26(1):125–32.

95. Gao J, Aksoy BA, Dogrusoz U, Dresdner G, Gross B, Sumer SO, et al. Integrative Analysis of Complex Cancer Genomics and Clinical Profiles Using the cBioPortal. Sci Signal. 2013 Apr 2;6(269):pl1–pl1.

96. Cerami E, Gao J, Dogrusoz U, Gross BE, Sumer SO, Aksoy BA, et al. The cBio Cancer Genomics Portal: An Open Platform for Exploring Multidimensional Cancer Genomics Data. Cancer Discov. 2012 May 1;2(5):401–4.

97. Bignold LP, Coghlan BLD, Jersmann HPA. Hansemann, Boveri, chromosomes and the gametogenesis-related theories of tumours. Cell Biol Int. 2006 Jul;30(7):640–4.

98. Rajagopalan H, Nowak MA, Vogelstein B, Lengauer C. The significance of unstable chromosomes in colorectal cancer. Nat Rev Cancer. 2003 Sep;3(9):695–701.

99. Hardy PA, Zacharias H. Reappraisal of the Hansemann-Boveri hypothesis on the origin of tumors. Cell Biol Int. 2005 Dec;29(12):983–92.

100. Weaver BAA, Silk AD, Montagna C, Verdier-Pinard P, Cleveland DW. Aneuploidy Acts Both Oncogenically and as a Tumor Suppressor. Cancer Cell. 2007 Jan;11(1):25–36.

101. Williams BR, Prabhu VR, Hunter KE, Glazier CM, Whittaker CA, Housman DE, et al. Aneuploidy affects proliferation and spontaneous immortalization in mammalian cells. Science. 2008 Oct 31;322(5902):703–9.

102. Baranovskaya S, Soto JL, Perucho M, Malkhosyan SR. Functional significance of concomitant inactivation of hMLH1 and hMSH6 in tumor cells of the microsatellite mutator phenotype. Proc Natl Acad Sci U S A. 2001 Dec 18;98(26):15107–12.

103. Loeb LA, Loeb KR, Anderson JP. Multiple mutations and cancer. Proc Natl Acad Sci U S A. 2003 Feb 4;100(3):776–81.

104. Perucho M. Cancer of the microsatellite mutator phenotype. Biol Chem. 1996 Nov;377(11):675–84.

105. Haigis KM, Caya JG, Reichelderfer M, Dove WF. Intestinal adenomas can develop with a stable karyotype and stable microsatellites. Proc Natl Acad Sci U S A. 2002 Jun 25;99(13):8927–31.

106. Solomon DA, Kim T, Diaz-Martinez LA, Fair J, Elkahloun AG, Harris BT, et al. Mutational inactivation of STAG2 causes aneuploidy in human cancer. Science. 2011 Aug 19;333(6045):1039–43.

107. Singh D, Chan JM, Zoppoli P, Niola F, Sullivan R, Castano A, et al. Transforming fusions of FGFR and TACC genes in human glioblastoma. Science. 2012 Sep 7;337(6099):1231–5.

108. Lengauer C, Kinzler KW, Vogelstein B. Genetic instability in colorectal cancers. Nature. 1997 Apr 10;386(6625):623–7.

109. Diaz-Cano SJ. Tumor Heterogeneity: Mechanisms and Bases for a Reliable Application of Molecular Marker Design. Int J Mol Sci. 2012 Feb 13;13(2):1951–2011.

110. Morgan WF, Murnane JP. A role for genomic instability in cellular radioresistance? Cancer Metastasis Rev. 1995 Mar 1;14(1):49–58.

111. Lee AJX, Endesfelder D, Rowan AJ, Walther A, Birkbak NJ, Futreal PA, et al. Chromosomal Instability Confers Intrinsic Multi-Drug Resistance. Cancer Res. 2011 Mar 1;71(5):1858–70.

112. Gisselsson D. Classification of chromosome segregation errors in cancer. Chromosoma. 2008 Dec 1;117(6):511–9.

113. Geigl JB, Obenauf AC, Schwarzbraun T, Speicher MR. Defining “chromosomal instability.” Trends Genet TIG. 2008 Feb;24(2):64–9.

114. Bonassi S, Znaor A, Ceppi M, Lando C, Chang WP, Holland N, et al. An increased micronucleus frequency in peripheral blood lymphocytes predicts the risk of cancer in humans. Carcinogenesis. 2006 Sep 14;28(3):625–31.

115. Zyss D, Gergely F. Centrosome function in cancer: guilty or innocent? Trends Cell Biol. 2009 Jul;19(7):334–46.

116. Koutsami MK, Tsantoulis PK, Kouloukoussa M, Apostolopoulou K, Pateras IS, Spartinou Z, et al. Centrosome abnormalities are frequently observed in non-small-cell lung cancer and are associated with aneuploidy and cyclin E overexpression. J Pathol. 2006 Aug;209(4):512–21.

117. Lingle WL, Lutz WH, Ingle JN, Maihle NJ, Salisbury JL. Centrosome hypertrophy in human breast tumors: implications for genomic stability and cell polarity. Proc Natl Acad Sci U S A. 1998 Mar 17;95(6):2950–5.

118. Hut HMJ, Lemstra W, Blaauw EH, van Cappellen GWA, Kampinga HH, Sibon OCM. Centrosomes Split in the Presence of Impaired DNA Integrity during Mitosis. Mol Biol Cell. 2003 May;14(5):1993–2004.

119. Lingle WL, Salisbury JL. Altered Centrosome Structure Is Associated with Abnormal Mitoses in Human Breast Tumors. Am J Pathol. 1999 Dec;155(6):1941–51.

120. Yang Z, Lončarek J, Khodjakov A, Rieder CL. Extra centrosomes and/or chromosomes prolong mitosis in human cells. Nat Cell Biol. 2008 Jun;10(6):748–51.

121. Dalton WB, Yang VW. THE ROLE OF PROLONGED MITOTIC CHECKPOINT ACTIVATION IN THE FORMATION AND TREATMENT OF CANCER. Future Oncol Lond Engl. 2009 Nov;5(9):1363–70.

122. Friedberg EC. DNA damage and repair. Nature. 2003 Jan 23;421(6921):436–40.

123. Yu T, Bachman J, Lai Z-C. Mutation analysis of large tumor suppressor genes LATS1 and LATS2 supports a tumor suppressor role in human cancer. Protein Cell. 2014 Dec 9;1–6.

124. Xu T, Wang W, Zhang S, Stewart RA, Yu W. Identifying tumor suppressors in genetic mosaics: the Drosophila lats gene encodes a putative protein kinase. Dev Camb Engl. 1995 Apr;121(4):1053–63.

125. Eeken JCJ, Klink I, van Veen BL, Pastink A, Ferro W. Induction of epithelial tumors in Drosophila melanogaster heterozygous for the tumor suppressor gene wts. Environ Mol Mutagen. 2002;40(4):277–82.

126. Hisaoka M, Tanaka A, Hashimoto H. Molecular alterations of h-warts/LATS1 tumor suppressor in human soft tissue sarcoma. Lab Investig J Tech Methods Pathol. 2002 Oct;82(10):1427–35.

127. Orr BA, Bai H, Odia Y, Jain D, Anders RA, Eberhart CG. Yes-Associated Protein 1 (YAP1) Is Widely Expressed in Human Brain Tumors and Promotes Glioblastoma Growth. J Neuropathol Exp Neurol. 2011 Jul;70(7):568–77.

128. Santarius T, Shipley J, Brewer D, Stratton MR, Cooper CS. A census of amplified and overexpressed human cancer genes. Nat Rev Cancer. 2010 Jan;10(1):59–64.

129. Zender L, Spector MS, Xue W, Flemming P, Cordon-Cardo C, Silke J, et al. Identification and Validation of Oncogenes in Liver Cancer Using an Integrative Oncogenomic Approach. Cell. 2006 Jun 30;125(7):1253–67.

130. Baia GS, Caballero OL, Orr BA, Lal A, Ho JSY, Cowdrey C, et al. Yes-Associated Protein 1 Is Activated and Functions as an Oncogene in Meningiomas. Mol Cancer Res. 2012 Jul 1;10(7):904–13.

131. Wang W, Huang J, Chen J. Angiomotin-like proteins associate with and negatively regulate YAP1. J Biol Chem. 2011 Feb 11;286(6):4364–70.

132. Levy D, Adamovich Y, Reuven N, Shaul Y. Yap1 Phosphorylation by c-Abl Is a Critical Step in Selective Activation of Proapoptotic Genes in Response to DNA Damage. Mol Cell. 2008 Feb 15;29(3):350–61.

133. Zhao B, Li L, Tumaneng K, Wang C-Y, Guan K-L. A coordinated phosphorylation by Lats and CK1 regulates YAP stability through SCFβ-TRCP. Genes Dev. 2010 Jan 1;24(1):72–85.

134. Iida S-I, Hirota T, Morisaki T, Marumoto T, Hara T, Kuninaka S, et al. Tumor suppressor WARTS ensures genomic integrity by regulating both mitotic progression and G1 tetraploidy checkpoint function. Oncogene. 2004 Jul 8;23(31):5266–74.

135. Hergovich A, Cornils H, Hemmings BA. Mammalian NDR protein kinases: from regulation to a role in centrosome duplication. Biochim Biophys Acta. 2008 Jan;1784(1):3–15.

136. Visser S, Yang X. LATS tumor suppressor: A new governor of cellular homeostasis. Cell Cycle. 2010 Oct 1;9(19):3892–903.

137. Park HW, Guan K-L. Regulation of the Hippo pathway and implications for anticancer drug development. Trends Pharmacol Sci. 2013 Oct;34(10):581–9.

138. Johnson R, Halder G. The two faces of Hippo: targeting the Hippo pathway for regenerative medicine and cancer treatment. Nat Rev Drug Discov. 2014 Jan;13(1):63–79.

139. Meyer J, Pusch S, Balss J, Capper D, Mueller W, Christians A, et al. PCR- and restriction endonuclease-based detection of IDH1 mutations. Brain Pathol Zurich Switz. 2010 Mar;20(2):298–300.

140. Bakhoum SF, Thompson SL, Manning AL, Compton DA. Genome stability is ensured by temporal control of kinetochore-microtubule dynamics. Nat Cell Biol. 2009 Jan;11(1):27–35.